A General Platform for Systematic Quantitative Evaluation of Small-Molecule Permeability in Bacteria

Tony D. Davis,[†] Christopher J. Gerry,[‡] and Derek S. Tan*[,†,‡,§]

[†]*Pharmacology Program–Weill Cornell Graduate School of Medical Sciences,*
[‡]*Gerstner Sloan Kettering Summer Undergraduate Research Program,*
[§]*Molecular Pharmacology & Chemistry Program and Tri-Institutional Research Program,*
Memorial Sloan Kettering Cancer Center
1275 York Avenue, Box 422, New York, New York 10065

Supporting Information

A. Supporting Information Figures S1–S15 S2
B. Supporting Information Tables S1–S4 S17
C. Materials and methods S20
D. Synthesis of acyl-AMS analogues S22
E. LC-MS/MS analysis S31
F. Compound accumulation studies S32
G. Principal component analysis S34
H. ^{1}H-NMR and ^{13}C-NMR spectra S43

A. Supporting Information Figures S1–S14

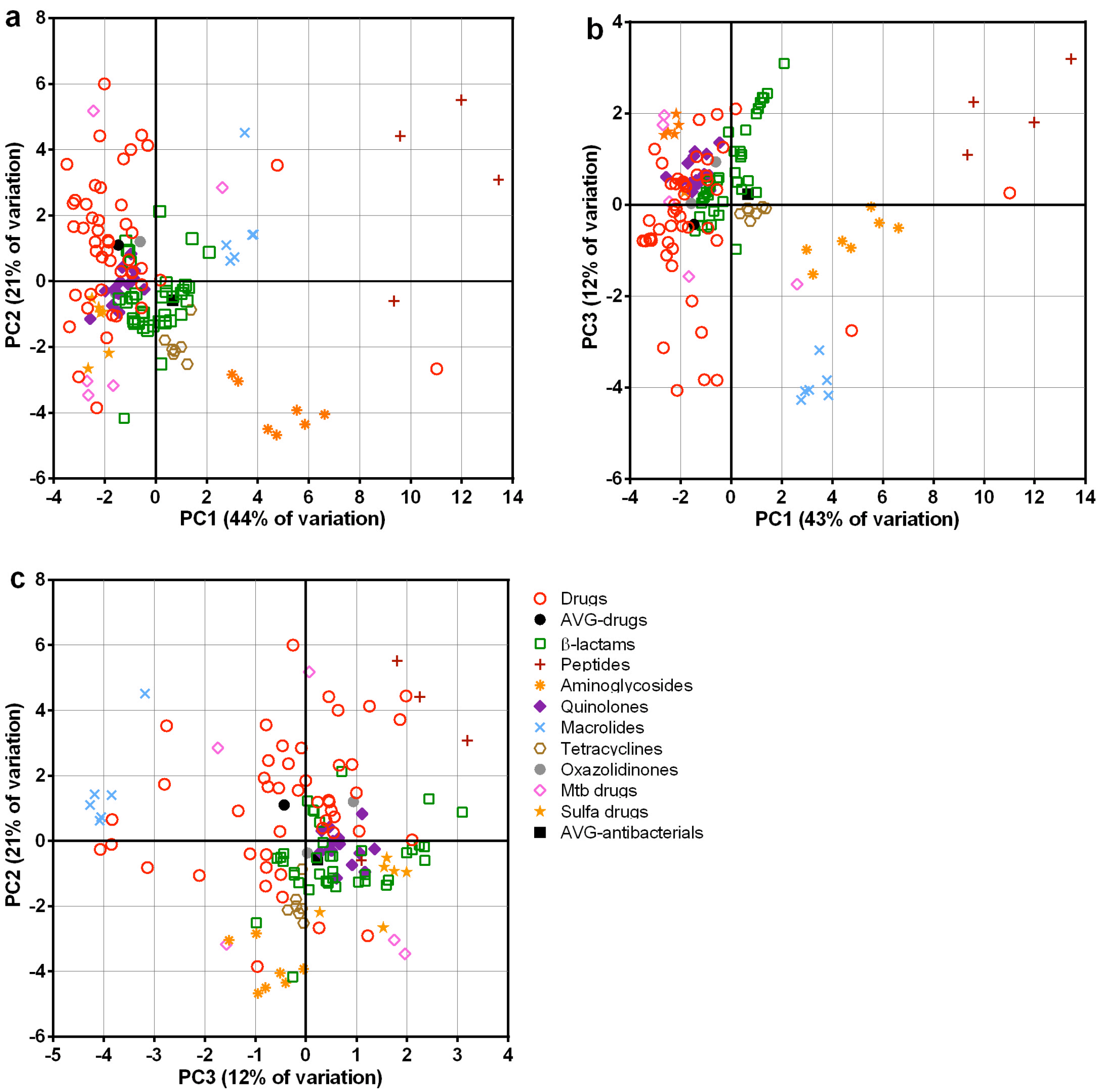

Figure S1. Principal component analysis (PCA) indicates that many antibacterial drugs have distinct structural and physicochemical properties compared to other drug classes. PCA plots of 91 antibacterial drugs and 50 top-selling, brand-name non-antiinfective drugs (Drugs): **(a)** PC1 vs. PC2, **(b)** PC1 vs. PC3, **(c)** PC3 vs. PC2; percent contribution for each principal component is indicated on the axes; *Mtb* = *Mycobacterium tuberculosis*; AVG = hypothetical average for a given dataset.

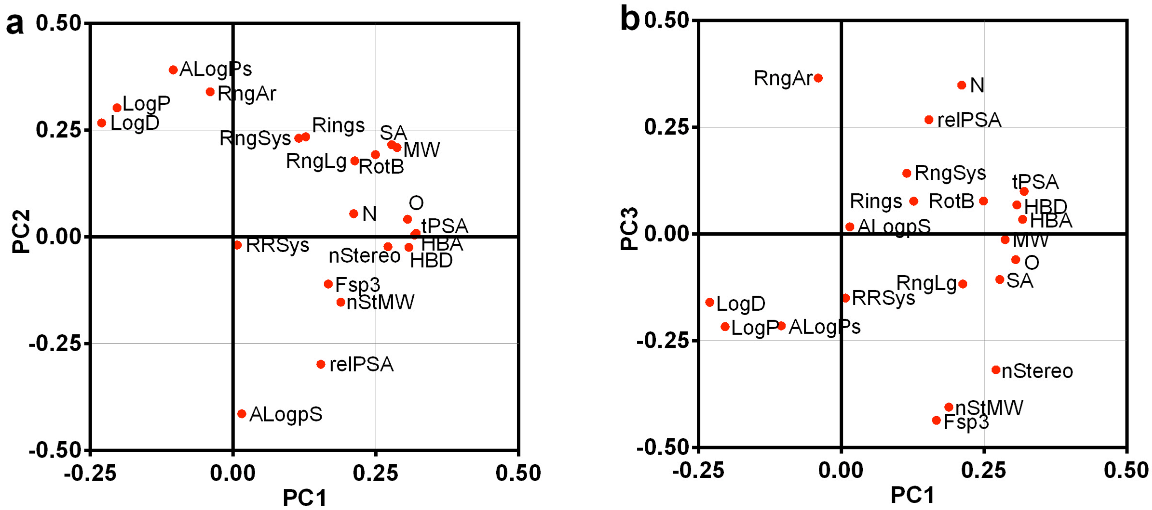

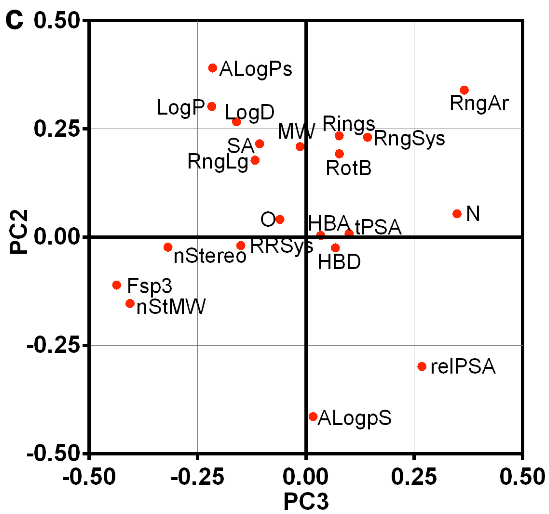

d

	PC1	PC2	PC3
MW	**0.2870**	0.2093	-0.0133
SA	0.2776	0.2159	-0.1066
N	0.2111	0.0543	**0.3485**
O	**0.3055**	0.0414	-0.0598
HBD	**0.3075**	-0.0243	0.0683
HBA	**0.3178**	0.0044	0.0345
LogD	-0.2301	0.2668	-0.1599
LogP	-0.2032	**0.3021**	-0.2169
ALogPs	-0.1048	**0.3910**	-0.2147
ALogpS	0.0153	**-0.4139**	0.0168
tPSA	**0.3204**	0.0084	0.0999
relPSA	0.1535	**-0.2983**	0.2677
nStereo	0.2712	-0.0228	**-0.3176**
nStMW	0.1886	-0.1526	**-0.4050**
Fsp3	0.1668	-0.1100	**-0.4362**
RotB	0.2493	0.1926	0.0775
Rings	0.1271	0.2343	0.0770
RngAr	-0.0402	**0.3396**	**0.3654**
RngLg	0.2131	0.1781	-0.1168
RngSys	0.1147	0.2310	0.1423
RRSys	0.0074	-0.0188	-0.1497

Figure S2. Loading plots and component loading values indicate the influence of each structural and physicochemical parameter on the positioning of compounds in the PCA plot. Corresponding loading plots for PCA of 91 antibacterial drugs and 50 top-selling, brand-name non-antiinfective drugs in **Figure 1a** and **Figure S1**: **(a)** PC1 vs. PC2, **(b)** PC1 vs. PC3, and **(c)** PC3 vs. PC2, (**d**) Component loadings of 20 structural and physicochemical parameters on the first three principal components; the five most influential parameters for each principal component are highlighted (yellow).

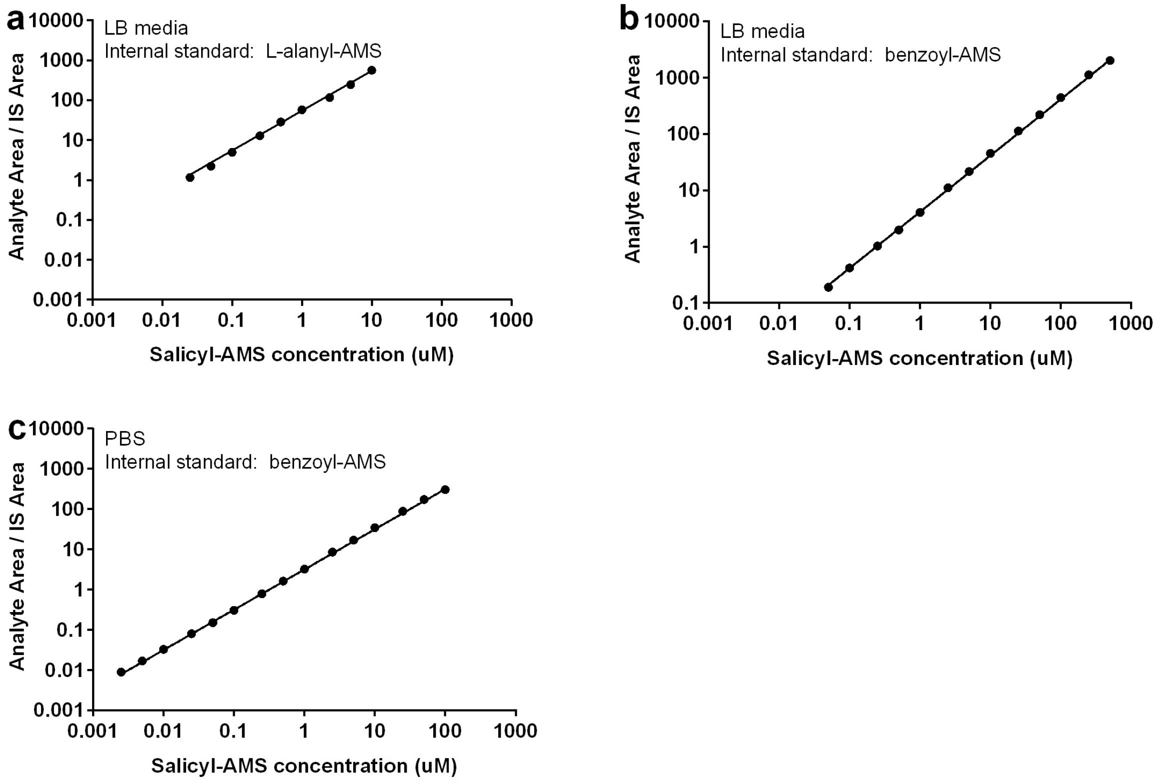

Figure S3. Standard calibration curves of salicyl-AMS indicate that media and internal standard influence limits of detection. Calibration curves in: **(a)** LB media, L-alanyl-AMS internal standard; quantifiable from 0.025–10 μM (2.6 logs), **(b)** LB media, benzoyl-AMS internal standard; quantifiable from 0.050–500 μM (4.0 logs), and **(c)** PBS, benzoyl-AMS internal standard; quantifiable from 0.0025–100 μM (4.6 logs).

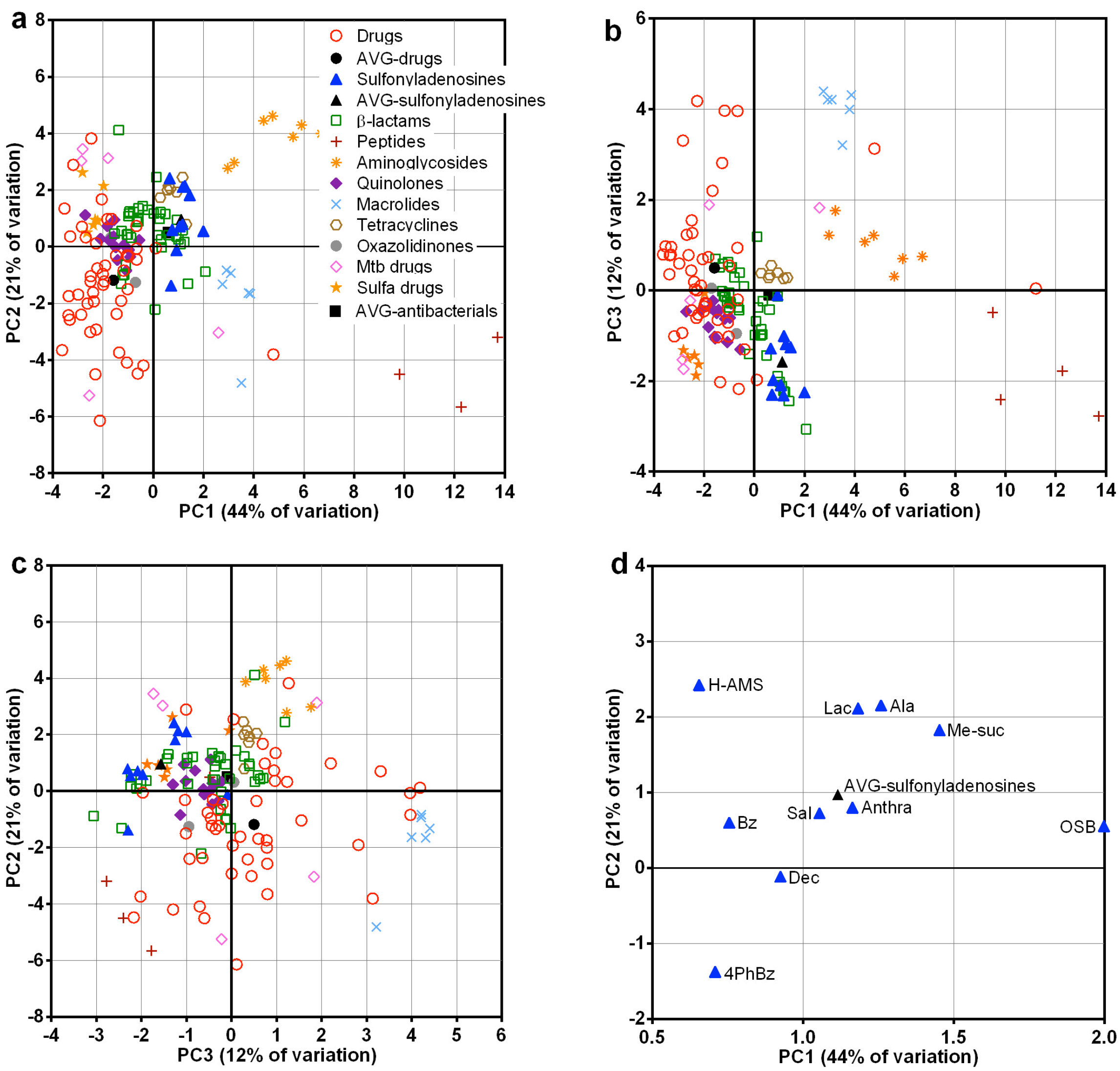

Figure S4. PCA indicates that sulfonyladenosines have structural and physicochemical properties similar to those of antibacterial drugs and distinct from non-antiinfective drugs. PCA plots of 25 sulfonyladenosines (AMS), 91 antibacterial drugs, and 50 top-selling, brand-name non-antiinfective drugs (Drugs): **(a)** PC1 vs. PC2, **(b)** PC1 vs. PC3, **(c)** PC3 vs. PC2; percent contribution for each principal component is indicated on the axes; *Mtb* = *Mycobacterium tuberculosis*; AVG = hypothetical average for a given dataset. Although the PC2 and PC3 axes were inverted compared to Figure S1, the signs of all PC axes are arbitrary. **(d)** Expanded view of panel (a) to visual positions of sulfonyladenosines.

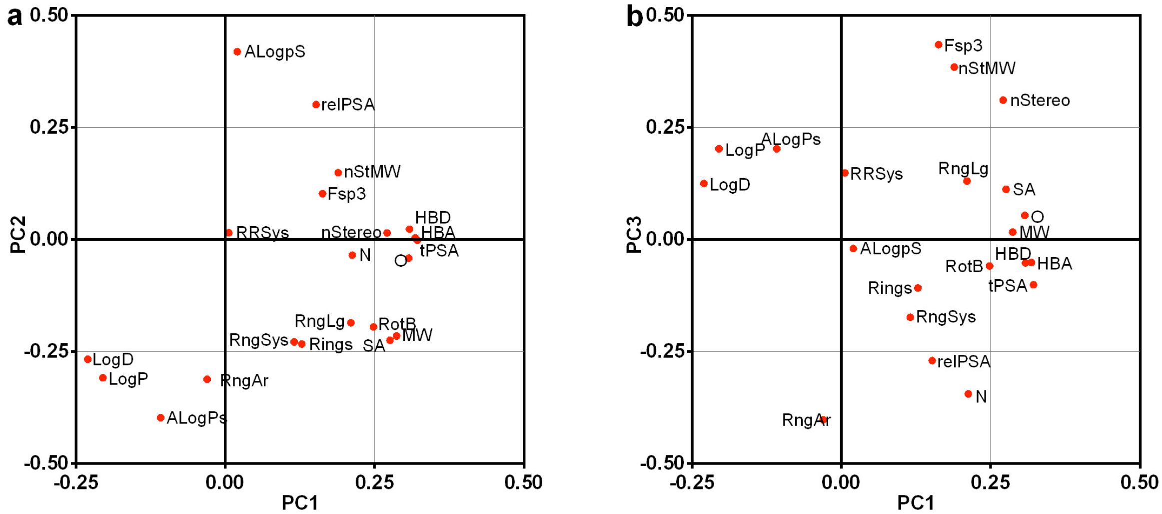

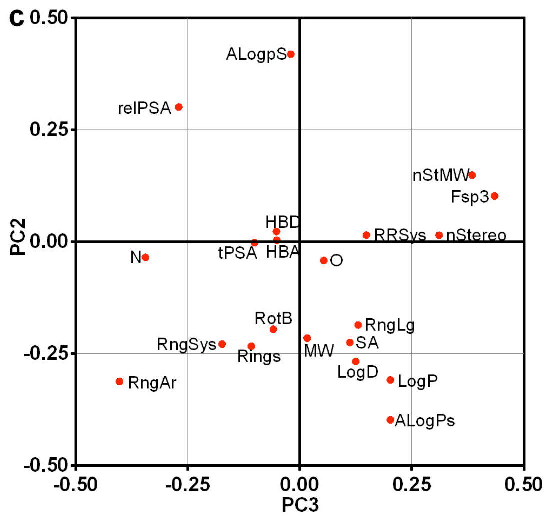

d

	PC1	PC2	PC3
MW	**0.2868**	-0.2152	0.0165
SA	0.2758	-0.2247	0.1118
N	0.2125	-0.0347	**-0.3445**
O	**0.3072**	-0.0417	0.0534
HBD	**0.3085**	0.0228	-0.0521
HBA	**0.3181**	0.0036	-0.0516
LogD	-0.2301	-0.2672	0.1248
LogP	-0.2048	**-0.3084**	0.2023
ALogPs	-0.1081	**-0.3974**	0.2020
ALogpS	0.0201	**0.4187**	-0.0202
tPSA	**0.3217**	-0.0018	-0.1012
relPSA	0.1521	**0.3009**	-0.2700
nStereo	0.2708	0.0144	**0.3110**
nStMW	0.1891	0.1488	**0.3846**
Fsp3	0.1628	0.1022	**0.4344**
RotB	0.2482	-0.1952	-0.0591
Rings	0.1281	-0.2333	-0.1080
RngAr	-0.0305	**-0.3119**	**-0.4022**
RngLg	0.2104	-0.1860	0.1302
RngSys	0.1153	-0.2284	-0.1735
RRSys	0.0058	0.0148	0.1485

Figure S5. Loading plots and component loading values indicate a similar influence of structural and physicochemical parameters on the positioning of compounds in the PCA plots with sulfonyladenosines. Corresponding loading plots for PCA of 25 sulfonyladenosines, 91 antibacterial drugs, and 50 top-selling, brand-name non-antiinfective drugs in **Figure S4**: **(a)** PC1 vs. PC2, **(b)** PC1 vs. PC3, and **(c)** PC3 vs. PC2, (**d**) Component loadings of 20 structural and physicochemical parameters on the first three principal components; the five most influential parameters for each principal component are highlighted (yellow).

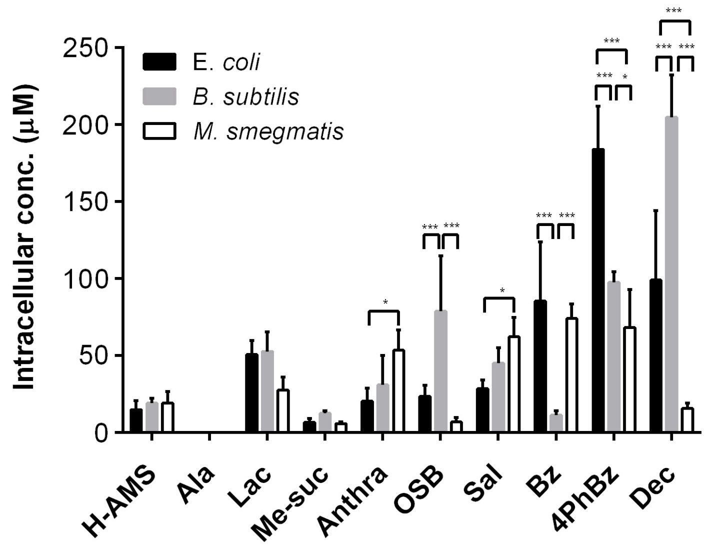

Figure S6. Accumulation of sulfonyladensine compounds across bacteria with different cellular envelopes. Alternative view of **Figure 4** from the manuscript. Data are reported as mean ± SD for 4 experiments. Statistical significance was assessed using two-way ANOVA and Tukey's multiple comparison test and 95% confidence intervals. $^{*}p < 0.05$, $^{**}p < 0.01$, $^{***}p < 0.001$.

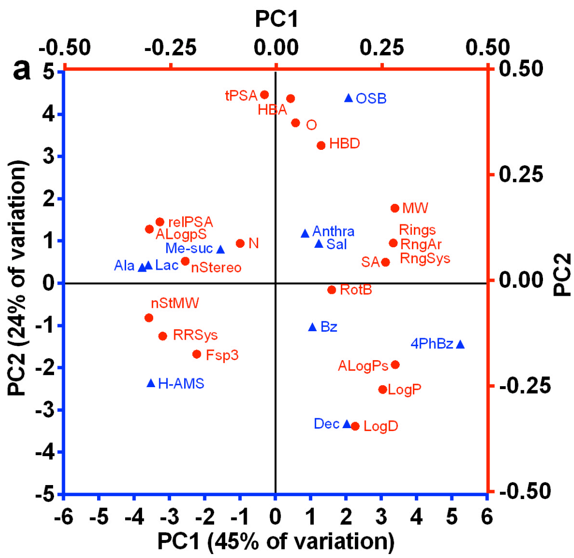

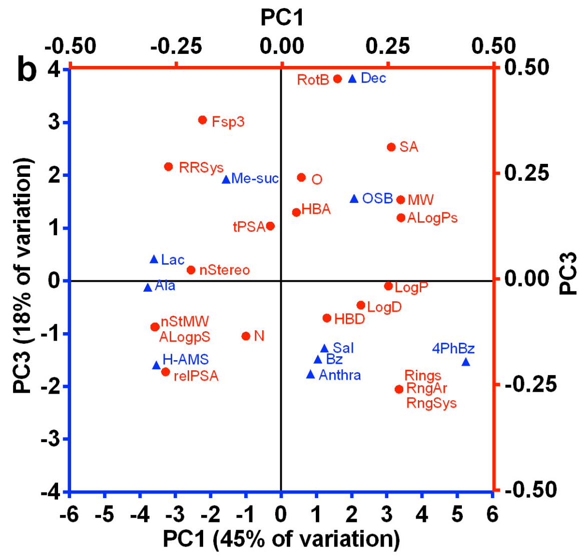

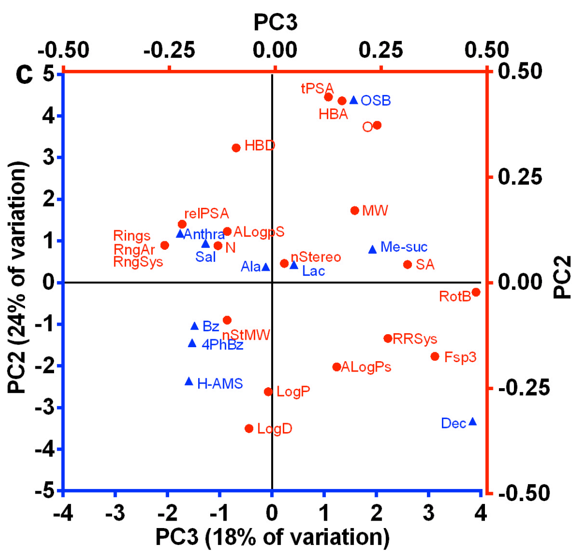

d

	PC1	PC2	PC3
MW	**0.2800**	0.1709	0.1879
SA	0.2576	0.0433	**0.3125**
N	-0.0858	0.0879	-0.1353
O	0.0450	**0.3732**	0.2407
HBD	0.1057	**0.3193**	-0.0922
HBA	0.0337	**0.4305**	0.1576
LogD	0.1862	**-0.3454**	-0.0618
LogP	0.2510	-0.2580	-0.0164
ALogPs	**0.2808**	-0.1993	0.1454
ALogpS	**-0.2998**	0.1214	-0.1131
tPSA	-0.0283	**0.4398**	0.1256
relPSA	-0.2754	0.1385	-0.2198
nStereo	-0.2154	0.0457	0.0216
nStMW	**-0.3012**	-0.0885	-0.1134
Fsp3	-0.1883	-0.1745	**0.3768**
RotB	0.1308	-0.0221	**0.4739**
Rings	**0.2761**	0.0885	**-0.2611**
RngAr	0.2761	0.0885	-0.2611
RngSys	0.2761	0.0885	-0.2611
RRSys	-0.2686	-0.1318	**0.2662**

Figure S7. PCA biplots indicate relationships between the 10 sulfonyladenosines and structural and physicochemical parameters. Combined PCA and loading plots: **(a)** PC1 vs. PC2, **(b)** PC1 vs. PC3, and **(c)** PC3 vs. PC2; percent contribution for each principal component is indicated on the axes; ▲ = sulfonyladenosine compounds; ● = physicochemical parameters. **(d)** Component loadings of 20 structural and physicochemical parameters on the first three principal components; the five most influential parameters for each principal component are highlighted (yellow).

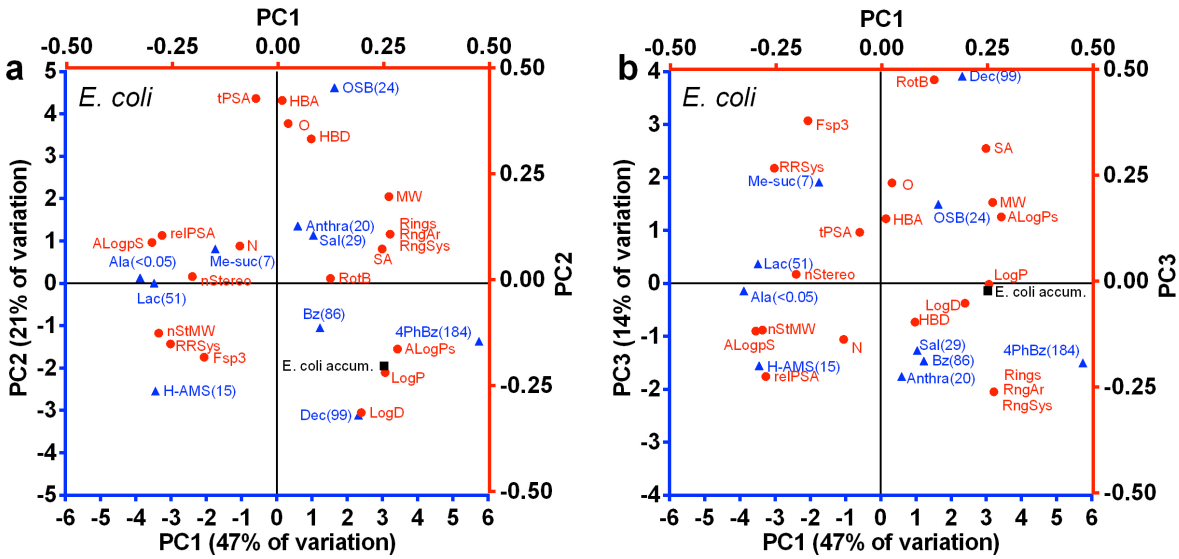

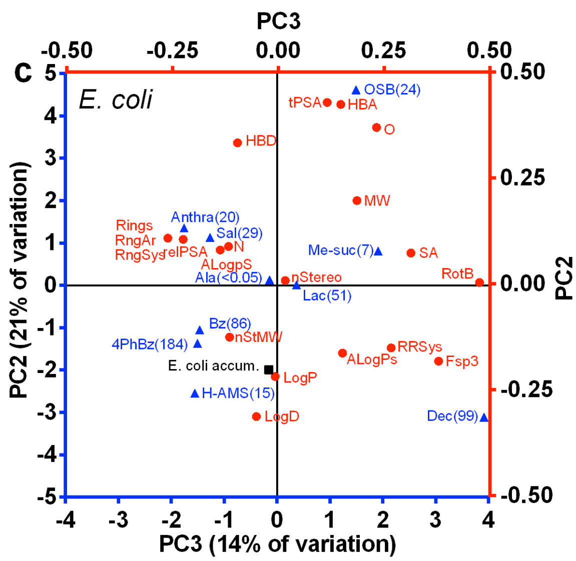

d

	PC1	PC2	PC3
MW	0.2623	0.1964	0.1860
SA	0.2463	0.0729	**0.3134**
N	-0.0904	0.0799	-0.1371
O	0.0239	**0.3691**	0.2323
HBD	0.0786	**0.3326**	-0.0963
HBA	0.0096	**0.4234**	0.1479
LogD	0.1968	**-0.3136**	-0.0518
LogP	0.2534	-0.2190	-0.0075
ALogPs	**0.2828**	-0.1636	0.1519
ALogpS	**-0.2981**	0.0882	-0.1178
tPSA	-0.0523	**0.4282**	0.1157
relPSA	**-0.2745**	0.1048	-0.2248
nStereo	-0.2027	0.0076	0.0163
nStMW	**-0.2825**	-0.1262	-0.1150
Fsp3	-0.1748	-0.1829	**0.3790**
RotB	0.1239	0.0030	**0.4758**
Rings	**0.2654**	0.1076	**-0.2611**
RngAr	0.2654	0.1076	-0.2611
RngSys	0.2654	0.1076	-0.2611
RRSys	-0.2543	-0.1515	**0.2667**
E. coli accum	0.2509	-0.2033	-0.0224

Figure S8. PCA biplots of sulfonyladenosine congeners indicate structural and physicochemical parameters that correlate with accumulation in *E. coli*. Combined PCA and loading plots of: **(a)** PC1 vs. PC2, **(b)** PC1 vs. PC3, and **(c)** PC3 vs. PC2; mean sulfonyladenosine intracellular concentrations (μM) are noted in parentheses; percent contribution for each principal component is indicated on the axes; ▲ = sulfonyladenosine compounds; ● = physicochemical parameters; ■ = accumulation parameters. **(d)** Component loadings of 21 structural, physicochemical, and accumulation parameters on the first three principal components; the five most influential parameters for each principal component are highlighted (yellow).

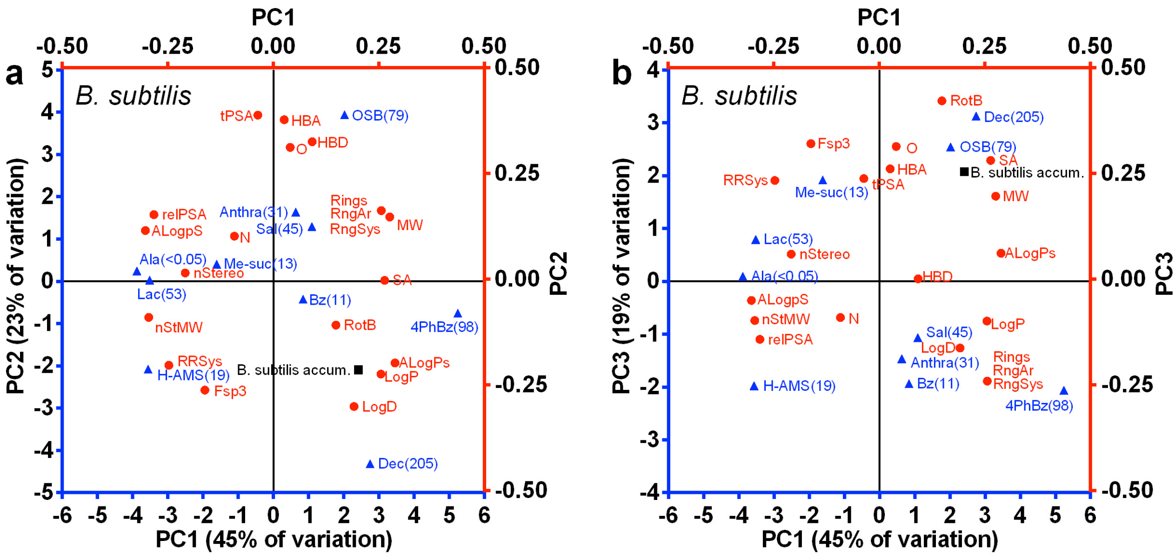

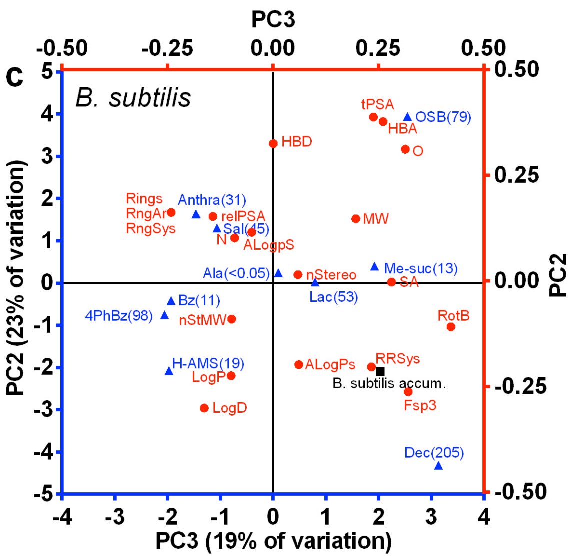

d

	PC1	PC2	PC3
MW	**0.2761**	0.1471	0.1966
SA	0.2640	-0.0029	**0.2811**
N	-0.0917	0.1020	-0.0905
O	0.0403	**0.3117**	**0.3139**
HBD	0.0921	**0.3252**	0.0010
HBA	0.0262	**0.3773**	**0.2611**
LogD	0.1916	**-0.3011**	-0.1626
LogP	0.2551	-0.2245	-0.0990
ALogPs	**0.2884**	-0.1980	0.0614
ALogpS	**-0.3028**	0.1151	-0.0501
tPSA	-0.0363	**0.3881**	0.2383
relPSA	**-0.2827**	0.1529	-0.1422
nStereo	-0.2086	0.0146	0.0592
nStMW	**-0.2946**	-0.0901	-0.0978
Fsp3	-0.1617	-0.2623	**0.3208**
RotB	0.1485	-0.1084	**0.4219**
Rings	0.2561	0.1621	-0.2412
RngAr	0.2561	0.1621	-0.2412
RngSys	0.2561	0.1621	-0.2412
RRSys	-0.2471	-0.2036	0.2336
B. subtilis accum	0.2020	-0.2145	0.2545

Figure S9. PCA biplots of sulfonyladenosine congeners indicate structural and physicochemical parameters that correlate with accumulation in *B. subtilis*. Combined PCA and loading plots of: **(a)** PC1 vs. PC2, **(b)** PC1 vs. PC3, and **(c)** PC3 vs. PC2; mean sulfonyladenosine intracellular concentrations (μM) are noted in parentheses; percent contribution for each principal component is indicated on the axes; ▲ = sulfonyladenosine compounds; ● = physicochemical parameters; ■ = accumulation parameters. **(d)** Component loadings of 21 structural, physicochemical, and accumulation parameters on the first three principal components; the five most influential parameters for each principal component are highlighted (yellow).

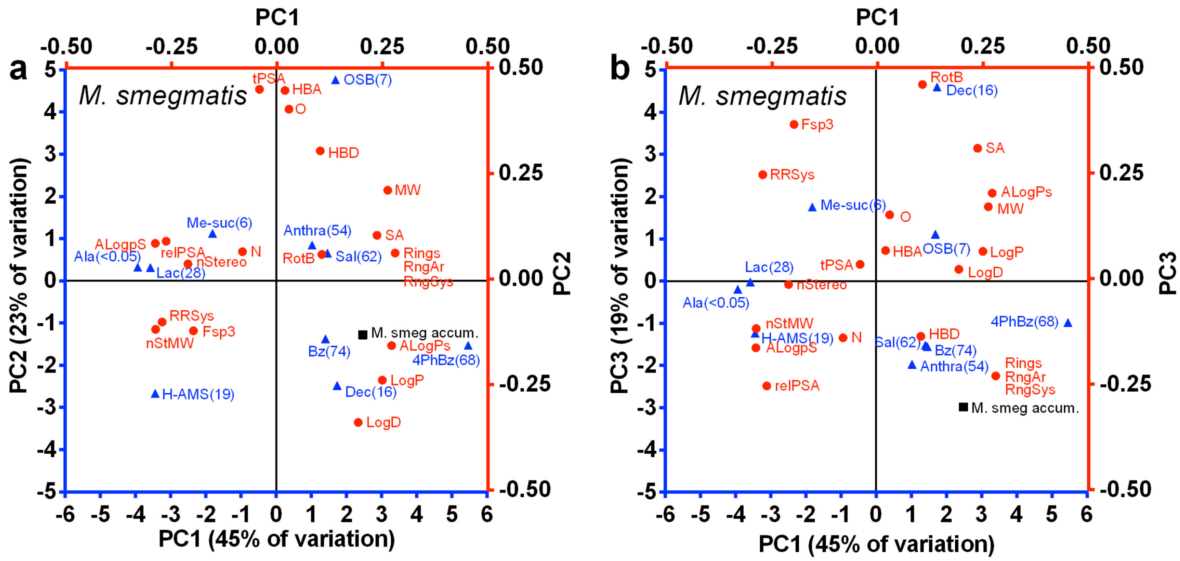

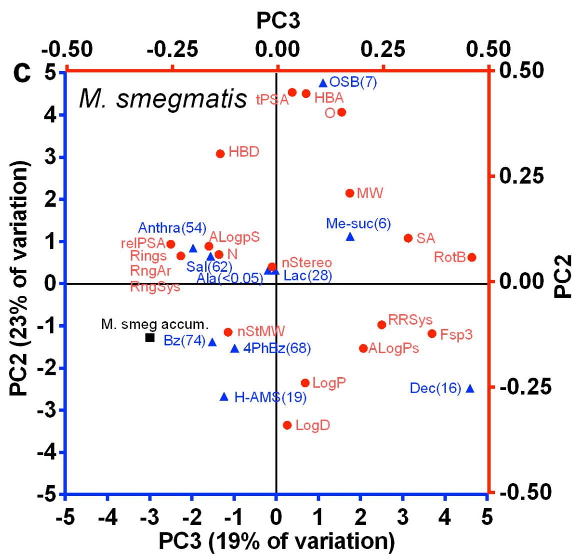

d

	PC1	PC2	PC3
MW	**0.2624**	0.2103	0.1707
SA	0.2369	0.1035	**0.3088**
N	-0.0821	0.0649	-0.1400
O	0.0280	**0.4021**	0.1516
HBD	0.1024	**0.3034**	-0.1365
HBA	0.0186	**0.4465**	0.0669
LogD	0.1925	**-0.3396**	0.0223
LogP	0.2492	-0.2399	0.0650
ALogPs	0.2713	-0.1578	0.2027
ALogpS	**-0.2890**	0.0843	-0.1634
tPSA	-0.0420	**0.4492**	0.0338
relPSA	-0.2632	0.0895	**-0.2540**
nStereo	-0.2115	0.0357	-0.0137
nStMW	**-0.2882**	-0.1192	-0.1183
Fsp3	-0.1986	-0.1225	**0.3657**
RotB	0.1061	0.0583	**0.4604**
Rings	**0.2800**	0.0615	-0.2302
RngAr	0.2800	0.0615	-0.2302
RngSys	0.2800	0.0615	-0.2302
RRSys	**-0.2729**	-0.1017	0.2465
***M. smeg.* Accum**	0.2031	-0.1325	**-0.3034**

Figure S10. PCA biplots of sulfonyladenosine congeners indicate structural and physicochemical parameters that correlate with accumulation in *M. smegmatis*. Combined PCA and loading plots of: **(a)** PC1 vs. PC2, **(b)** PC1 vs. PC3, and **(c)** PC3 vs. PC2; mean sulfonyladenosine intracellular concentrations (μM) are noted in parentheses; percent contribution for each principal component is indicated on the axes; ▲ = sulfonyladenosine compounds; ● = physicochemical parameters; ■ = accumulation parameters. **(d)** Component loadings of 21 structural, physicochemical, and accumulation parameters on the first three principal components; the five most influential parameters for each principal component are highlighted (yellow).

	MW	SA	N	O	HBD	HBA	LogD	LogP	ALogPs	ALogpS	tPSA	relPSA	nStereo	nStMW	Fsp3	RotB	Rings	RngAr	RngSys	RRSys
MW	**1.00**	**0.93**	-0.17	0.56	0.40	0.56	0.15	0.39	**0.67**	**-0.77**	0.37	**-0.77**	-0.38	-0.87	-0.35	0.62	0.61	0.61	0.61	-0.60
SA	**0.93**	**1.00**	-0.20	0.41	0.18	0.37	0.30	0.51	**0.80**	**-0.84**	0.18	**-0.90**	-0.35	**-0.81**	-0.03	**0.83**	0.37	0.37	0.37	-0.35
N	-0.17	-0.20	**1.00**	-0.27	0.22	0.15	-0.14	-0.20	-0.33	0.21	0.26	0.30	0.38	0.28	-0.03	-0.29	-0.08	-0.08	-0.08	0.04
O	0.56	0.41	-0.27	**1.00**	**0.43**	**0.88**	-0.61	-0.44	-0.13	0.04	0.82	-0.07	-0.04	-0.40	-0.09	0.40	0.05	0.05	0.05	-0.11
HBD	0.40	0.18	0.22	**0.43**	**1.00**	**0.63**	-0.19	0.03	-0.09	0.01	0.63	0.08	-0.33	-0.44	-0.52	-0.02	0.39	0.39	0.39	-0.53
HBA	0.56	0.37	0.15	**0.88**	**0.63**	**1.00**	**-0.66**	**-0.44**	-0.21	0.06	0.96	0.04	0.15	-0.29	-0.19	0.26	0.12	0.12	0.12	-0.21
LogD	0.15	0.30	-0.14	-0.61	-0.19	**-0.66**	**1.00**	**0.87**	**0.77**	**-0.65**	**-0.78**	**-0.64**	-0.42	-0.35	-0.09	0.14	0.35	0.35	0.35	-0.28
LogP	0.39	0.51	-0.20	-0.44	0.03	**-0.44**	**0.87**	**1.00**	**0.88**	**-0.81**	-0.57	**-0.73**	-0.59	-0.57	-0.20	0.33	0.50	0.50	0.50	-0.45
ALogPs	**0.67**	**0.80**	-0.33	-0.13	-0.09	-0.21	**0.77**	**0.88**	**1.00**	**-0.96**	-0.41	**-0.95**	-0.47	**-0.70**	-0.10	0.59	0.49	0.49	0.49	-0.41
ALogpS	**-0.77**	**-0.84**	0.21	0.04	0.01	0.06	**-0.65**	**-0.81**	**-0.96**	**1.00**	0.25	**0.94**	0.45	**0.75**	0.23	-0.56	-0.62	-0.62	-0.62	0.54
tPSA	0.37	0.18	0.26	0.82	0.63	0.96	**-0.78**	-0.57	-0.41	0.25	**1.00**	0.25	0.18	-0.15	-0.13	0.15	-0.01	-0.01	-0.01	-0.08
relPSA	**-0.77**	**-0.90**	0.30	-0.07	0.08	0.04	**-0.64**	**-0.73**	**-0.95**	**0.94**	0.25	**1.00**	0.44	**0.77**	0.04	**-0.72**	-0.42	-0.42	-0.42	0.36
nStereo	**-0.38**	-0.35	0.38	-0.04	-0.33	0.15	-0.42	-0.59	-0.47	0.45	0.18	0.44	**1.00**	**0.77**	0.39	-0.29	-0.45	-0.45	-0.45	0.49
nStMW	-0.87	**-0.81**	0.28	-0.40	-0.44	-0.29	-0.35	-0.57	**-0.70**	**0.75**	-0.15	**0.77**	**0.77**	**1.00**	0.45	-0.57	**-0.64**	**-0.64**	**-0.64**	**0.66**
Fsp3	-0.35	-0.03	-0.03	-0.09	-0.52	-0.19	-0.09	-0.20	-0.10	0.23	-0.13	0.04	0.39	0.45	**1.00**	0.45	**-0.90**	**-0.90**	**-0.90**	**0.94**
RotB	0.62	**0.83**	-0.29	0.40	-0.02	0.26	0.14	0.33	0.59	-0.56	0.15	**-0.72**	-0.29	-0.57	0.45	**1.00**	-0.15	-0.15	-0.15	0.16
Rings	0.61	0.37	-0.08	0.05	0.39	0.12	0.35	0.50	0.49	-0.62	-0.01	-0.42	-0.45	**-0.64**	**-0.90**	-0.15	**1.00**	**1.00**	**1.00**	**-0.98**
RngAr	0.61	0.37	-0.08	0.05	0.39	0.12	0.35	0.50	0.49	-0.62	-0.01	-0.42	-0.45	**-0.64**	**-0.90**	-0.15	**1.00**	**1.00**	**1.00**	**-0.98**
RngSys	0.61	0.37	-0.08	0.05	0.39	0.12	0.35	0.50	0.49	-0.62	-0.01	-0.42	-0.45	**-0.64**	**-0.90**	-0.15	**1.00**	**1.00**	**1.00**	**-0.98**
RRSys	-0.60	-0.35	0.04	-0.11	-0.53	-0.21	-0.28	-0.45	-0.41	0.54	-0.08	0.36	0.49	**0.66**	**0.94**	0.16	**-0.98**	**-0.98**	**-0.98**	**1.00**

Figure S11. Heatmap of Pearson pairwise correlation coefficients of 20 physicochemical properties from 10 sulfonyladenosine compounds used in bacterial compound accumulation assays reveal correlations between the physicochemical parameters. Positive correlations in red; negative correlations in blue; correlations in bold are statistically significant as assessed using two-tailed unpaired *t*-test and 95% confidence intervals ($p < 0.05$).

a

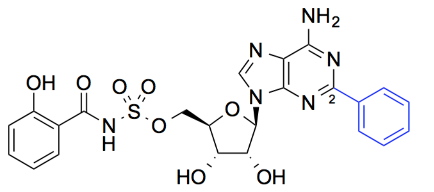

salicyl-(2-phenyl-AMS)

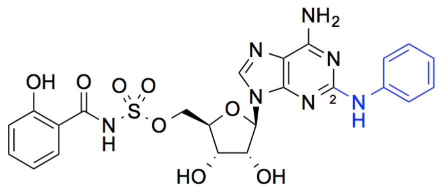

salicyl-(2-phenylamino-AMS)

	sal-AMS (1)	salicyl-(2-phenyl-AMS)	salicyl-(2-phenylamino-AMS)
MW	466	543	558
SA	563	671	688
N	6	6	7
O	8	8	8
HBD	5	5	6
HBA	12	12	13
LogD	-1.43	0.75	0.69
LogP	-2.11	1.88	1.52
ALogPs	-0.44	1.58	1.81
ALogpS	-2.21	-3.06	-3.16
tPSA	212	212	224
relPSA	38	32	33
nStereo	4	4	4
nStMW ‡	8.6	7.4	7.2
Fsp3	0.29	0.22	0.22
RotB	5	6	7
Rings	4	5	5
RngAr	3	4	4
RngLg	6	6	6
RngSys	3	4	4
RRSys	1.33	1.25	1.25

‡ For clarity, values shown are [nStMW x 1000]

b

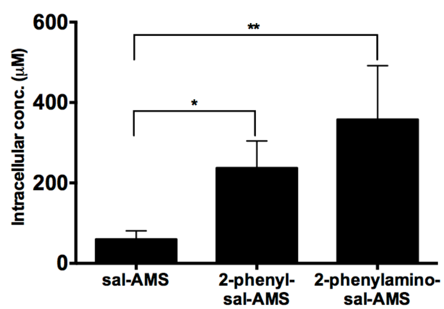

Figure S12. Accumulation of C2-substituted salicyl-AMS analogues in *E. coli* is consistent with correlations identified using sulfonyladenosine variants in the acyl region. (a) Structures and physicochemical properties of C2-subsituted sulfonyladenosines, synthesized as previously described.[3d] **(b)** Accumulation of C2-subsituted sulfonyladenosines in *E. coli* (100 μM extracellular, 30 min, LB media). Data are reported as mean ± SD for 4 experiments. Statistical significance was assessed relative to cells treated with salicyl-AMS using one-way ANOVA and Tukey's multiple comparison test and 95% confidence intervals: * $p < 0.05$, ** $p < 0.01$.

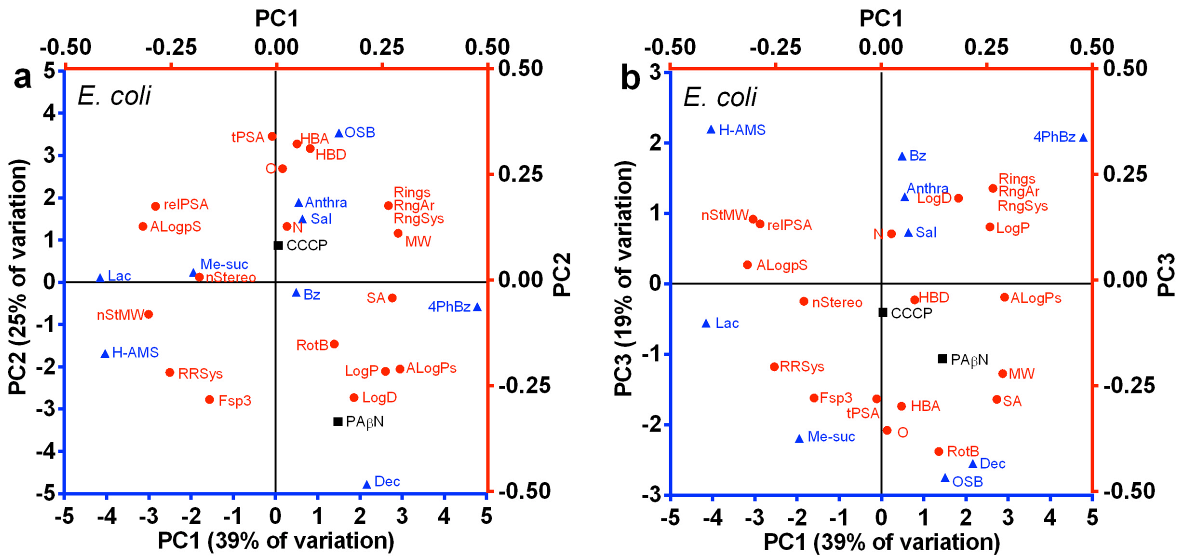

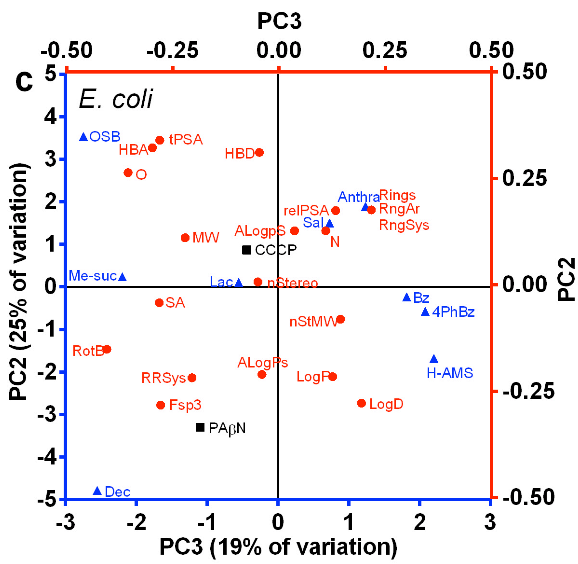

d

	PC1	PC2	PC3
MW	**0.2875**	0.1112	-0.2212
SA	0.2739	-0.0418	**-0.2819**
N	0.0242	0.1275	0.1099
O	0.0139	0.2640	**-0.3553**
HBD	0.0793	**0.3116**	-0.0466
HBA	0.0480	**0.3224**	**-0.2981**
LogD	0.1830	**-0.2776**	0.1940
LogP	0.2578	-0.2156	0.1262
ALogPs	**0.2922**	-0.2104	-0.0403
ALogpS	**-0.3170**	0.1275	0.0364
tPSA	-0.0105	**0.3403**	**-0.2806**
relPSA	**-0.2867**	0.1746	0.1332
nStereo	-0.1831	0.0071	-0.0496
nStMW	**-0.3034**	-0.0807	0.1443
Fsp3	-0.1588	**-0.2824**	-0.2787
RotB	0.1364	-0.1511	**-0.4053**
Rings	0.2648	0.1763	0.2175
RngAr	0.2648	0.1763	0.2175
RngSys	0.2648	0.1763	0.2175
RRSys	-0.2532	-0.2182	-0.2046
CCCP	0.0041	0.0822	-0.0759
PAβN	0.1452	-0.3343	-0.1856

Figure S13. PCA biplots of sulfonyladenosine congeners indicate structural and physicochemical parameters that correlate with efflux sensitivity in *E. coli*. Combined PCA and loading plots of: **(a)** PC1 vs. PC2, **(b)** PC1 vs. PC3, and **(c)** PC3 vs. PC2; percent contribution for each principal component is indicated on the axes; ▲ = sulfonyladenosine compounds; ● = physicochemical parameters; ■ = efflux parameters (calculated for each compound as relative accumulation level compared to concentration in the absence of the efflux pump inhibitor). **(d)** Component loadings of 22 structural, physicochemical, and efflux parameters on the first three principal components; the five most influential parameters for each principal component are highlighted (yellow).

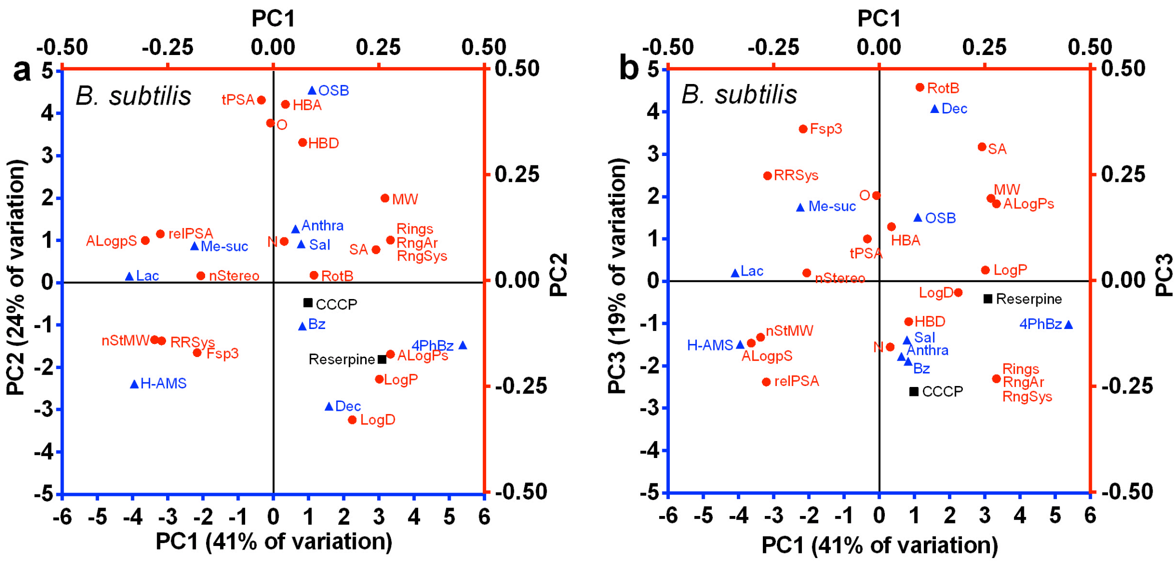

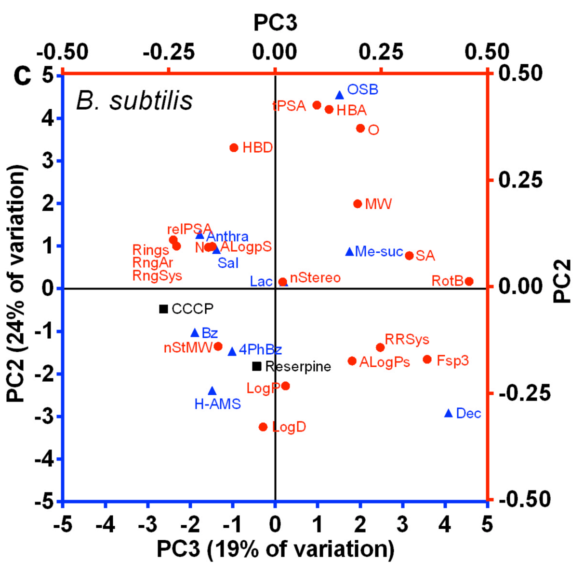

d

	PC1	PC2	PC3
MW	0.2646	0.1947	0.1943
SA	0.2436	0.0730	0.3161
N	0.0261	0.0926	-0.1568
O	-0.0063	**0.3724**	0.2010
HBD	0.0699	**0.3263**	-0.0967
HBA	0.0288	**0.4166**	0.1273
LogD	0.1871	**-0.3288**	-0.0283
LogP	0.2513	-0.2325	0.0249
ALogPs	**0.2776**	-0.1739	0.1813
ALogpS	**-0.3033**	0.0947	-0.1479
tPSA	-0.0280	**0.4266**	0.0984
relPSA	**-0.2672**	0.1103	-0.2394
nStereo	-0.1713	0.0115	0.0180
nStMW	**-0.2810**	-0.1399	-0.1341
Fsp3	-0.1801	-0.1704	**0.3582**
RotB	0.0966	0.0126	**0.4567**
Rings	**0.2777**	0.0957	**-0.2318**
RngAr	0.2777	0.0957	-0.2318
RngSys	0.2777	0.0957	-0.2318
RRSys	-0.2644	-0.1421	**0.2479**
CCCP	0.0825	-0.0524	**-0.2623**
Reserpine	0.2579	-0.1864	-0.0433

Figure S14. PCA biplots of sulfonyladenosine congeners indicate structural and physicochemical parameters that correlate with efflux sensitivity in *B. subtilis*. Combined PCA and loading plots of: **(a)** PC1 vs. PC2, **(b)** PC1 vs. PC3, and **(c)** PC3 vs. PC2; percent contribution for each principal component is indicated on the axes; ▲ = sulfonyladenosine compounds; ● = physicochemical parameters; ■ = efflux parameters (calculated for each compound as relative accumulation level compared to concentration in the absence of the efflux pump inhibitor). **(d)** Component loadings of 22 structural, physicochemical, and efflux parameters on the first three principal components; the five most influential parameters for each principal component are highlighted (yellow).

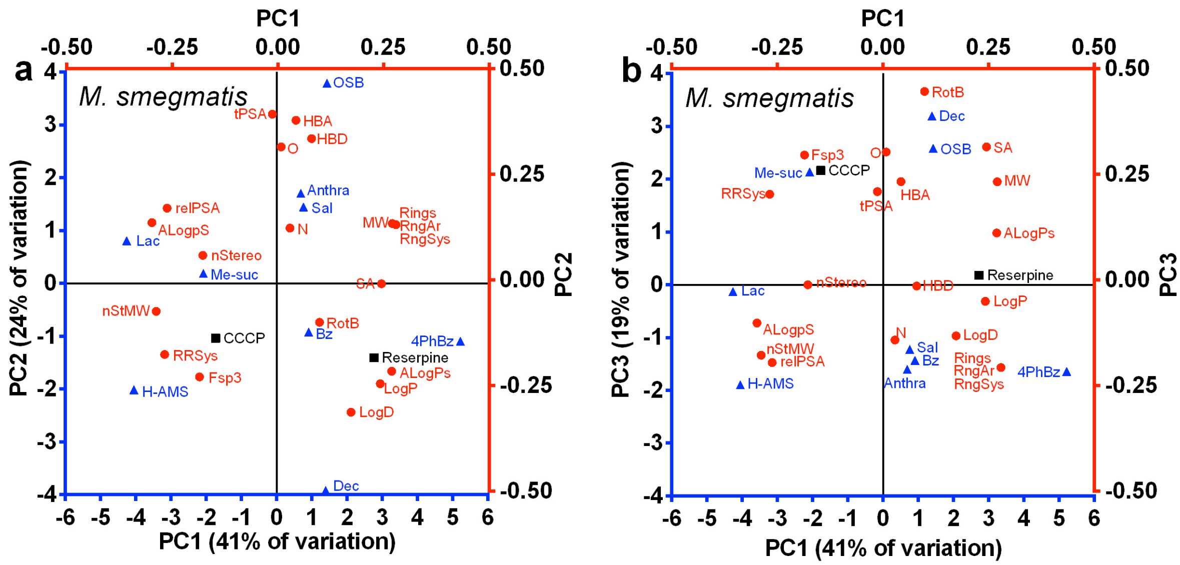

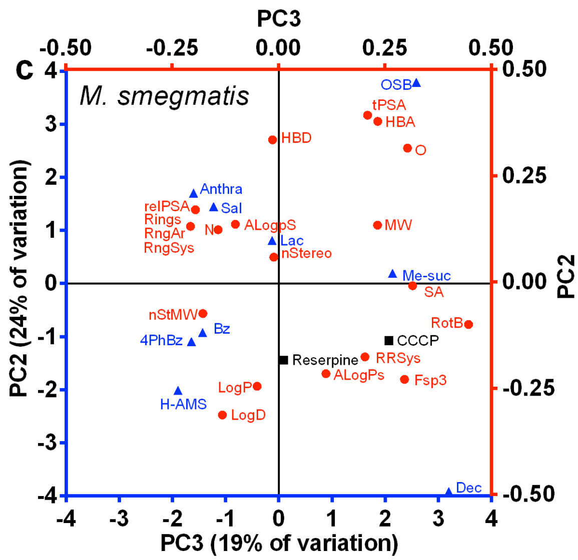

d

	PC1	PC2	PC3
MW	**0.2705**	0.1340	0.2325
SA	0.2453	-0.0085	**0.3154**
N	0.0286	0.1232	-0.1417
O	0.0076	**0.3153**	0.3031
HBD	0.0799	**0.3346**	-0.0141
HBA	0.0427	**0.3780**	**0.2333**
LogD	0.1733	**-0.3129**	-0.1318
LogP	0.2421	-0.2453	-0.0503
ALogPs	0.2695	-0.2156	0.1113
ALogpS	**-0.2983**	0.1359	-0.1014
tPSA	-0.0130	**0.3926**	0.2092
relPSA	**-0.2625**	0.1703	-0.1954
nStereo	-0.1775	0.0584	-0.0111
nStMW	**-0.2883**	-0.0739	-0.1776
Fsp3	-0.1857	-0.2291	**0.2961**
RotB	0.0986	-0.0999	**0.4463**
Rings	**0.2793**	0.1309	-0.2068
RngAr	0.2793	0.1309	-0.2068
RngSys	0.2793	0.1309	-0.2068
RRSys	-0.2683	-0.1760	0.2030
CCCP	-0.1471	-0.1377	**0.2593**
Reserpine	0.2274	-0.1835	0.0113

Figure S15. PCA biplots of sulfonyladenosine congeners indicate structural and physicochemical parameters that correlate with efflux sensitivity in *M. smegmatis*. Combined PCA and loading plots of: **(a)** PC1 vs. PC2, **(b)** PC1 vs. PC3, and **(c)** PC3 vs. PC2; percent contribution for each principal component is indicated on the axes; ▲ = sulfonyladenosine compounds; ● = physicochemical parameters; ■ = efflux parameters (calculated for each compound as relative accumulation level compared to concentration in the absence of the efflux pump inhibitor). **(d)** Component loadings of 22 structural, physicochemical, and efflux parameters on the first three principal components; the five most influential parameters for each principal component are highlighted (yellow).

B. Supporting Information Tables S1–S4

Table S1. Non-antiinfective drugs and antibacterials used in PCA

Series	Compounds				
Top-selling Non-antiinfective Drugs (50 entries)	Nexium	Diovan	MethylphenidateER	Flovent	Lexapro
	Abilify	Lyrica	Androgel	Budesonide	Benicar
	Crestor	Lipitor	Lidoderm	Cialis	Lunesta
	Advair	Celebrex	Atorvastatin	Aciphex	Evista
	Cymbalta	Gleevec	Tricor	AderallXR	Enoxaparin
	Singulair	Namenda	Alimta	Restasis	Synthroid
	Plavix	Actos	Viagra	Pradaxa	Xeloda
	Spiriva	Vyvanse	ProairHFA	Gilenya	Ventolin HFA
	Oxycontin	Seroquel	Niaspan	Vesicare	Velcade
	Januvia	Zetia	Nasonex	Dexilant	Sensipar
β-Lactams (38 entries)	Amoxicillin	Cefditoren pivoxil	Cefpiramide	Cloxacillin	Methicilin
	Ampicillin	Cefepime	Cefprozil	Dicloxacillin	Mezlocillin
	Azlocillin	Cefixime	Ceftaroline fosamil	Ertapenem	Oxacillin
	Carbenicillin	Cefmenoxime	Ceftazidime	Flucloxacillin	Penicillin G
	Cefaclor	Cefmetazole	Ceftriaxone	Hetacillin	Penicillin V
	Cefadroxil	Ceforanide	Cefuroxime	Loracarbef	Piperacillin
	Cefalotin	Cefotaxime	Cephalexin	Meropenem	Ticarcillin
	Cefdinir	Cefotiam	Clavulanate		
Peptides (4 entries)	Colistin	Daptomycin	Vancomycin	Telavancin	
Aminoglycosides (7 entries)	Gentamicin	Kanamycin	Netilmicin	Streptomycin	Tobramycin
	Amikacin	Neomycin			
Quinolones (15 entries)	Besifloxacin	Gatifloxacin	Levofloxacin	Nalidixic acid	Perfloxacin
	Ciprofloxacin	Gemifloxacin	Lomefloxacin	Norfloxacin	Sparfloxacin
	Enoxacin	Grepafloxacin	Moxifloxacin	Ofloxacin	Trovafloxacin
Macrolides (7 entries)	Azithromycin	Dirithromycin	Fidaxomicin	Roxithromycin	Telithromycin
	Clarithromycin	Erythromycin			
Tetracyclines (7 entries)	Oxytetracycline	Demeclocycline	Minocycline	Tetracycline	Tigecycline
	Clomocycline	Doxycycline			
Oxazolidinones (2 entries)	Linezolid	Ranbezolid			
Tuberculosis Drugs (5 entries)	Bedaquiline	Ethambutol	Isoniazid	Pyrazinamide	Rifampicin
Sulfa Drugs (6 entries)	Sulfadiazine	Sulfamethoxazole	Sulfanilamide	Sulfapyridine	Tinidazole
	Sulfamethizole				

Table S2. Structural and physicochemical properties used in PCA

Parameter	Description	Method of Determination
MW	molecular weight	Instant JChem
SA	surface area	Instant JChem
N	number of nitrogens	Instant JChem
O	number of oxygens	Instant JChem
HBD	number of hydrogen bond donors	Instant JChem
HBA	number of hydrogen bond acceptors	Instant JChem
LogD	calc *n*-octanol/water partition coefficient (pH 7.4)	Instant JChem
LogP	calc *n*-octanol/water partition coefficient	Instant JChem
ALogPs	calc *n*-octanol/water partition coefficient (Tetko)	http://www.vcclab.org
ALogpS	calc aqueous solubility (Tetko)	http://www.vcclab.org
tPSA	topological polar surface area	Instant JChem
relPSA	tPSA ÷ SA	Instant JChem
nStereo	number of chiral atoms	Instant JChem
nStMW	nStereo ÷ MW (stereochemical density)	Instant JChem
Fsp3	number of sp3 carbons ÷ number of carbons	Instant JChem
RotB	# rotatable bonds	Instant JChem
Rings	number of rings	Instant JChem
RngAr	number of aromatic rings	Instant JChem
RngLg	number of atoms in largest ring	Instant JChem
RngSys	number of ring systems	Instant JChem
RRSys	Rings ÷ RngSys (ring complexity)	Instant JChem

Table S3. Average structural and physicochemical properties by compound class.

	Non-antiinfective Drugs	Sulfonyladenosines	All antibacterials	β-Lactams	Peptides	Aminoglycoside	Quinolones	Macrolides	Tetracyclines	Oxazolidinones	Tuberculosis Drugs	Sulfa Drugs
MW	417.21	477.33	493.34	440.57	1495.25	526.72	355.92	813.56	480.88	399.39	368.60	240.44
SA	593.38	597.80	664.30	538.55	2083.50	743.00	473.87	1327.71	613.71	562.00	539.60	321.83
N	2.46	6.32	4.07	4.29	13.25	5.29	3.27	1.29	2.57	4.00	2.80	3.17
O	3.94	7.88	6.86	5.63	22.50	10.29	3.33	14.00	8.14	5.00	3.60	2.50
HBD	2.04	4.48	4.45	3.03	20.50	10.71	1.80	5.14	6.29	1.00	2.80	1.67
HBA	4.96	11.84	8.88	7.16	24.50	15.43	6.60	14.00	9.57	6.00	5.60	4.33
LogD	1.35	-2.44	-3.23	-3.51	-12.06	-13.14	-0.33	1.86	-4.86	1.06	0.84	-0.17
LogP	2.82	-2.62	-1.12	-1.04	-7.01	-6.32	-0.08	3.63	-3.68	1.08	1.59	0.26
ALogP	2.72	-0.53	0.44	0.63	0.42	-2.51	-0.04	3.19	-0.31	1.06	1.74	0.31
ALogS	-4.00	-2.41	-2.99	-3.32	-4.39	-1.14	-2.87	-3.61	-2.71	-2.89	-2.58	-2.36
tPSA	90.36	213.24	163.99	143.13	580.32	281.67	81.97	204.38	186.42	97.60	93.43	93.87
relPSA	14.58	36.08	25.34	26.72	27.90	37.85	17.40	15.35	30.78	17.02	23.76	29.57
nStereo	2.50	4.16	5.13	3.00	15.50	14.71	0.93	17.71	5.00	1.00	2.60	0.00
nStMW ‡	5.54	8.86	8.86	7.20	10.49	27.90	2.41	22.26	10.56	2.57	4.87	0.00
Fsp3	0.44	0.43	0.47	0.40	0.57	0.96	0.42	0.91	0.43	0.46	0.35	0.14
RotB	6.62	5.80	6.31	6.00	26.50	7.86	3.07	9.86	3.00	5.50	4.80	2.33
Rings	3.16	3.80	3.47	3.50	6.25	3.14	3.73	3.29	4.00	3.50	2.40	1.67
RngAr	1.98	2.60	1.36	1.32	3.25	0.00	2.07	0.14	1.00	1.50	1.80	1.67
RngLg	6.44	7.04	7.45	5.92	21.50	6.00	6.07	14.71	6.00	6.00	8.40	5.83
RngSys	2.22	2.56	2.42	2.50	3.25	3.14	2.47	3.14	1.00	3.50	1.40	1.67
RRSys	1.60	1.69	1.55	1.43	1.83	1.00	1.56	1.05	4.00	1.00	1.23	1.00

‡ For clarity, values shown are [nStMW x 1000]

Table S4. Structural and physicochemical properties of sulfonyladenosines evaluated in bacterial compound accumulation assays

	H-AMS (2)	L-ala-AMS (3)	L-lac-AMS (4)	Me-suc-AMS (5)	anthra-AMS (6)	OSB-AMS (7)	sal-AMS (1)	Bz-AMS (8)	4-PhBz-AMS (9)	dec-AMS (10)
MW	346	417	418	460	465	550	466	450	526	500
SA	450	523	519	583	567	679	563	554	661	725
N	6	7	6	6	7	6	6	6	6	6
O	6	7	8	9	7	10	8	7	7	7
HBD	4	4	4	4	5	5	5	4	4	4
HBA	10	12	12	12	12	14	12	11	11	11
LogD	-2.61	-3.91	-3.85	-3.60	-1.89	-5.41	-1.43	-1.71	-0.07	0.25
LogP	-2.61	-3.90	-4.66	-4.33	-2.58	-3.30	-2.11	-2.41	-0.76	-0.49
ALogPs	-1.26	-1.36	-1.23	-0.97	-0.70	-0.49	-0.44	-0.35	1.25	1.37
ALogpS	-1.77	-1.96	-1.87	-2.05	-2.40	-2.61	-2.21	-2.47	-3.54	-3.26
tPSA	189	218	212	218	218	246	212	195	192	192
relPSA	45	42	41	37	38	36	38	35	29	26
nStereo	4	5	5	4	4	4	4	4	4	4
nStMW ‡	11.6	12	12	8.7	8.6	7.3	8.6	8.9	7.6	8
Fsp3	0.50	0.54	0.54	0.53	0.29	0.33	0.29	0.29	0.22	0.70
RotB	4	5	5	8	5	9	5	5	6	12
Rings	3	3	3	3	4	4	4	4	5	3
RngAr	2	2	2	2	3	3	3	3	4	2
RngLg	6	6	6	6	6	6	6	6	6	6
RngSys	2	2	2	2	3	3	3	3	4	2
RRSys	1.50	1.50	1.50	1.50	1.33	1.33	1.33	1.33	1.25	1.50

‡ For clarity, values shown are [nStMW x 1000]

Physicochemical properties shown are for the non-ionized forms of sulfonyladenosines (as shown in **Figure 3** of the manuscript), because the algorithm used to compute ALogPs and ALogpS (vcclab.org) of the ionized compounds as they would exist at pH 7.4 neutralizes the negatively charged sulfamate nitrogen by addition of an ammonium counterion: for OSB-AMS, the algorithm adds two ammonium counterions to neutralize both the sulfamate and the carboxylate; for L-alanyl-AMS, the algorithm adds ammonium and chloride to neutralize the sulfamate and positively charge amine, respectively. Computation of the physicochemical properties of compounds in their ionized state at pH 7.4 did not substantially change the values. The largest observed differences between the non-ionized and pH 7.4 ionized compounds were the ALogPs values for L-alanyl-AMS (ALogPs –1.03 for ionized form vs. –1.36 for non-ionized form) and OSB-AMS (ALogPs 0.19 for ionized form vs. –0.49 for non-ionized form).

C. Materials and Methods

Reagents

Reagents were obtained from Aldrich Chemical (www.sigma-aldrich.com) or Acros Organics (www.fishersci.com) and used without further purification. Phenylalanine-arginine-beta-naphthylamide (PAβN) was purchased from MP Biomedicals. Optima or HPLC grade solvents were obtained from Fisher Scientific (www.fishersci.com), degassed with Ar, and purified on a solvent drying system as described[1] unless otherwise indicated.

Reactions

All reactions were performed in flame-dried glassware under positive Ar pressure with magnetic stirring unless otherwise noted. Liquid reagents and solutions were transferred through rubber septa via syringes flushed with Ar prior to use. Cold baths were generated as follows: 0 °C, wet ice/water; –10 °C, wet ice/brine; –20 °C, dry ice/isopropanol monitored with a thermometer; –44 °C, dry ice/CH_3CN; –63 °C, dry ice/chloroform; –78 °C, dry ice/acetone; –100 °C, dry ice/Et_2O.

Chromatography

TLC was performed on 0.25 mm E. Merck silica gel 60 F254 plates and visualized under UV light (254 nm) or by staining with potassium permanganate ($KMnO_4$), cerium ammonium molybdenate (CAM), phosphomolybdic acid (PMA), iodine (I_2), or *p*-anisaldehyde. Silica flash chromatography was performed on E. Merck 230–400 mesh silica gel 60. Lyophilization of small aqueous samples was performed using a GeneVac HT-4X centrifugal evaporator. Lyophilization of larger aqueous samples was performed using a Labconco Freezone 2.5 instrument.

Analytical Instrumentation

IR spectra were recorded on a Bruker Optics Tensor 27 FTIR spectrometer with peaks reported in cm^{-1}. NMR spectra were recorded on a Bruker UltraShield Plus 500 MHz Avance III NMR or UltraShield Plus 600 MHz Avance III NMR with DCH CryoProbe at 24 °C in $CDCl_3$ unless otherwise indicated. Chemical shifts are expressed in ppm relative to TMS (^1H, 0 ppm) or solvent signals: $CDCl_3$ (^{13}C, 77.0 ppm), C_6D_6 (^1H, 7.16 ppm; ^{13}C, 128.0 ppm) or acetone-d_6 (^{13}C, 206.2 ppm); coupling constants are expressed in Hz. NMR spectra were processed using Bruker TopSpin or nucleomatica iNMR (www.inmr.net) software. Mass spectra were obtained at the MSKCC Analytical Core Facility on a Waters Acuity SQD LC-MS or PE SCIEX API 100 by electrospray (ESI) ionization or atmospheric pressure chemical ionization (AP-CI). High resolution mass spectra were obtained on a Waters Acuity Premiere XE TOF LC-MS by electrospray ionization.

Liquid chromatography tandem mass spectrometry (LC-MS/MS) was carried out on an Agilent Technologies 6410 triple quad LC-MS/MS system with autosampler in electrospray ionization (ESI) mode, with an Agilent Zorbax Eclipse XDB-C18 reverse phase column (50 × 4.6 mm, 5 µm) using a flow rate of 0.4 mL/min and an isocratic mobile phase of CH_3CN in 0.1% aq formic acid (mixture optimized for each analyte, see **Table S5**) over 5 min.

---

[1] Pangborn, A. B.; Giardello, M. A.; Grubbs, R. H.; Rosen, R. K.; Timmers, F. J. *Organometallics* **1996,** *15*, 1518–1520.

Nomenclature

Atom numbers shown in chemical structures herein correspond to the standard nucleoside numbering system used in the text of the article and Supporting Information and not to IUPAC nomenclature, which was used solely to name each compound. Compounds not cited in the paper are numbered herein from **S1**.

Microbiology

*Bacillus subtilis subtilis (*ATCC 6051) was cultured at 30 °C in Lennox LB broth (Fisher). *Escherichia coli* (ATCC 25922) was cultured at 37 °C in tryptic soy broth (BD Biosciences). *Mycobacterium smegmatis* (ATCC 700084) was cultured at 37 °C in Middlebrook 7H9 (BD Biosciences) supplemented with 0.1% Tween and 10% ADN (5% BSA, 2% dextrose, 0.85% NaCl).[2]

---

[2] Tatham, E.; Sundaram Chavadi, S.; Mohandas, P.; Edupuganti, U. R.; Angala, S. K.; Chatterjee, D.; Quadri, L. E. *BMC Microbiol* **2012**, *12*, 118.

D. Synthesis of acyl-AMS Analogues (2-10)

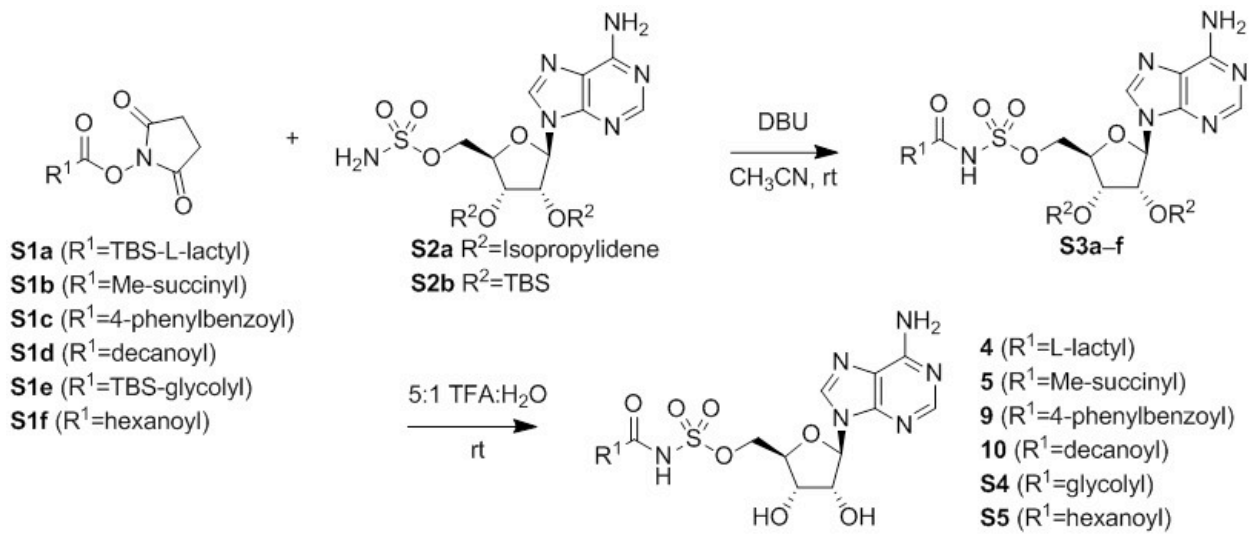

Figure S16. General synthetic approach to access acyl-AMS derivatives not previously reported in the literature. (TBS = t-butyldimethylsilyl; DBU = 1,8-Diazabicyclo[5.4.0]undec-7-ene; TFA = 2,2,2-trifluoroacetic acid)

Salicyl-AMS (**1**), sulfamoyladenosine (**2**), L-alanyl-AMS (**3**), anthranilyl-AMS (**6**), OSB-AMS (**7**), benzoyl-AMS (**8**), glycyl-AMS (**Figure S17**), 2-phenyl-salicyl-AMS, and 2-phenylamino-salicyl-AMS were prepared as previously described.[3]

General procedure for preparation of N-hydroxysuccinamide esters S1a–f

N-hydroxysuccinamide esters **S1a–f** were prepared using the procedures described by Anderson, *et al*.[4]

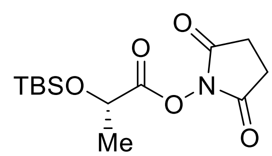

2,5-Dioxopyrrolidin-1-yl(S)-2-((tert-butyldimethylsilyl)oxy)propanoate (S1a). Synthesized from (S)-2-((tert-butyldimethylsilyl)oxy)propanoic acid,[5] white solid (421 mg, 57%). **TLC**: R_f 0.56 (1:1 hexanes/EtOAc). **IR** (ZnSe, film): 2954, 1819, 1788, 1743, 1364, 1257, 1207, 1109, 1085, 1067, 968, 913, 836, 815, 783, 735. **^{1}H-NMR** (500 MHz): δ 4.65 (q, J = 6.8 Hz, 1H), 2.83 (s, 4H), 1.58 (d, J = 6.8 Hz, 3H), 0.92 (s, 9H), 0.13 (d, J = 6.5 Hz, 6H). **^{13}C-NMR** (125 MHz): δ 169.70, 169.00, 67.05, 25.84, 25.72, 21.80, 18.42, -5.20. **ESI-MS** *m/z* (rel int):

---

[3] (a) Ferreras, J. A.; Ryu, J. S.; Di Lello, F.; Tan, D. S.; Quadri, L. E. *Nat. Chem. Biol.* **2005**, *1*, 29. (b) Cisar, J. S.; Ferreras, J. A.; Soni, R. K.; Quadri, L. E.; Tan, D. S. *J. Am. Chem. Soc.* **2007**, *129*, 7752. (c) Qiao, C.; Gupte, A.; Boshoff, H. I.; Wilson, D. J.; Bennett, E. M.; Somu, R. V.; Barry, C. E.; Aldrich, C. C. *J. Med. Chem.* **2007**, *50*, 6080. (d) Lu, X.; Zhou, R.; Sharma, I.; Li, X.; Kumar, G.; Swaminathan, S.; Tonge, P. J.; Tan, D. S. *Chembiochem* **2012**, *13*, 129. (d) Neres, J., Labello, N. P., Somu, R. V., Boshoff, H. I., Wilson, D. J., Vannada, J., Chen, L., Barry, C. E., Bennett, E. M., and Aldrich, C. C. *J. Med. Chem.* **2008**, 51, 5349.

[4] Anderson, G. W.; Zimmerman, J. E.; Callahan, F. M. *J. Am. Chem. Soc.* **1964**, *86*, 1839.

[5] Blonski, C.; Gefflaut, T.; Perie, J. *Bioorg Med Chem* **1995**, *3*, 1247.

(pos) 324.3 ([M+Na]$^+$, 100); (neg) 300.3 ([M–H]$^-$, 100). **HRMS** *m/z* calcd for $C_{13}H_{23}NO_5NaSi$ ([M+H]$^+$) 324.1251; found 324.1243.

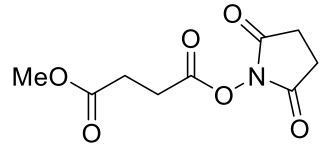

2,5-Dioxopyrrolidin-1-yl methyl succinate (S1b). Synthesized from methyl succinate, white solid (795.0 mg, 92%). **TLC**: R_f 0.24 (1:1 hexanes/EtOAc). **IR** (ZnSe, film): 2954, 2933, 2857, 1815, 1784, 1738, 1438, 1365, 1206, 1093, 1071, 996, 843, 747, 702. **^{1}H-NMR** (500 MHz): δ 3.72 (d, *J* = 2.5 Hz, 3H), 2.95 (td, *J* = 7.0, 2.3 Hz, 2H), 2.83 (s, 4H), 2.75 (td, *J* = 7.0, 2.4 Hz, 2H). **^{13}C-NMR** (125 MHz): δ 171.6, 169.1, 167.9, 52.4, 28.8, 26.6, 25.8. **ESI-MS** *m/z* (rel int): (pos) 252.0 ([M+Na]$^+$, 100), 267.9 ([M+K]$^+$, 20), 481.1 ([2M+Na]$^+$, 5). **HRMS** *m/z* calcd for $C_9H_{11}NO_6Na$ ([M+Na]$^+$) 252.0484; found 252.0485.

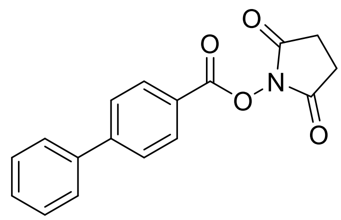

2,5-Dioxopyrrolidin-1-yl[1,1'-biphenyl]-4-carboxylate (S1c). Synthesized from 4-phenylbenzoic acid, white solid (414.9 mg, 56%). **TLC**: R_f 0.13 (3:1 hexanes/EtOAc). **IR** (ZnSe, film): 2952, 2930, 2856, 1770, 1740, 1606, 1367, 1258, 1248, 1211, 1707, 999, 848, 838, 778, 741. **^{1}H-NMR** (500 MHz): δ 8.20 (dd, *J* = 8.3, 3.4 Hz, 2H), 7.73 (dd, *J* = 8.1, 3.3 Hz, 2H), 7.65-7.63 (m, 2H), 7.51-7.47 (m, 2H), 7.44-7.42 (m, 1H), 2.92 (s, 4H). **^{13}C-NMR** (125 MHz): δ 169.5, 162.0, 147.9, 139.7, 131.4, 129.3, 128.9, 127.72, 127.61, 124.0, 26.0.

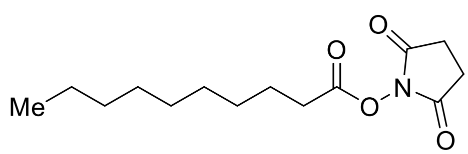

2,5-Dioxopyrrolidin-1-yl decanoate (S1d). Synthesized from decanoic acid, white solid (864.0 mg, 84%). **TLC**: R_f 0.26 (3:1 hexanes/EtOAc). **IR** (ZnSe, film): 2955, 2923, 1853, 1787, 1727, 1378, 1212, 1073, 997, 912, 869, 815, 736. **^{1}H-NMR** (500 MHz): δ 2.83 (d, *J* = 0.6 Hz, 4H), 2.60 (t, *J* = 7.5 Hz, 2H), 1.74 (t, *J* = 7.6 Hz, 2H), 1.40 (t, *J* = 7.6 Hz, 2H), 1.33-1.27 (m, 10H), 0.88 (t, *J* = 6.9 Hz, 3H). **^{13}C-NMR** (125 MHz): δ 169.4, 168.9, 32.1, 31.2, 29.56, 29.46, 29.33, 29.0, 25.8, 24.8, 22.9, 14.4. **ESI-MS** *m/z* (rel int): (pos) 292.1 ([M+Na]$^+$, 20), 561.3 ([2M+Na]$^+$, 5); (neg) 268.1 ([M–H]$^-$, 25), 537.3 ([2M–H]$^-$, 25). **HRMS** *m/z* calcd for $C_{14}H_{23}NO_4Na$ ([M+Na]$^+$) 292.1525; found 292.1537.

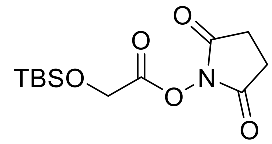

2,5-Dioxopyrrolidin-1-yl 2-((tert-butyldimethylsilyl)oxy)acetate (S1e). Synthesized from 2-((tert-butyldimethylsilyl)oxy)acetic acid,[6] white solid (894 mg, 54%). **TLC**: R_f 0.56 (3:1 hexanes/EtOAc). **IR** (ZnSe, film): 2956, 2932, 2859, 1841, 1741, 1469, 1430, 1362, 1255, 1205, 1101, 1070, 874, 838, 785, 702. **^{1}H-NMR** (500 MHz): δ 4.58 (s, 2H), 2.85 (s, 4H), 0.92 (s, J = 5.9 Hz, 9H), 0.13 (d, J = 6.2 Hz, 6H). **^{13}C-NMR** (125 MHz): δ 169.0, 167.5, 59.9, 25.8, 18.5. **ESI-MS** *m/z* (rel int): (pos) 310.3 ([M+Na]$^+$, 100); (neg) 286.2 ([M–H]$^-$, 100). **HRMS** *m/z* calcd for $C_{12}H_{21}NO_5NaSi$ ([M+H]$^+$) 310.1088; found 310.1087.

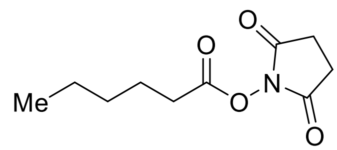

2,5-Dioxopyrrolidin-1-yl hexanoate (S1f). Synthesized from hexanoic acid, white solid (1.4548 g, 85%). **TLC**: R_f 0.51 (3:1 hexanes/EtOAc). **IR** (ZnSe, film): 2960, 2874, 1815, 1785, 1741, 1730, 1209, 1069, 915, 866, 815, 734. **^{1}H-NMR** (500 MHz): δ 2.83 (s, 4H), 2.60 (t, J = 7.5 Hz, 2H), 1.74 (q, J = 7.5 Hz, 2H), 1.41-1.34 (m, 4H), 0.91 (t, J = 7.1 Hz, 3H). **^{13}C-NMR** (125 MHz): δ 169.4, 168.9, 77.5, 31.2, 25.8, 24.5, 22.4, 14.1. **ESI-MS** *m/z* (rel int): (pos) 252.0 ([M+K]$^+$, 50), 449.4 ([2M+Na]$^+$, 10); (neg) 211.9 ([M–H]$^-$, 75). **HRMS** *m/z* calcd for $C_{10}H_{14}NO_4$ ([M+H]$^+$) 212.0923; found 212.0914.

General procedure for coupling N-hydroxysuccinamide esters S1a–f with 5´-O-sulfamoyl-adenosine S2a or S2b

In a 25 mL conical flask, protected sulfamoyl adenosine[3a, 7] **S2a** or **S2b** (1.3 mmol, 1.0 equiv) and the *N*-hydroxysuccinimidyl ester **S1a–f** (2.0 mmol, 1.5 equiv) were dissolved in 13 mL CH_3CN. DBU (0.28 mL, 2.0 mmol, 1.5 equiv) was added and the mixture was stirred at rt for 2 h. The reaction mixture was poured into 150 mL EtOAc, washed with satd aq NH_4Cl (1 x 15 mL), satd aq $NaHCO_3$ (1 x 15 mL), and brine (1 x 15 mL), dried ($MgSO_4$), filtered, and concentrated by rotary evaporation. Purification by silica flash chromatography (95:5 → 4:1 CH_2Cl_2/MeOH) yielded the protected acyl sulfamoyl adenosines **S3**.

---

[6] Vo, C. V.; Mitchell, T. A.; Bode, J. W. *J Am Chem Soc* **2011**, *133*, 14082.
[7] Castro-Pichel, J.; Garcia-Lopez, M. T.; De las Heras, F. G. *Tetrahedron* **1987**, *43*, 383.

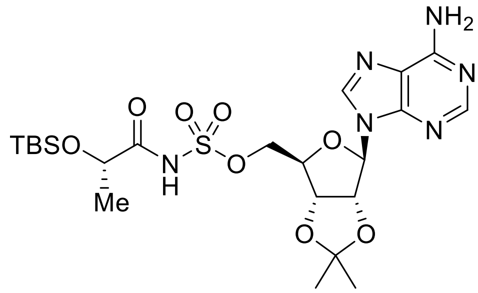

2´,3´-*O*-Isopropylidene-5´-*O*-[*N*-(*O*-*t*-butyldimethylsilyl-L-lactyl)sulfamoyl]adenosine (S3a). Synthesized from **S1a** and **S2a**, white solid (549.2 mg, 76%). **TLC**: R_f 0.33 (4:1 CH_2Cl_2/MeOH). **IR** (ZnSe, film): 2954, 2932, 2858, 1654, 1471, 1254, 1213, 1130, 1103, 1058, 1045, 973, 832, 800, 782. **^{1}H-NMR** (500 MHz, CD_3OD): δ 8.42 (s, 1H), 8.21 (s, 1H), 6.24 (d, *J* = 3.0 Hz, 1H), 5.38 (dd, *J* = 6.1, 3.0 Hz, 1H), 5.15 (dd, *J* = 6.1, 2.4 Hz, 1H), 4.54-4.52 (m, 1H), 4.27 (dd, *J* = 10.8, 4.2 Hz, 2H), 4.20 (q, *J* = 9.4, 4.8 Hz, 1H), 1.61 (s, 3H), 1.38 (s, 2H), 1.31 (d, *J* = 6.7 Hz, 3H), 0.89 (s, 9H), 0.07 (s, 3H), 0.05 (s, 3H). **^{13}C-NMR** (125 MHz): δ 183.5, 154.2, 150.4, 141.6, 140.6, 93.7, 92.0, 87.3, 86.7, 85.9, 83.5, 73.1, 69.9, 59.2, 27.7, 26.7, 26.4, 25.8, 22.8, 22.0, 19.5, 19.1, -4.3, -4.5, -4.79, -4.97. **ESI-MS** *m/z* (rel int): (pos) 611.1 ($[M+K]^+$, 60), 595.1 ($[M+Na]^+$, 20), 573.2 ($[M+H]^+$, 10); (neg) 571.2 ($[M–H]^-$, 100). **HRMS** *m/z* calcd for $C_{22}H_{37}N_6O_8SiS$ ($[M+H]^+$) 573.2162; found 573.2163

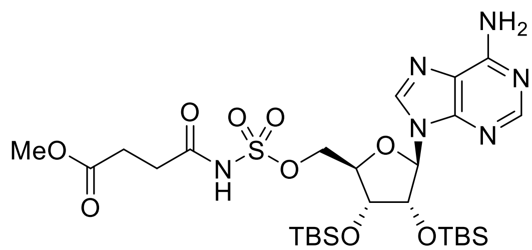

2´,3´-*O*,*O*-Bis(*t*-butyldimethylsilyl)-5´-*O*-[*N*-(methyl-succinyl)sulfamoyl]adenosine (S3b). Synthesized from **S1b** and **S2b**, white solid (83.2 mg, 70%). **TLC**: R_f 0.55 (4:1 CH_2Cl_2/MeOH). **IR** (ZnSe, film): 2953, 2932, 2858, 1733, 1618, 1575, 1472, 1363, 1295, 1253, 1144, 1094, 989, 956, 834, 778, 713. **^{1}H-NMR** (500 MHz, CD_3OD): δ 8.50 (s, 1H), 8.20 (s, 1H), 6.10 (d, *J* = 7.0 Hz, 1H), 4.78 (m, 1H), 4.44 (d, *J* = 4.4 Hz, 1H), 4.38 (dd, *J* = 11.1, 4.0 Hz, 1H), 4.32-4.27 (m, 2H), 3.63 (s, 3H), 2.62-2.59 (m, 2H), 2.56-2.54 (m, 2H), 0.97 (s, 9H), 0.73 (s, 9H), 0.17 (d, *J* = 9.0 Hz, 6H), -0.33 (s, 3H), -0.02 (s, 3H). **^{13}C-NMR** (125 MHz): δ 181.7, 175.7, 157.5, 154.1, 151.2, 141.7, 120.4, 88.8, 85.9, 77.4, 74.7, 69.5, 52.3, 50.0, 35.0, 31.0, 26.6, 26.4, 19.1, 18.9, -4.06, -4.13, -5.0. **HRMS** *m/z* calcd for $C_{27}H_{49}N_6O_9Si_2S$ ($[M+H]^+$) 689.2820; found 689.2800.

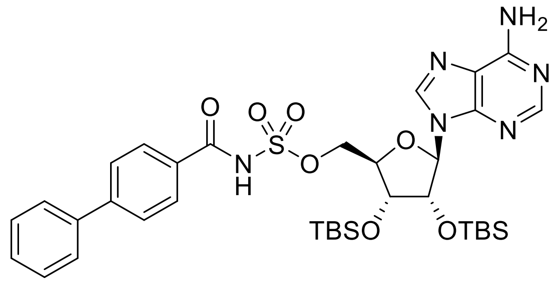

2´,3´-*O*,*O*-Bis(*t*-butyldimethylsilyl)-5´-*O*-[*N*-(4-phenylbenzoyl)sulfamoyl]adenosine (S3c). Synthesized from **S1c** and **S2b**, white solid (108 mg, 82%). **TLC**: R_f 0.61 (4:1 CH_2Cl_2/MeOH). **IR** (ZnSe, film): 2952, 2931, 2857, 1618, 1541, 1472, 1350, 1297, 1254, 1162, 1125, 990, 915, 843, 779, 750. **^{1}H-NMR** (500 MHz, CD_3OD): δ 8.52 (s, 1H), 8.18 (d, *J* = 8.5 Hz, 2H), 8.14 (s, 1H), 7.60-7.56 (m, 4H), 7.43-7.39 (m, 2H), 7.35-7.32 (m, 1H), 6.09 (d, *J* = 6.9 Hz, 1H), 4.89 (dd, *J* = 6.9, 4.4 Hz, 1H), 4.53 (dd, *J* = 11.3, 4.0 Hz, 1H), 4.46 (dd, *J* = 4.4, 1.6 Hz, 1H), 4.43 (dd, *J* = 11.3, 3.5 Hz, 1H), 4.30 (td, *J* = 3.6, 1.7 Hz, 1H), 0.93 (s, 9H), 0.70 (s, 9H), 0.13 (d, *J* = 5.6 Hz, 6H), -0.37 (s, 3H), -0.06 (s, 3H). **^{13}C-NMR** (125 MHz): δ 175.3, 157.5, 154.1, 151.1, 145.7, 141.8, 141.6, 137.2, 131.1, 130.1, 129.0, 128.2, 127.6, 120.4, 89.0, 86.0, 77.3, 74.7, 69.5, 26.5, 26.3, 19.1, 18.8, -4.0, -4.1, -4.2, -5.0. **HRMS** *m/z* calcd for $C_{35}H_{51}N_6O_7Si_2S$ ($[M+H]^+$) 755.3079; found 755.3041.

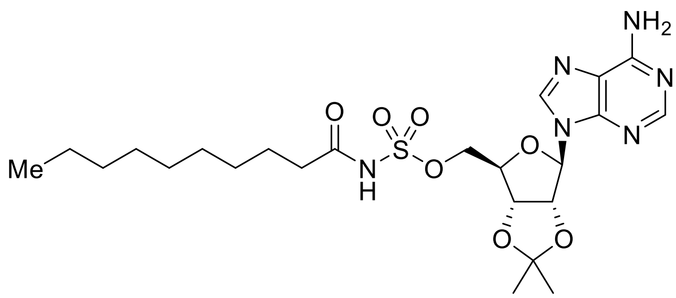

2´,3´-*O*-Isopropylidene-5´-*O*-[*N*-(decanoyl)sulfamoyl]adenosine (S3d). Synthesized from **S1d** and **S2a**, white solid (55.1 mg, 65%). **TLC**: R_f 0.24 (9:1 CH_2Cl_2/MeOH). **IR** (ZnSe, film): 2954, 2928, 2857, 1653, 1605, 1468, 1428, 1379, 1216, 1146, 1108, 1047, 999, 829, 782, 739, 704. **^{1}H-NMR** (500 MHz, CD_3OD): δ 8.40 (s, 1H), 8.21 (s, 1H), 6.23 (d, *J* = 2.9 Hz, 1H), 5.36 (dd, *J* = 6.1, 3.0 Hz, 1H), 5.12 (dd, *J* = 6.1, 2.4 Hz, 1H), 4.54-4.52 (m, 1H), 4.26 (qd, *J* = 12.9, 4.3 Hz, 2H), 2.16 (t, *J* = 7.6 Hz, 2H), 1.64-1.60 (m, 3H), 1.60 (s, 3H), 1.38 (s, 3H), 1.28 (s, 9H), 1.24 (s, 8H), 0.88 (q, *J* = 7.4 Hz, 5H). **^{13}C-NMR** (125 MHz): δ 184.0, 157.5, 154.2, 150.6, 141.7, 120.4, 115.6, 91.9, 85.9, 83.3, 69.9, 40.5, 33.2, 30.8, 30.7, 30.62, 30.59, 30.4, 27.5, 26.5, 25.8, 23.9, 14.6. **ESI-MS** *m/z* (rel int): (neg) 539.2 ($[M–H]^-$, 100), 1079.3 (($[2M–H]^-$, 5). **HRMS** *m/z* calcd for $C_{23}H_{37}N_6O_7S$ ($[M+H]^+$) 541.2431; found 541.2444.

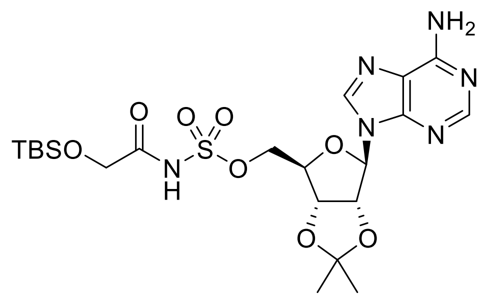

2´,3´-*O*-Isopropylidene-5´-*O*-[*N*-(*O*-*t*-butyldimethylsilyl-glycolyl)sulfamoyl]adenosine (S3e). Synthesized from **S1e** and **S2a**, white solid (519.6 mg, 75%). **TLC**: R_f 0.22 (4:1 CH_2Cl_2/MeOH). **IR** (ZnSe, film): 2954, 2933, 2858, 1642, 1473, 1428, 1385, 1296, 1256, 1213, 1149, 1112, 1006, 836, 785, 703. **^{1}H-NMR** (500 MHz, CD_3OD): δ 8.44 (s, 1H), 8.21 (s, 1H), 6.24 (d, *J* = 3.1 Hz, 1H), 5.37 (dd, *J* = 6.1, 3.1 Hz, 1H), 5.13 (dd, *J* = 6.1, 2.2 Hz, 1H), 4.55-4.52 (m, 1H), 4.24 (qd, *J* = 9.6, 4.0 Hz, 2H), 4.10 (s, 2H), 1.61 (s, 3H), 1.39 (s, 3H), 0.90 (s, 9H), 0.08 (s, 6H). **^{13}C-NMR** (125 MHz): δ 180.2, 154.2, 141.6, 115.5, 92.0, 85.93, 85.89, 83.5, 69.8, 66.4, 27.7, 26.64, 26.45, 25.8, 19.6, -4.9. **ESI-MS** *m/z* (rel int): (pos) 581.1 ([M+Na]$^+$, 30), 559.1 ([M+H]$^+$, 10); (neg) 557.1 ([M–H]$^-$, 100). **HRMS** *m/z* calcd for $C_{21}H_{35}N_6O_8SiS$ ([M+H]$^+$) 559.2012; found 559.2006.

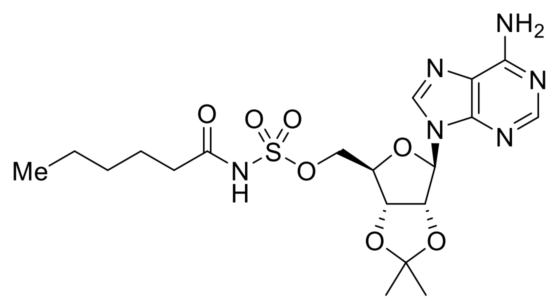

2´,3´-*O*-Isopropylidene-5´-*O*-[*N*-(hexanoyl)sulfamoyl]adenosine (S3f). Synthesized from **S1f** and **S2a**, white solid (55.1 mg, 43%). **TLC**: R_f 0.17 (9:1 CH_2Cl_2/MeOH). **IR** (ZnSe, film): 2959, 2935, 2863, 1653, 1606, 1474, 1383, 1275, 1219, 1151, 1111, 1054, 862, 836, 708. **^{1}H-NMR** (500 MHz, CD_3OD): δ 8.37 (s, 1H), 8.21 (s, 1H), 6.23 (d, *J* = 2.8 Hz, 1H), 5.37 (dd, *J* = 6.1, 2.8 Hz, 1H), 5.12 (dd, *J* = 6.1, 2.5 Hz, 1H), 4.52 (d, *J* = 2.6 Hz, 1H), 4.30-4.21 (m, 2H), 2.15 (t, *J* = 7.6 Hz, 2H), 1.60 (s, 3H), 1.55 (dd, *J* = 14.5, 7.5 Hz, 2H), 1.38 (s, 3H), 1.33-1.24 (m, 4H), 0.86 (t, *J* = 6.9 Hz, 3H). **^{13}C-NMR** (125 MHz): δ 184.2, 157.5, 154.2, 150.5, 141.7, 120.4, 115.6, 91.9, 86.0, 85.8, 83.3, 69.9, 40.5, 32.9, 27.6, 27.2, 25.7, 23.7, 14.5. **ESI-MS** *m/z* (rel int): (pos) 523.1 ([M+K]$^+$, 10), 485.2 ([M+Na]$^+$, 10); (neg) 483.1 ([M–H]$^-$, 100). **HRMS** *m/z* calcd for $C_{19}H_{29}N_6O_7S$ ([M+H]$^+$) 485.1804; found 485.1818.

General procedure for deprotection of S3a–f

In a 20 mL vial, *N*-acyl sulfamoyl adenosine **S3a–f** (70 μmol), 344 μL H_2O was added and cooled to 0 °C. TFA (1.7 mL) was added and the reaction was warmed to rt and stirred for 2–24 h. The solution was cooled to 0 °C, then MeOH was added (5 mL) and the mixture was concentrated by rotary evaporation. The mixture was azeotroped from MeOH (2 x 5 mL) and cyclohexane (3 x 5 mL). Purification by silica flash chromatography (5:1 → 3:1 EtOAc/MeOH) yielded the acyl sulfamoyl adenosines.

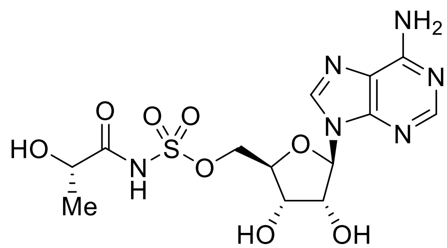

5´-*O*-[*N*-(L-Lactyl)sulfamoyl]adenosine (4, L-lactyl-AMS). Synthesized from **S3a**, white solid (33.7 mg, 79%). **TLC**: R_f 0.10 (3:1 EtOAc/MeOH). **IR** (ZnSe, film): 2473 1622, 1121, 1093, 973, 902, 825, 763. **^{1}H-NMR** (500 MHz, CD_3OD): δ 8.49 (s, 1H), 8.19 (s, 1H), 6.09 (d, *J* = 5.5 Hz, 1H), 4.66 (t, *J* = 5.2 Hz, 1H), 4.39 (t, *J* = 4.2 Hz, 1H), 4.35 (dd, *J* = 11.7, 3.8 Hz, 1H), 4.30 (dt, *J* = 7.8, 3.6 Hz, 2H), 4.12-4.08 (m, 1H), 1.35 (d, *J* = 6.7 Hz, 3H). **^{13}C-NMR** (125 MHz): δ 183.5, 157.4, 154.0, 151.0, 141.4, 94.1, 89.5, 84.6, 76.3, 72.3, 70.9, 69.4, 22.1. **ESI-MS** *m/z* (rel int): (pos) 419.0 ($[M+H]^+$, 100), 441.2 ($[M+Na]^+$, 100); (neg) 417.7 ($[M–H]^-$, 100). **HRMS** *m/z* calcd for $C_{13}H_{19}N_6O_8S$ ($[M+H]^+$) 419.0982; found 419.0985.

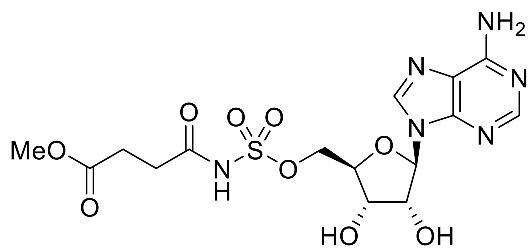

5´-*O*-[*N*-(Methyl-succinyl)sulfamoyl]adenosine (5, methyl-succinyl-AMS). Synthesized from **S3b**, white solid (11.0 mg, 42%). **TLC**: R_f 0.05 (4:1 CH_2Cl_2/MeOH). **IR** (ZnSe, film): 1725, 1681, 1647, 1603, 1581, 1298, 1208, 1147, 1002, 840, 800, 723. **^{1}H-NMR** (500 MHz, CD_3OD): δ 8.48 (s, 1H), 8.20 (s, 1H), 6.09 (d, *J* = 5.7 Hz, 1H), 4.67 (t, *J* = 5.4 Hz, 1H), 4.38 (dd, *J* = 5.0, 3.1 Hz, 1H), 4.30 (dt, *J* = 13.0, 8.0 Hz, 3H), 3.62 (s, 3H), 2.59-2.56 (m, 2H), 2.53-2.51 (m, 2H). **^{13}C-NMR** (125 MHz): δ 175.7, 157.5, 154.0, 151.0, 141.3, 89.4, 84.7, 76.2, 72.5, 69.4, 52.3, 34.7, 30.9. **HRMS** *m/z* calcd for $C_{15}H_{21}N_6O_9S$ ($[M+H]^+$) 461.1091; found 461.1079.

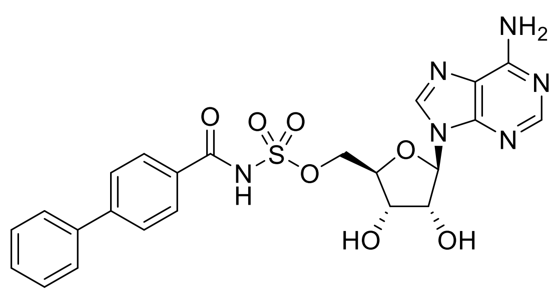

5´-*O*-[*N*-(4-Phenylbenzoyl)sulfamoyl]adenosine (9, 4-phenylbenzoyl-AMS). Synthesized from **S3c**, white solid (30.7 mg, 100%). **TLC**: R_f 0.10 (4:1 CH_2Cl_2/MeOH). **IR** (ZnSe, film): 1675, 1336, 1302, 1203, 1134, 978, 914, 845, 801, 751, 725. **^{1}H-NMR** (500 MHz, CD_3OD): δ 8.44 (s, 1H), 8.15-8.11 (m, 3H), 7.60 (dd, *J* = 16.1, 7.8 Hz, 4H), 7.44-7.41 (m, 2H), 7.35 (d, *J* = 7.3 Hz, 1H), 6.08 (d, *J* = 5.2 Hz, 1H), 4.73-4.71 (m, 1H), 4.63-4.60 (m, 2H), 4.50-4.41 (m, 3H), 4.36-4.35 (m, 1H). **^{13}C-NMR** (125 MHz): δ 175.5, 163.5, 163.3, 157.4, 154.0, 150.8, 145.6, 141.8, 141.2, 137.2, 130.9, 130.1, 129.0, 128.2, 127.6, 120.4, 119.5, 117.1, 89.8, 84.5, 76.0, 72.4, 69.8. **ESI-MS** *m/z* (rel int): (pos) 565.2 ($[M+K]^+$, 100), 549.2 ($[M+Na]^+$, 40), 527.2 ($[M+H]^+$, 10). **HRMS** *m/z* calcd for $C_{23}H_{23}N_6O_7S$ ($[M+H]^+$) 527.1349; found 527.1357.

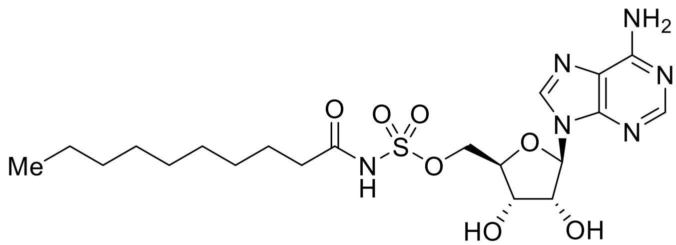

5´-*O*-[*N*-(Decanoyl)sulfamoyl]adenosine (10, decanoyl-AMS). Synthesized from **S3d**, white solid (17.1 mg, 76%). **TLC**: R_f 0.18 (4:1 CH_2Cl_2/MeOH). **IR** (ZnSe, film): 2925, 2853, 1684, 1630, 1355, 1301, 1208, 1143, 834, 802. **^{1}H-NMR** (500 MHz, CD_3OD): δ 8.45 (s, 1H), 8.20 (s, 1H), 6.08 (d, J = 5.5 Hz, 1H), 4.67 (t, J = 5.3 Hz, 1H), 4.40-4.34 (m, 2H), 4.29 (dt, J = 7.9, 3.8 Hz, 2H), 2.19 (t, J = 7.6 Hz, 2H), 1.60-1.57 (m, 2H), 1.29-1.25 (m, 6H), 1.23 (s, 7H), 0.87 (t, J = 7.0 Hz, 3H). **^{13}C-NMR** (125 MHz): δ 184.1, 154.1, 150.9, 141.3, 89.6, 84.5, 76.1, 72.4, 69.6, 40.5, 33.2, 30.83, 30.79, 30.74, 30.62, 27.6, 23.9, 14.6. **ESI-MS** *m/z* (rel int): (pos) 523.2 ($[M+Na]^+$, 100), 501.2(($[M+H]^+$, 75,) 1023.6 ($[2M+Na]^+$, 5); (neg) 499.1 ($[M–H]^-$, 100), 999.4 ($[2M–H]^-$, 20). **HRMS** *m/z* calcd for $C_{20}H_{33}N_6O_7S$ ($[M+H]^+$) 501.2131; found 501.2120.

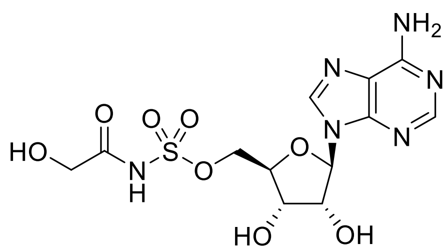

5´-*O*-[*N*-(Glycolyl)sulfamoyl]adenosine (S4, glycoyl-AMS). Synthesized from **S3e**, white solid (30.0 mg, 78%). **TLC**: R_f 0.38 (3:1 EtOAc/MeOH). **IR** (ZnSe, film): 2572, 2070, 1619, 1122, 1092, 973, 901, 823. **^{1}H-NMR** (500 MHz, CD_3OD): δ 8.51 (s, 1H), 8.20 (s, 1H), 6.09 (d, J = 5.6 Hz, 1H), 4.66 (t, J = 5.3 Hz, 1H), 4.39 (dd, J = 4.9, 3.5 Hz, 1H), 4.31 (ddd, J = 13.2, 9.1, 3.7 Hz, 3H), 3.97 (s, 2H). **^{13}C-NMR** (125 MHz): δ 180.5, 157.5, 154.0, 151.0, 141.3, 120.5, 89.4, 84.6, 76.3, 72.3, 69.2, 64.5. **ESI-MS** *m/z* (rel int): (neg) 403.1 ($[M–H]^-$, 100). **HRMS** *m/z* calcd for $C_{12}H_{15}N_6O_8S$ ($[M+H]^+$) 403.0674; found 403.0672.

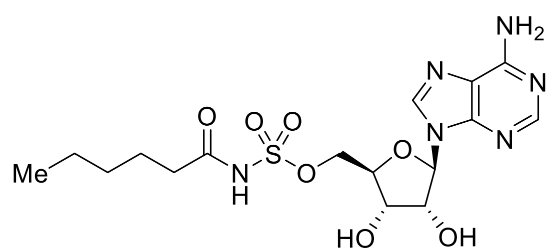

5´-*O*-[*N*-(Hexanoyl)sulfamoyl]adenosine (S5, hexanoyl-AMS). Synthesized from **S3f**, white solid (50.0 mg, 100%). **TLC**: R_f 0.20 (3:1 EtOAc/MeOH). **IR** (ZnSe, film): 2960, 2934, 1678, 1453, 1379, 1333, 1300, 1207, 1143, 982, 843, 801, 725. **^{1}H-NMR** (500 MHz, CD_3OD): δ 8.39 (s, 1H), 8.20 (s, 1H), 6.08 (d, J = 5.3 Hz, 1H), 4.68 (t, J = 5.2 Hz, 1H), 4.42-4.40 (m, 2H), 4.36-4.30 (m, 2H), 2.22-2.19 (m, 2H), 1.59-1.54 (m, 2H), 1.27 (dt, J = 7.6, 3.9 Hz, 4H), 0.86 (t, J =

7.0 Hz, 3H). **^{13}C-NMR** (125 MHz): δ 157.4, 154.1, 150.9, 141.2, 120.5, 89.9, 84.2, 75.9, 72.3, 70.2, 40.0, 32.8, 26.9, 23.6, 14.4. **HRMS** *m/z* calcd for $C_{16}H_{25}N_6O_7S$ ([M+H]$^+$) 445.1505; found 445.1518.

E. Liquid Chromatography-Tandem Mass Spectrometry (LC-MS/MS)

To quantify the amount of the sulfonyladenosine of interest in each sample, a standard curve (0.0025–100 μM) was constructed by mixing 200 μL analyte (in PBS) with 200 μL internal standard (2 μM, acetonitrile). Approximately 4 μL of sample were injected into the LC-MS/MS. For the purposes of platform methodology validation herein, we selected close structural analogues of each analyte for the internal standards to maximize sensitivity and linear range of detection. For example, we obtained a wider linear range of detection for salicyl-AMS when we used benzoyl-AMS, a close structural analogue as an internal standard, compared to when we used alanyl-AMS, a more structurally distinct compound (**Figure S3**). Full details regarding internal standards for each analyte and the multiple reaction monitoring (MRM) transitions are provided below in **Table S5**.

Table S5. Analytes, internal standards and MRM transitions used for LC-MS/MS

Analyte	Analyte MRM	Analyte ret. time (min)	Internal Standard	IS MRM transition	IS ret. time (min)	Eluent (% B)
H-AMS (2)	347/136	1.7	guanosine	284/152	1.6	10
L-Ala-AMS (3)	418/136	1.5	glycyl-AMS	404/136	1.4	10
L-Lac-AMS (4)	419/136	1.8	glycolyl-AMS	405/136	1.7	10
Me-suc-AMS (5)	461/136	1.4	hex-AMS	445/136	2.0	35
anthra-AMS (6)	466/136	1.4	Bz-AMS	451/136	1.5	30
OSB-AMS (7)	551/136	1.6	sal-AMS	467/136	1.6	30
sal-AMS (1)	467/136	1.5	Bz-AMS	451/136	1.4	35
Bz-AMS (8)	451/136	1.4	sal-AMS	467/136	1.5	35
4-PhBz-AMS (9)	527/136	3.8	sal-AMS	467/136	1.6	35
dec-AMS (10)	501/136	1.8	hex-AMS	445/136	1.4	60

Multiple reaction monitoring (MRM) transitions were monitored in the positive ionization mode. Mobile phase: A=0.1% formic acid in water, B=acetonitrile.

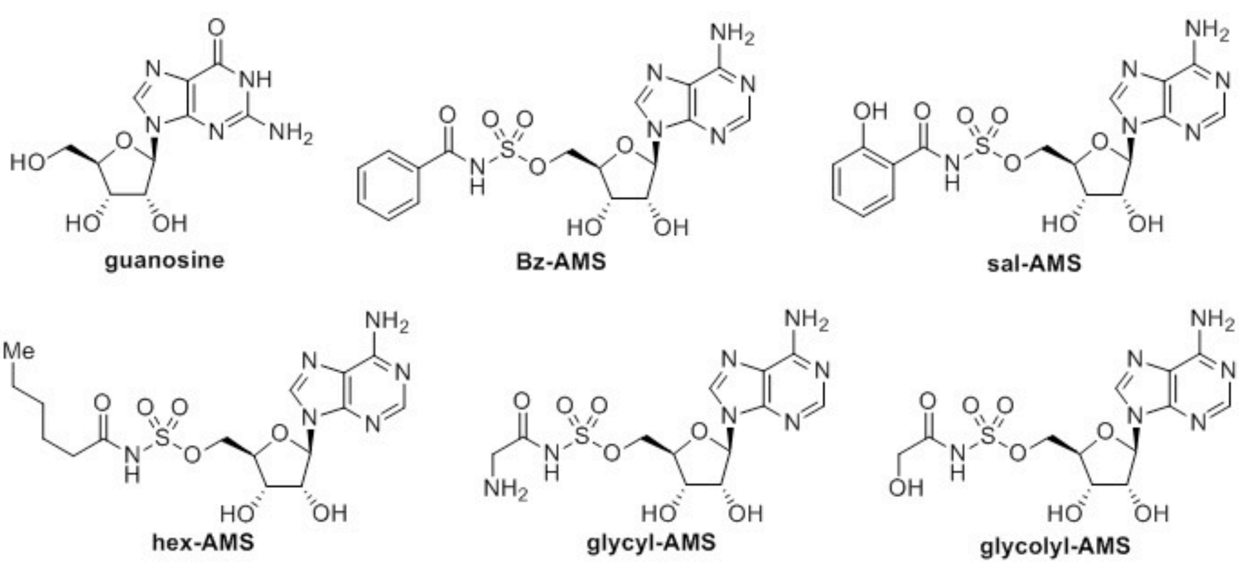

Figure S17. Structures of internal standards used for LC-MS/MS. (Bz = benzoyl; sal = salicyl; hex = hexanoyl).

F. COMPOUND ACCUMULATION STUDIES

Salicyl-AMS influx experiments

E. coli (OD_{600} = 0.5) was treated with salicyl-AMS (0.01–1000 μM, 37 °C, 0–60 min) in PBS, centrifuged (15,000 rpm, 4 °C, 5 min), resuspended, washed with cold PBS (4 x 200 μL), and lysed by sonication. The lysate and all wash supernatants were analyzed separately by LC-MS/MS with benzoyl-AMS (1 μM) as an internal standard. The intracellular concentration of salicyl-AMS was calculated based on CFU determination of the culture prior to centrifugation.

Salicyl-AMS efflux experiments

E. coli (OD_{600} = 0.5) was treated with CCCP (100 μM, 37 °C, 10 min) in PBS and then with salicyl-AMS (100 μM, 37°C, 15 min). Cells were washed and resuspended in cold PBS containing either glucose (0.2%) or CCCP (100 μM). The preloaded cells were incubated at 37 °C and aliquots were removed at various times (0–60 min) and processed as above.

Compound accumulation experiments

E. coli (OD_{600} = 0.5, tryptic soy broth, 37 °C), *B.* subtilis (OD_{600} = 0.5, LB media, 30 °C), or *M. smegmatis* (OD_{620} = 0.5, Middlebrook 7H9 + 10% ADN (5% BSA, 2% dextrose, 0.85% NaCl), 37 °C) was equilibrated (10 min) without or with indicated efflux pump inhibitors: CCCP (100 μM), reserpine (33 μM; 20 μg/mL), or PAβN (38 μM; 20 μg/mL). Then, bacteria were incubated with the appropriate sulfonyladenosine (100 μM, 30 min) and processed as above for salicyl-AMS influx experiments.

Calculation of cellular concentration

The total number of cells was determined via viable cell counts and plating of colony forming units (CFUs). After incubation with analyte, serial dilutions in fresh media were plated on agar. Colonies were grown for 16–24 h and plates containing 25–250 colonies were used to calculate the total number of cells. Individual cell volumes *of B. subtilis*,[8] *E. coli*,[9] and *M. smegmatis*[10] were taken from the literature and total cell volume and cellular analyte concentration was calculated using this information.

Optimization of Wash Protocol

To determine whether four washes were adequate to remove extracellular salicyl-AMS in the compound accumulation studies, we incubated *B. subtilis* with 1 mM salicyl-AMS for 1 h and varied the number of wash steps. We reasoned that cell-associated salicyl-AMS would reach an asymptote as the number of wash steps was increased. Indeed, the amount of cell associated salicyl-AMS decreased between no washes and three washes and reached an asymptote after three washes.

---

[8] Sharpe, M. E.; Hauser, P. M.; Sharpe, R. G.; Errington, J. *J Bacteriol* **1998**, *180*, 547.
[9] Kubitschek, H. E.; Friske, J. A. *J Bacteriol* **1986**, *168*, 1466.
[10] Nguyen, L.; Scherr, N.; Gatfield, J.; Walburger, A.; Pieters, J.; Thompson, C. J. *J Bacteriol* **2007**, *189*, 7896.

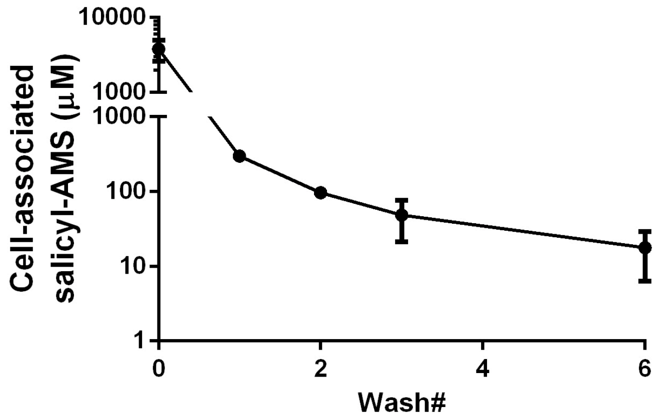

Figure S18. Optimization of wash steps in *B. subtilis*. Four washes are adequate to remove cell-associated salicyl-AMS. *B. subtilis* (OD_{600} = 0.5) was treated with salicyl-AMS (1.0 mM, 30 °C, 1 h, LB media) and the number of wash steps was varied. Cell-associated salicyl-AMS was quantified by LC-MS/MS. The concentration of cell-associated salicyl-AMS decreased between no washes and three washes, and reached an asymptote thereafter.

Assessment of day-to-day variation in accumulation experiments

To assess the interday variation in accumulation of salicyl-AMS, we conducted accumulation experiments under the following conditions: (1) 100 µM salicyl-AMS, 37 °C; (2) 100 µM salicyl-AMS, 100 µM CCCP, 37 °C; and (3) 100 µM salicyl-AMS, 20 µg/mL PAβN, 37 °C. Pretreatment with CCCP significantly increased the accumulation of salicyl-AMS in E. coli, whereas treatment with a competitive inhibitor of AcrAB-TolC, phenylalanine-arginine-β-naphthylamide (PAβN) did not substantially increase cellular salicyl-AMS. These trends were consistent for experiments conducted on three separate days.

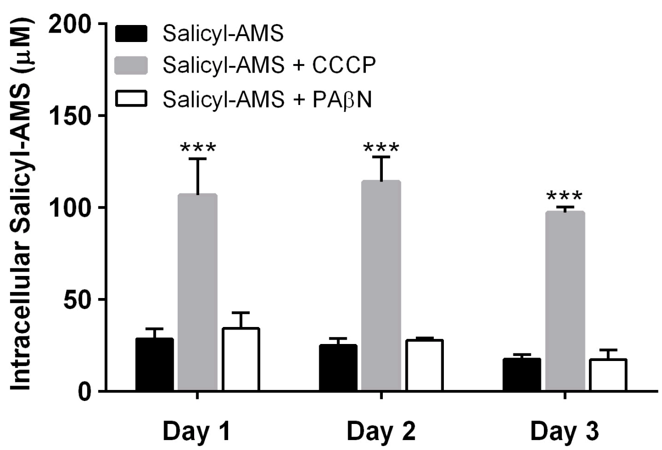

Figure S19. Interday variation in salicyl-AMS accumulation in *E. coli*. Trends in accumulation of salicyl-AMS are consistent across experiments on three separate days. (100 µM extracellular, 30 min, tryptic soy broth). Statistical significance compared to salicyl-AMS alone assessed using one-way ANOVA and Tukey's multiple comparison test and 95% confidence intervals: ***$p < 0.001$. CCCP = carbonyl cyanide *m*-chlorophenylhydrazone; PAβN = phenylalanine arginine-β-naphthylamide. All data are reported as mean ± SD for four replicates.

G. PRINCIPAL COMPONENT ANALYSIS

To generate the plots shown in **Figure 1** of the manuscript, a total of 141 compounds (**Table S1**) were compared by principal component analysis (PCA).[11]

The compounds analyzed by PCA included the following:

- 50 top selling brand-name, non-antiinfective small molecule drugs by revenue in 2012 (**Figure S20**)[12]
- 91 antibacterials (**Figure S21–S29**),[13] including:
    - 38 β-lactams (**Figure S21**)
    - 4 peptides (**Figure S22**)
    - 7 aminoglycosides (**Figure S23**)
    - 15 quinolones (**Figure S24**)
    - 7 macrolides (**Figure S25**)
    - 7 tetracyclines (**Figure S26**)
    - 2 oxazolidinones (**Figure S27**)
    - 5 *M. tuberculosis* targeting drugs (**Figure S28**)
    - 6 sulfa drugs (**Figure S29**)

The drug reference set consists of drugs with non-antiinfective indications and the different classes of antibacterials were chosen to demonstrate that the structural and physicochemical properties of most antibacterials are distinct from drugs targeting other therapeutic indications.

A set of 20 physicochemical descriptors (**Table S2**) were calculated using cheminformatics tools (Instant JChem, VCCLab[14]). The descriptors were selected based on several criteria. First, Lipinski's parameters[15] (MW ≤ 500, HBD ≤ 10, HBA ≤ 5, LogP ≤ 5) and Veber's parameters[12] (RotB ≤ 10, tPSA ≤ 140 Å^2) have been correlated with oral bioavailability.[16] While oral bioavailability is not an immediate goal of most academic screening campaigns, some attention to these parameters is useful to the extent that they partially correlate to cell permeability.[6] Second, Tetko's calculated logS aqueous solubility (ALogpS) and log P hydrophobicity (ALogPs) were included since a balance between compound solubility and hydrophobicity are critical for oral bioavailability.[6] The distribution coefficient ($\log D_{7.4}$) was included to approximate aqueous solubility of ionizable molecules at pH = 7.4. Third, several stereochemical parameters (nStereo, nStMW, Fsp^3) were included to approximate three-

[11] (a) Wenderski, T. A.; Stratton, C. F.; Bauer, R. A.; Kopp, F.; Tan, D. S. In *Methods Mol. Biol.* in press. (b) Bauer, R. A.; Wurst, J. M.; Tan, D. S. *Curr Opin Chem Biol* **2010**, *14*, 308. (c) Bauer, R. A.; Wenderski, T. A.; Tan, D. S. *Nat Chem Biol* **2013**, *9*, 21. (d) Kopp, F.; Stratton, C. F.; Akella, L. B.; Tan, D. S. *Nat Chem Biol* **2012**, *8*, 358. (e) Moura-Letts, G.; Diblasi, C. M.; Bauer, R. A.; Tan, D. S. *Proc Natl Acad Sci U S A* **2011**, *108*, 6745.

[12] Jon T. Njardarson Group Website – "Top 200 Brand-Name Drugs by Retail Dollars in 2012": cbc.arizona.edu/njardarson/group/sites/default/files/Top200%20Pharmacetical%20Products%20by%20US%20Retail%20Sales%20in%202012_0.pdf.

[13] (a) Jon T. Njardarson Group Website – "Anti-Infective Drug Poster": cbc.arizona.edu/njardarson/group/sites/default/files/Anti-Infective%20Drugs3.pdf. (b) O'Shea, R.; Moser, H. E. *J Med Chem* **2008**, *51*, 2871.

[14] (a) Tetko, I. V., Virtual Computational Chemistry Laboratory; http://www.vcclab.org/lab/alogps/ (b) Tetko, I. V.; Tanchuk, V. Y.; Kasheva, T. N.; Villa, A. E. *J Chem Inf Comput Sci* **2001**, *41*, 246.

[15] Lipinski, C. A.; Lombardo, F.; Dominy, B. W.; Feeney, P. J. *Advanced Drug Delivery Reviews* **1997**, *23*, 3.

[16] Rezai, T.; Yu, B.; Millhauser, G. L.; Jacobson, M. P.; Lokey, R. S. *J Am Chem Soc* **2006**, *128*, 2510.

dimensional complexity.[17] Fourth, most antibacterials are natural products or derived from natural products,[15] and additional parameters previously found to differentiate synthetic drugs and natural products were included.[18] Synthetic drugs tend to have higher nitrogen content, while natural products tend to have higher oxygen content (N, O). Natural products tend to have fewer aromatic rings and more complex, fused ring sytems (Rings, RngAr, RngSys, RngLg, RRSys). Lastly, relative polar surface area (relPSA) was included because it has been shown to be a distinguishing factor between Gram-positive and Gram-negative antibacterials.[19]

These data were assembled in a Microsoft Excel spreadsheet and average values for each parameter were calculated within each compound series. The hypothetical average values for each antibacterial class, non-antiinfectives, and the sulfonyladenosine datasets were included in the PCA analysis (**Table S3**).

---

[17] Lovering, F.; Bikker, J.; Humblet, C. *J Med Chem* **2009**, *52*, 6752.
[18] Feher, M.; Schmidt, J. M. *J Chem Inf Comput Sci* **2003**, *43*, 218.
[19] O'Shea, R.; Moser, H. E. *J Med Chem* **2008**, *51*, 2871.

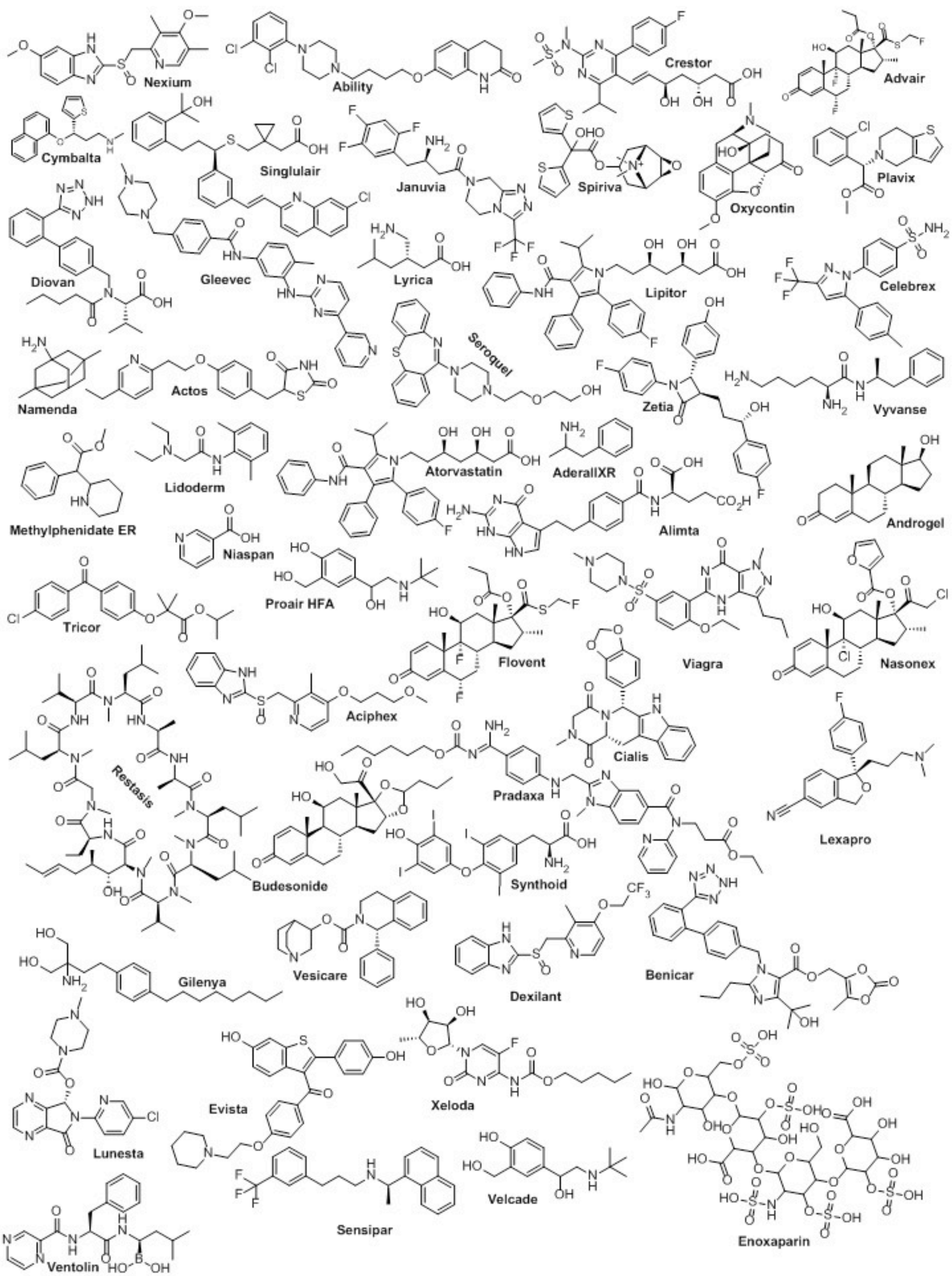

Figure S20. 2012 brand-name drug reference set for PCA (50 structures).

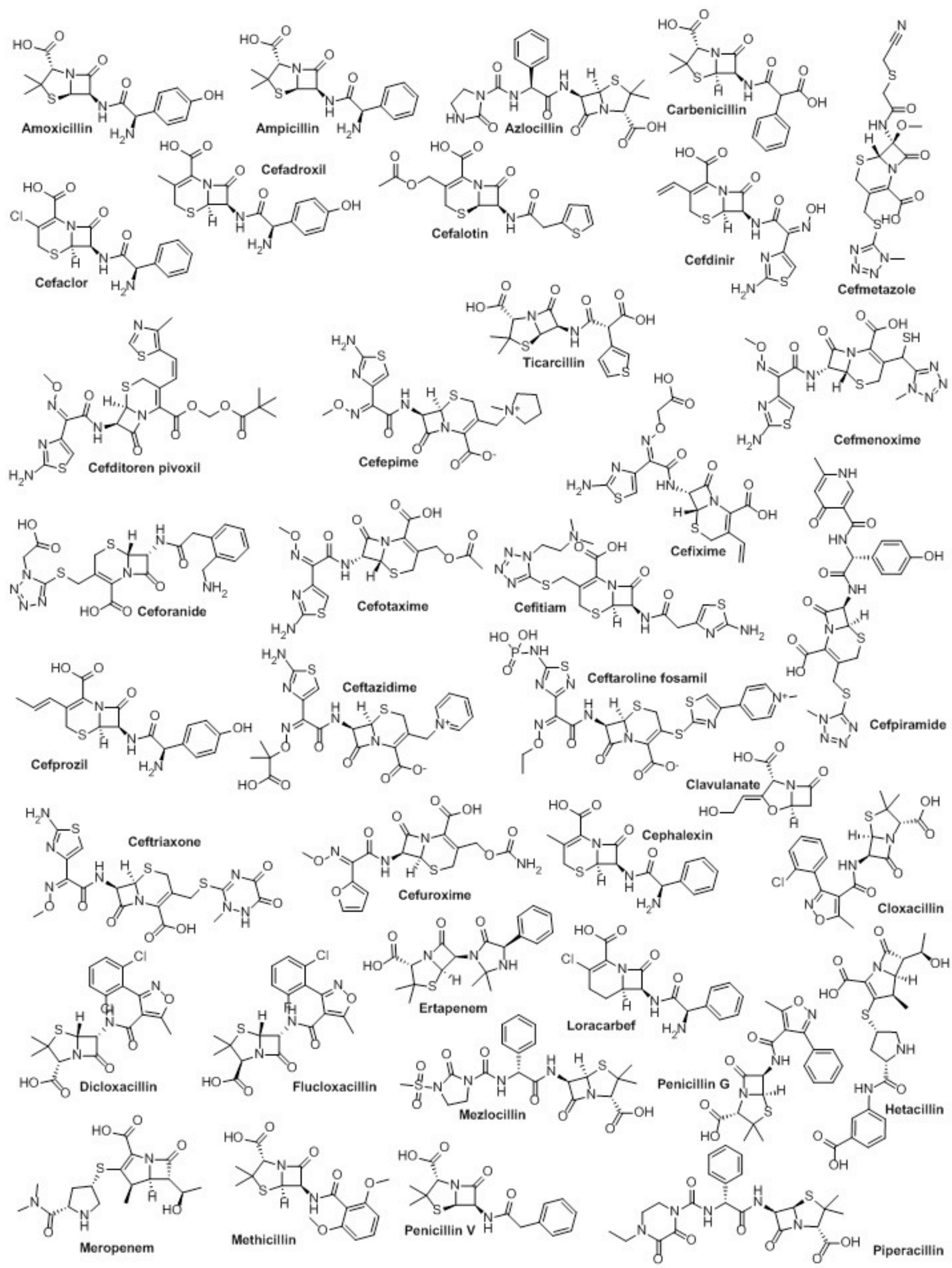

Figure S21. β-Lactam reference set for PCA (38 structures).

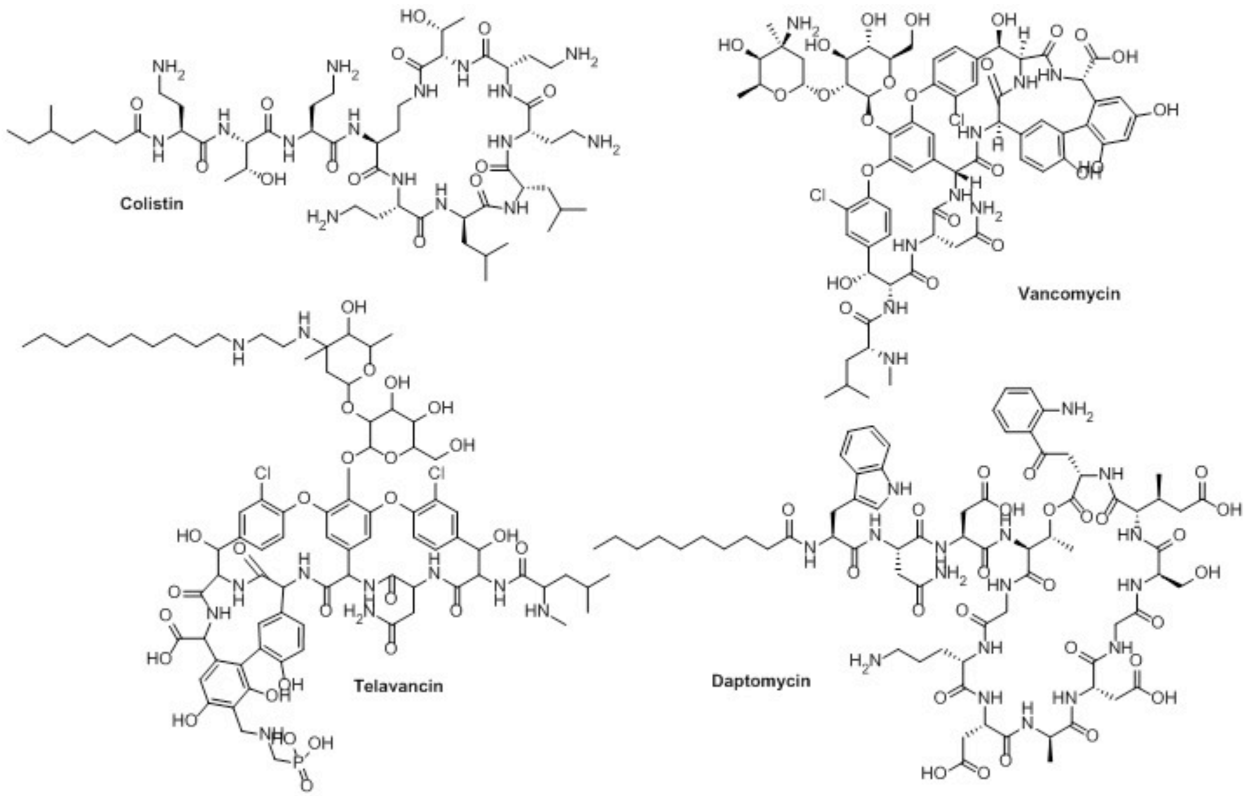

Figure S22. Peptide reference set for PCA (4 structures).

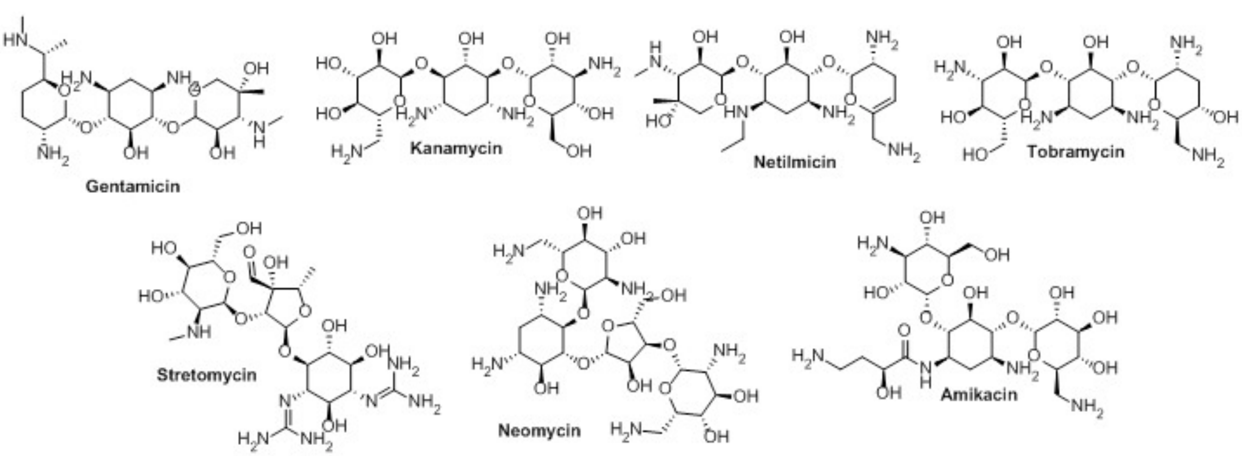

Figure S23. Aminoglycoside reference set for PCA (7 structures).

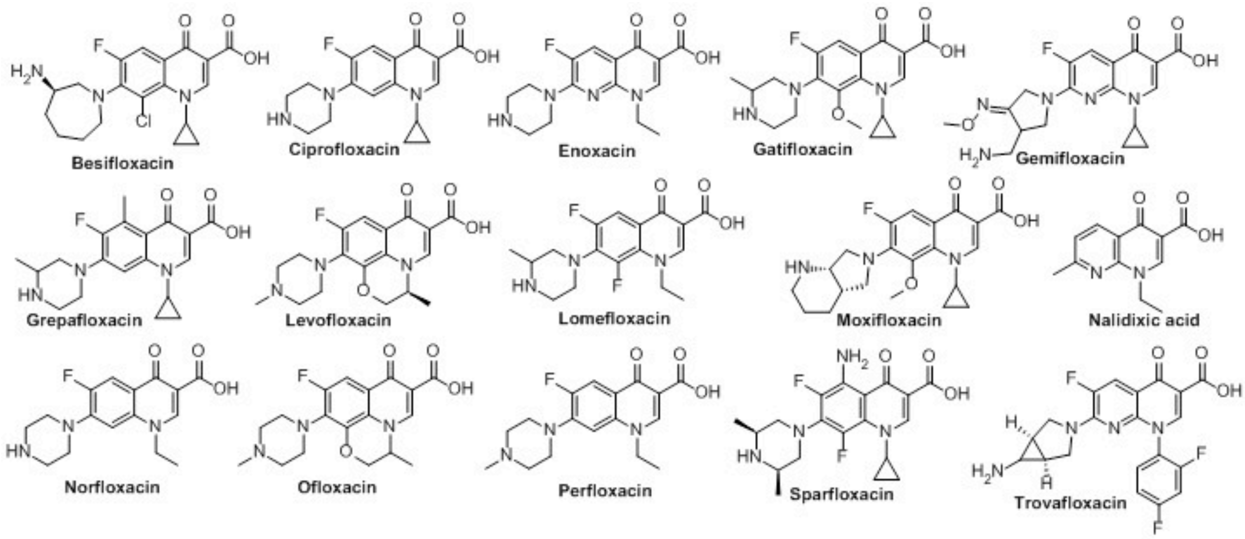

Figure S24. Quinolone reference set for PCA (15 structures).

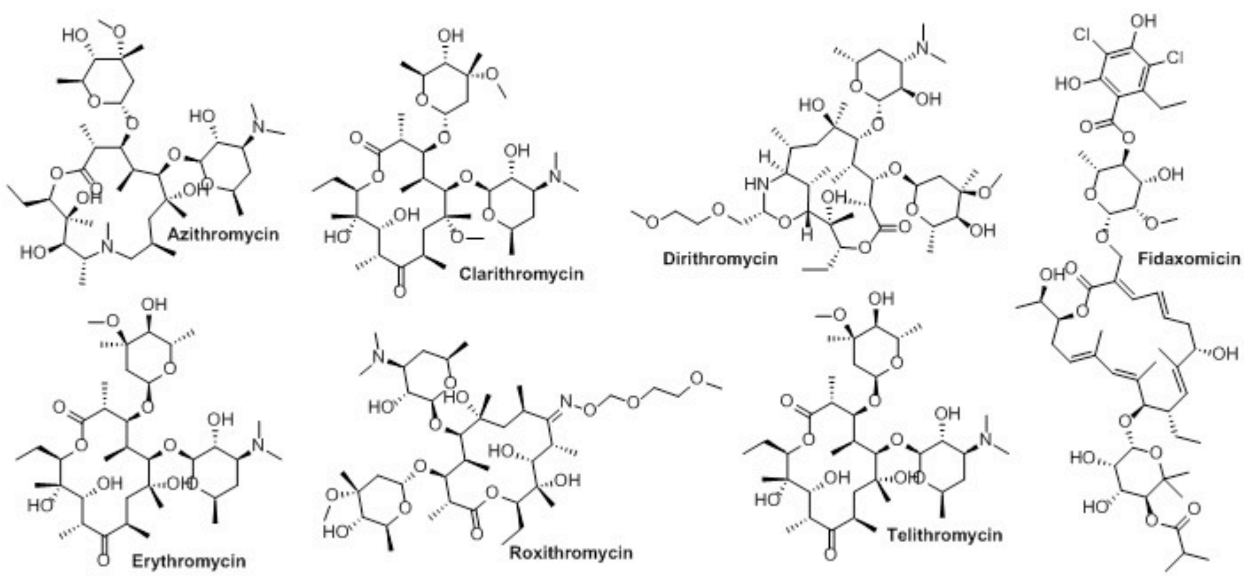

Figure S25. Macrolide reference set for PCA (7 structures).

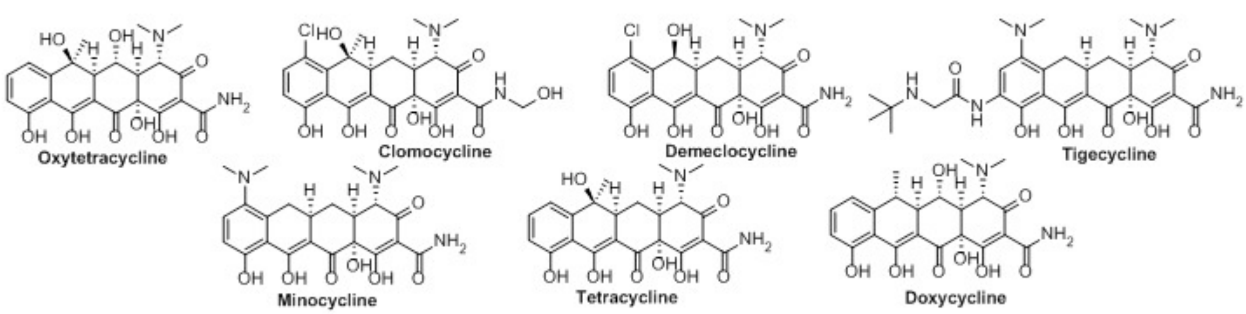

Figure S26. Tetracycline reference set for PCA (7 structures).

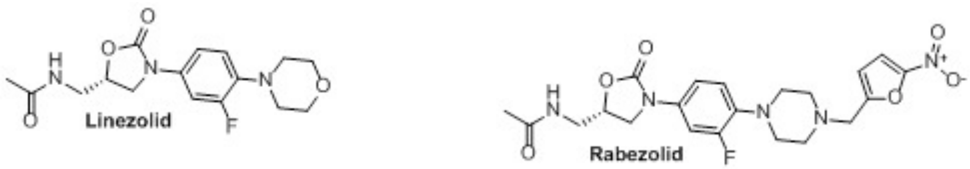

Figure S27. Oxazolidinone reference set for PCA (2 structures).

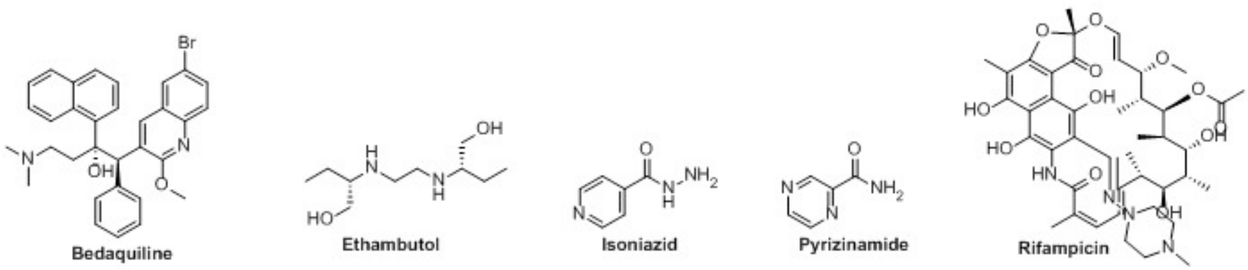

Figure S28. *M. tuberculosis* drug reference set for PCA (5 structures).

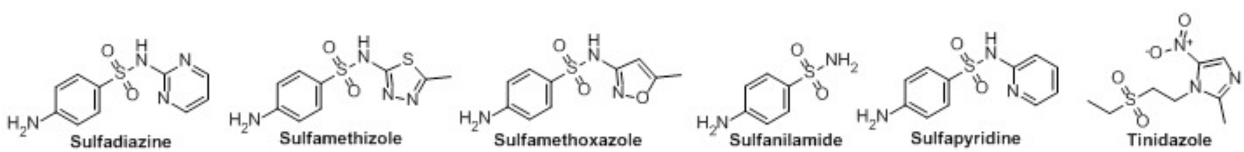

Figure S29. Sulfa drug reference set for PCA (6 structures).

Detailed PCA Protocol (Windows)

To provide a visual representation of the position of each component in chemical space, we conducted PCA with the "R" open source statistical computing package[20] to rotate the 20-dimensional vector corresponding to each compound to a 2-dimensional vector, with minimal loss of information. The detailed protocol is as follows:

1. In MS Excel, a "Raw" worksheet was created with compounds in rows and physicochemical descriptors in columns.

2. Mean and standard deviation values were calculated for each column.

3. A "Norm" worksheet was created and mean-centered, standardized values were generated for each column using the equation:
   normval = (val – column mean) / column standard deviation

4. With the upper cell left blank (R requires this to recognize a header row), the Number format was designated for all data columns to 4 decimal places.

5. Excel workbook was saved.

[20] The R Project for Statistical Computing; http://www.r-project.org/

6. The “Norm” worksheet was saved as “AntibacterialsNorm.txt” (Text-Tab Delimited) on the Desktop (Windows).

7. Close Excel workbook and discard changes.

8. The “R” open source computing package was opened and the following commands were entered:

9. R>a<-read.table("C:\\Users\\Tony\\Desktop\\AntibacterialsNorm.txt", header=T, sep="\t", row.names=1) #read data into dataframe a

10. R>prcomp(a)->b #PCA of dataframe b, results to c

11. R>summary(b) #prints summary of % PC contributions

12. R>b #prints the rotation (loading) matrix

13. R>b$x #prints the rotated data (scores)

14. The command in step 13 prints the rotated data (scores). Select and copy the first section of this data (PC1–PC10, without top headers).

15. Paste results into a MS Word text file and change font to Courier New 5 pt.

16. Save MS Word file as: “PC Scores.txt” (Select “Windows (Default)” for text encoding, end lines with “CR/LF” from dropdown menu. Uncheck the boxes marked “insert line breaks” and “allow character substitution”).

17. Open MS Excel workbook from earlier, create a new worksheet “Scores” and import the .txt file by selecting “Get External Data” in the Data menu, then select “From Text.”

18. Check the delimited button, click next, and select the “space” delimiter. Check the box marked “treat consecutive delimiters as one.” Click Finish.

19. The first three columns (compound numbers, PC1, PC2, and PC3) were copied into a new worksheet “PCA”, and the Number format was designated to 4 decimal places.

20. Each group of compounds was sorted in order of ascending PC1 to facilitate location on the PCA plot.

21. PCA plots of PC1 vs. PC2, PC1 vs. PC3, and PC3 vs. PC2 were generated by importing the scores in GraphPad Prism.

22. To obtain loading plots, repeat steps 14–21 for the component loadings in step 12.

23. To generate biplots, overlay the PCA plots with loading plots using the Layout feature in GraphPad Prism.

Following PCA, all 141 compounds were plotted on newly generated, unitless, orthogonal axes (principal components) that are based on linear combinations of the original 20 parameters (**Figure 1a, Figures S1**). Summary information from R is shown below in **Table S6**.

Table S6. Standard deviation and percent contribution for each principal component in PCA plot of antibacterials (R summary).

	PC1	PC2	PC3	PC4	PC5	PC6	PC7	PC8	PC9	PC10
Standard deviation	3.046	2.119	1.570	1.212	1.092	0.722	0.682	0.550	0.456	0.433
Proportion of Variance	0.442	0.214	0.117	0.070	0.057	0.025	0.022	0.014	0.010	0.009
Cumulative Proportion	0.442	0.656	0.773	0.843	0.900	0.924	0.947	0.961	0.971	0.980

These data indicate that 90% of the variation in the complete 20-dimensional dataset is accounted for by the five six principal components (PC1–PC5), due to correlations between some of the original 20 parameters. For visualization purposes, the first two principal components (PC1, PC2) were used to generate the plots shown in **Figure 1a** of the manuscript. Together, these principal components account for 66% of the variation in the complete dataset, with individual contributions of 44% and 21%, respectively (**Table S6**).

The component loadings generated from the PCA were used to construct loading plots using GraphPad Prism (**Figure S2**). These data indicate that MW, O, HBD, HBA, and tPSA have the largest loadings on PC1 and shift molecules to the right along PC1 in the PC1 vs. PC2 (**Figures S2a, d**) and PC1 vs. PC3 (**Figure S2b, d**) plots. The descriptors with the largest loadings on PC2 are ALogPs and RngAr, which shifts molecules to the top of the PC1 vs. PC2 (**Figure S2a, d**) and PC3 vs. PC2 (**Figures S2c, d**) plots, and ALogpS and relPSA, which shifts molecules to the bottom of these plots. The descriptors with the largest loadings on PC3 are nStMW and Fsp^3, which shifts molecules to the left along PC3, and N and RngAr, which shifts molecules to the right along PC3.

To compare the physicochemical properties of the 10 sulfonyladenosines evaluated in bacterial compound accumulation assays (**Figure 3**), we conducted an additional PCA incorporating these sulfonyladenosines, 50 top selling, brand-name, non-antiinfectives, and 91 antibacterials (**Figures S4–S5**).

To evaluate the robustness of PCA on a smaller dataset, we conducted separate PCAs on the 10 sulfonyladenosines used in the compound accumulation assays (**Figure S7**) and the 9 sulfonyladenosines that accumulated to detectable levels in the compound accumulation assays (data not shown). The relative positions of each compound were not substantially affected when each plot was compared to the other and the PCA with non-antiinfectives and antibacterials.

For PCA analyses that included sulfonyladenosines, we used the physicochemical properties of sulfonyladenosines in their non-ionized forms. Using the physicochemical properties of the pH 7.4 ionized forms did not substantially alter the PCA results for correlations between properties and *E. coli* accumulation shown in **Figure 5a** and **Figure S8**.

H. ^{1}H-NMR AND ^{13}C-NMR SPECTRA

1. Preparation of *N*-hydroxysuccinamide esters (S1a–f) S44

2. Coupling reactions between *N*-hydroxysuccinamide esters (S1a–f) and sulfamoyl adenosines (S2a or S2b) S50

3. Deprotection to acyl-AMS compounds S56

a. L-Lactyl-AMS (**4**) S56
b. Methyl-succinyl-AMS (**5**) S57
c. 4-Phenylbenzoyl-AMS (**9**) S58
d. Decanoyl-AMS (**10**) S59
e. Glycolyl-AMS (**S4**) S60
f. Hexanoyl-AMS (**S5**) S61

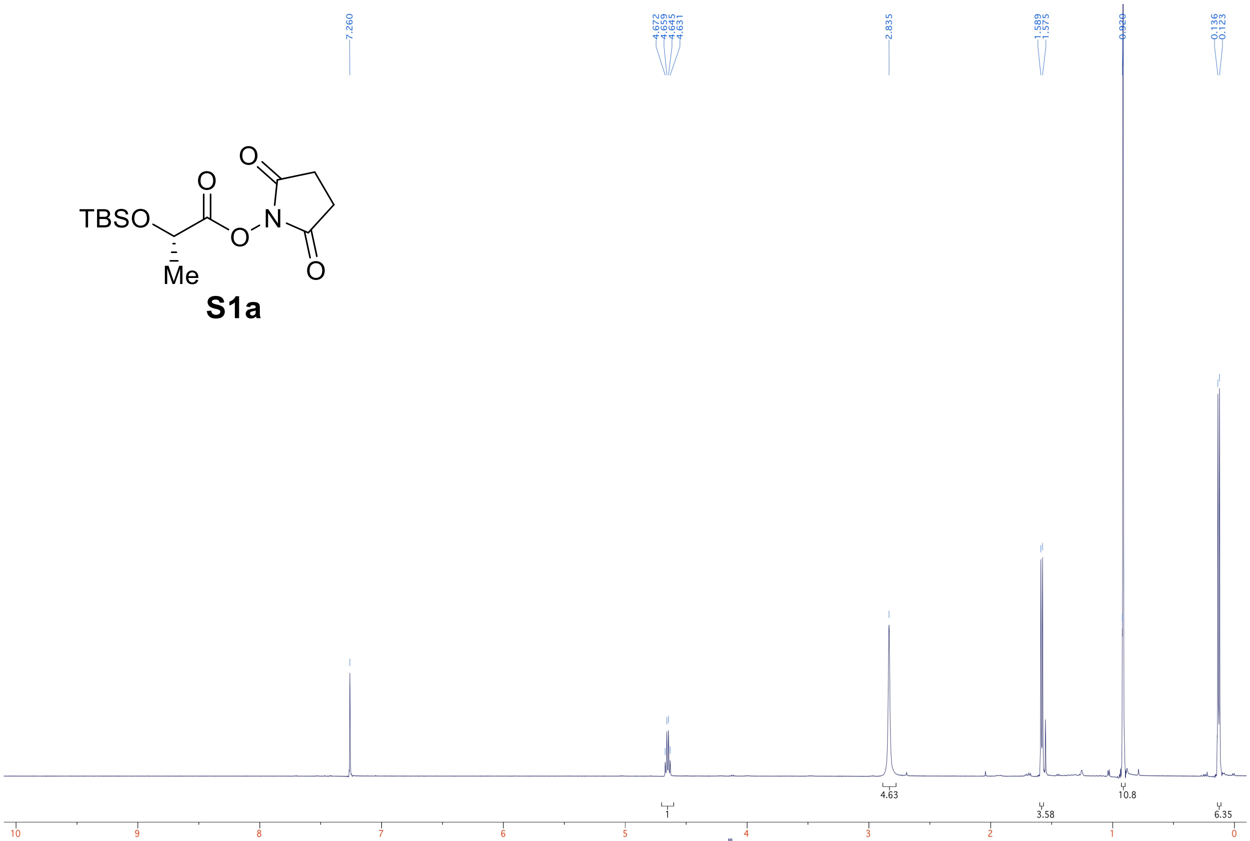
TBSO
O
O
N
O
O
Me
7.260
4.672
4.659
4.645
4.631
2.835
1.589
1.575
0.920
0.136
0.123
1
4.63
3.58
10.8
6.35

S1a

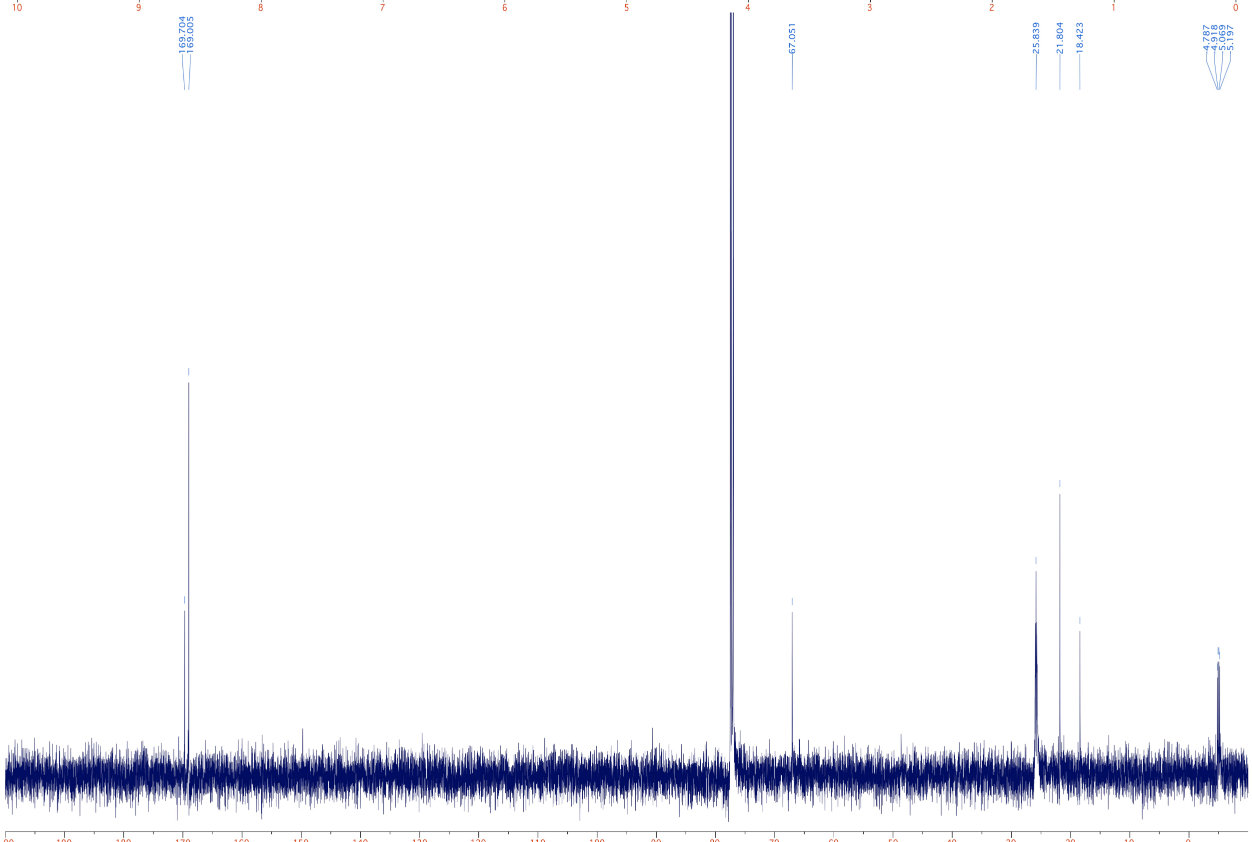
169.704
169.005
67.051
25.839
21.804
18.423
-4.787
-4.918
-5.069
-5.197

S1b

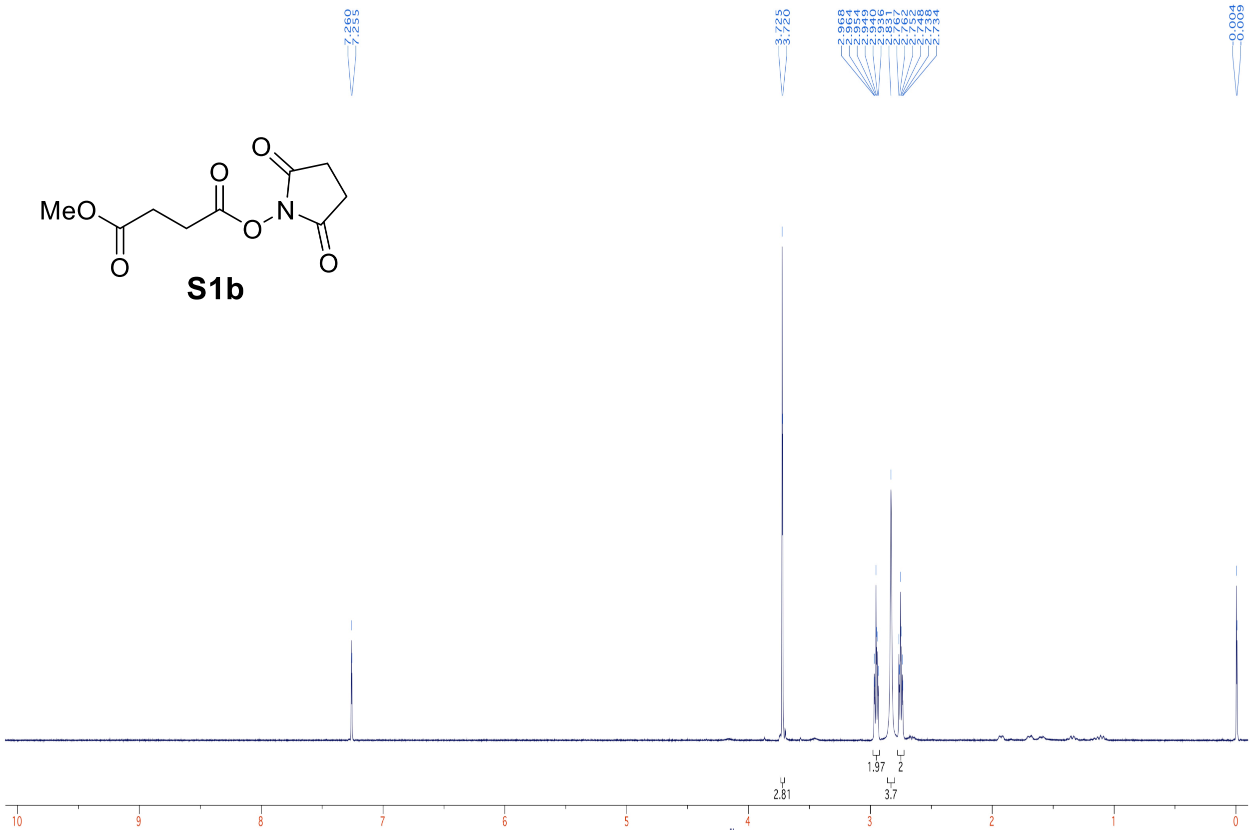
MeO
O
N
7.260
7.255
3.725
3.720
2.968
2.964
2.954
2.949
2.940
2.936
2.831
2.767
2.762
2.752
2.748
2.738
2.734
0.004
0.009
1.97
2
2.81
3.7
10 9 8 7 6 5 4 3 2 1 0

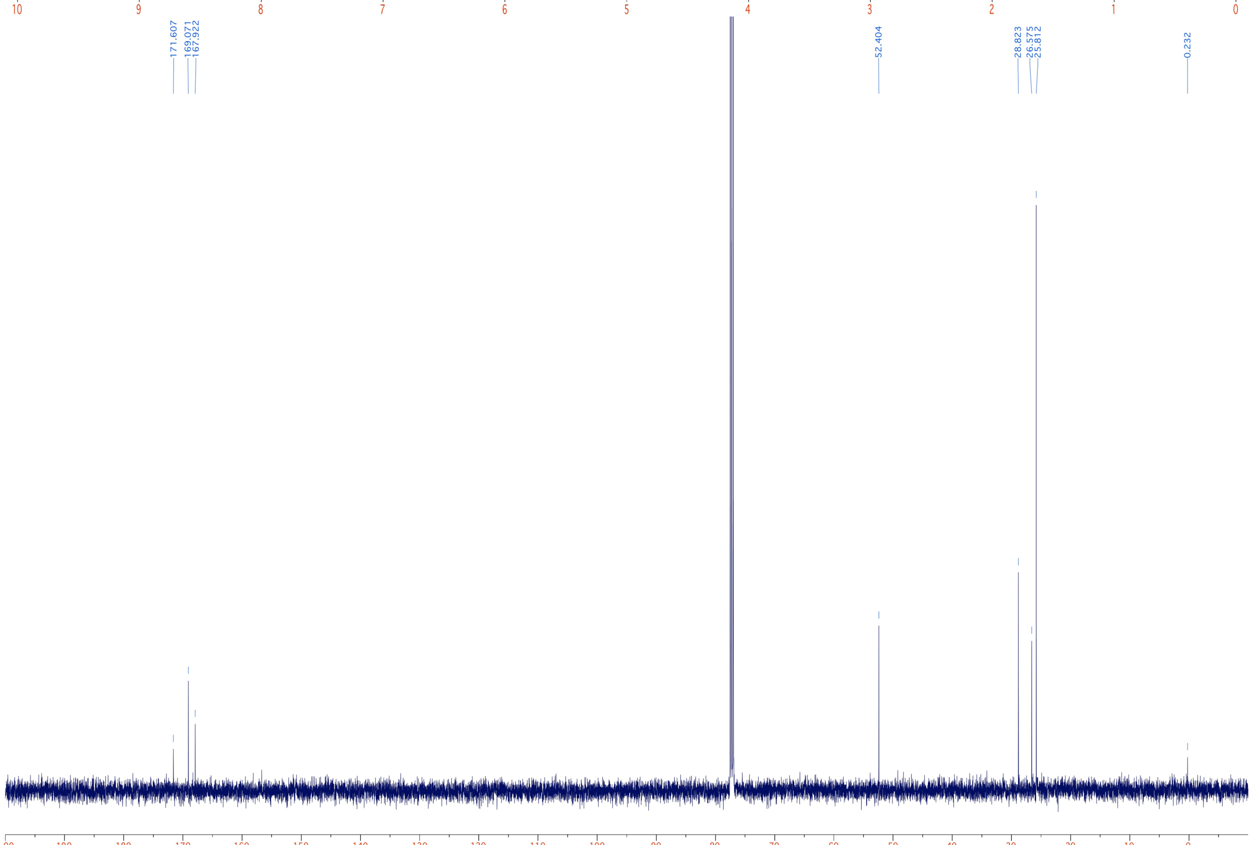
171.607
169.071
167.922
52.404
28.823
26.575
25.812
0.232
00 190 180 170 160 150 140 130 120 110 100 90 80 70 60 50 40 30 20 10 0

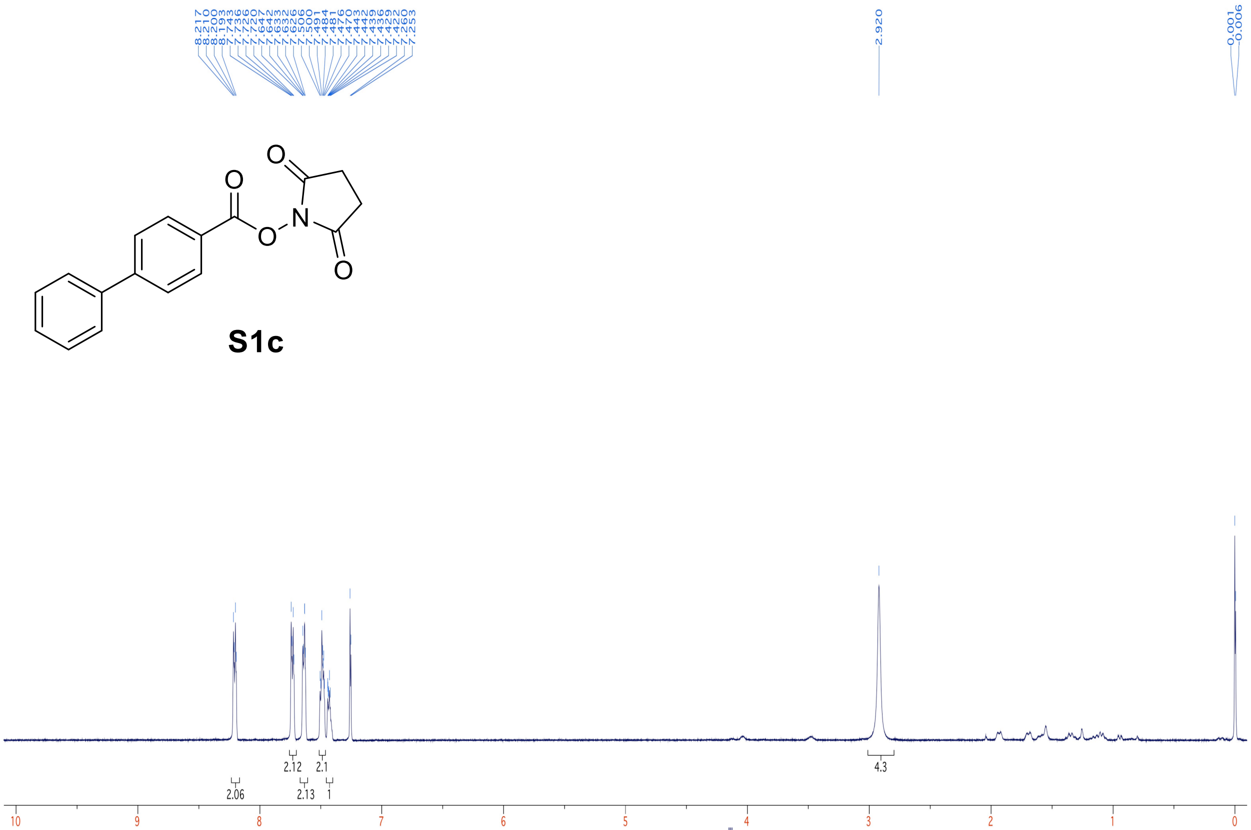
S1c
8.217
8.210
8.200
8.193
7.743
7.736
7.726
7.720
7.647
7.642
7.633
7.626
7.506
7.500
7.491
7.484
7.481
7.476
7.470
7.443
7.442
7.439
7.436
7.429
7.422
7.260
7.253
2.920
0.001
0.006
2.06
2.12
2.13
2.1
1
4.3
10 9 8 7 6 5 4 3 2 1 0

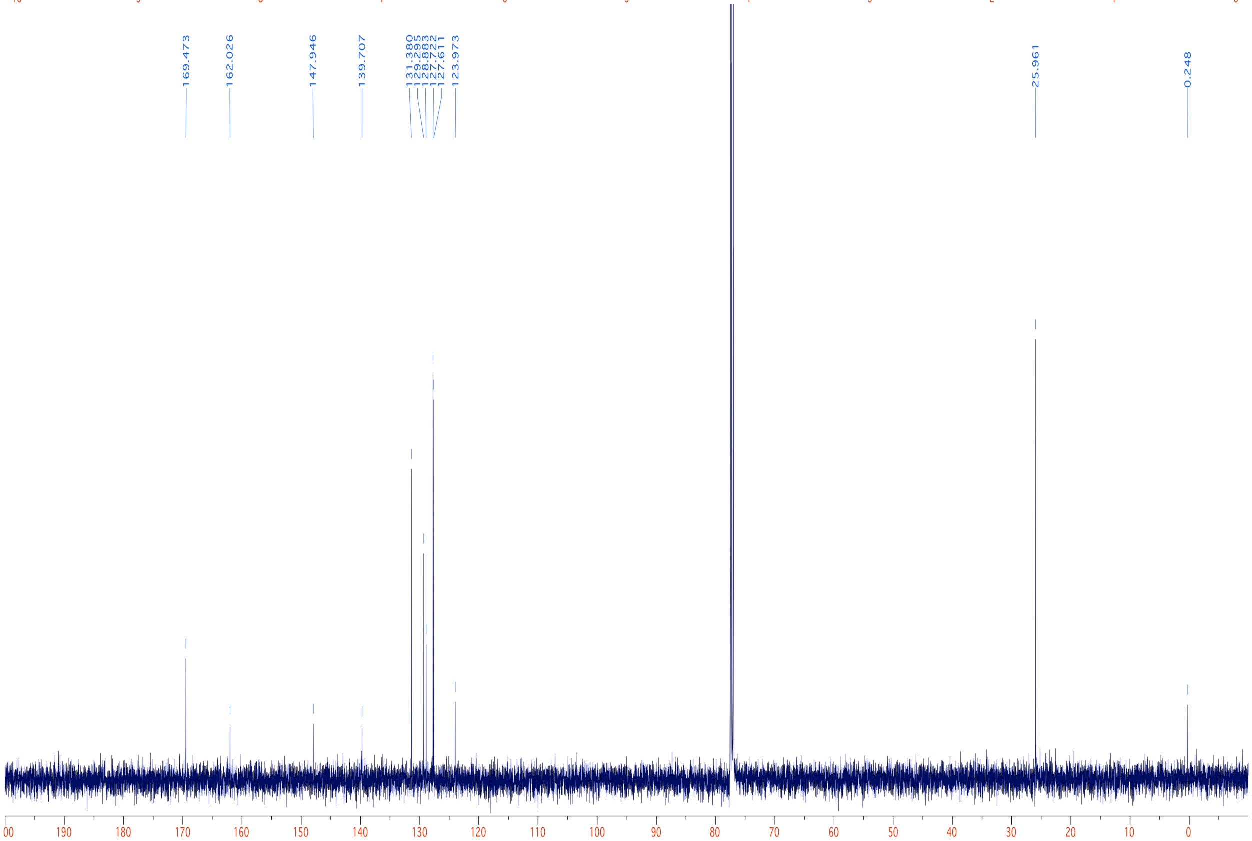
169.473
162.026
147.946
139.707
131.380
129.295
128.883
127.722
127.611
123.973
25.961
0.248
200 190 180 170 160 150 140 130 120 110 100 90 80 70 60 50 40 30 20 10 0

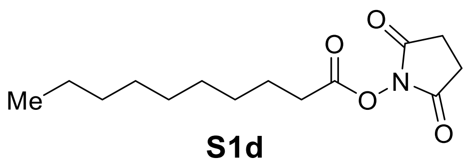
O
O
Me
O
N
O
O

S1d

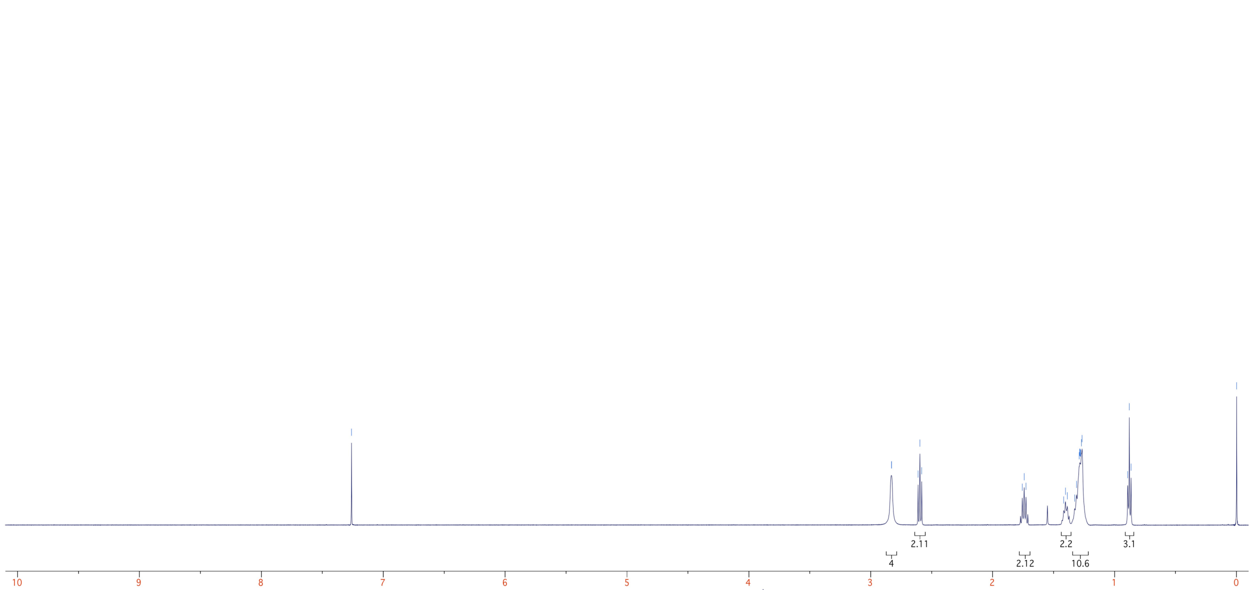
7.260
2.830
2.829
2.612
2.597
2.582
1.757
1.742
1.726
1.417
1.403
1.387
1.327
1.312
1.290
1.295
1.284
1.283
1.279
1.271
1.267
0.892
0.879
0.865
-0.002
4
2.11
2.12
2.2
10.6
3.1
10
9
8
7
6
5
4
3
2
1
0

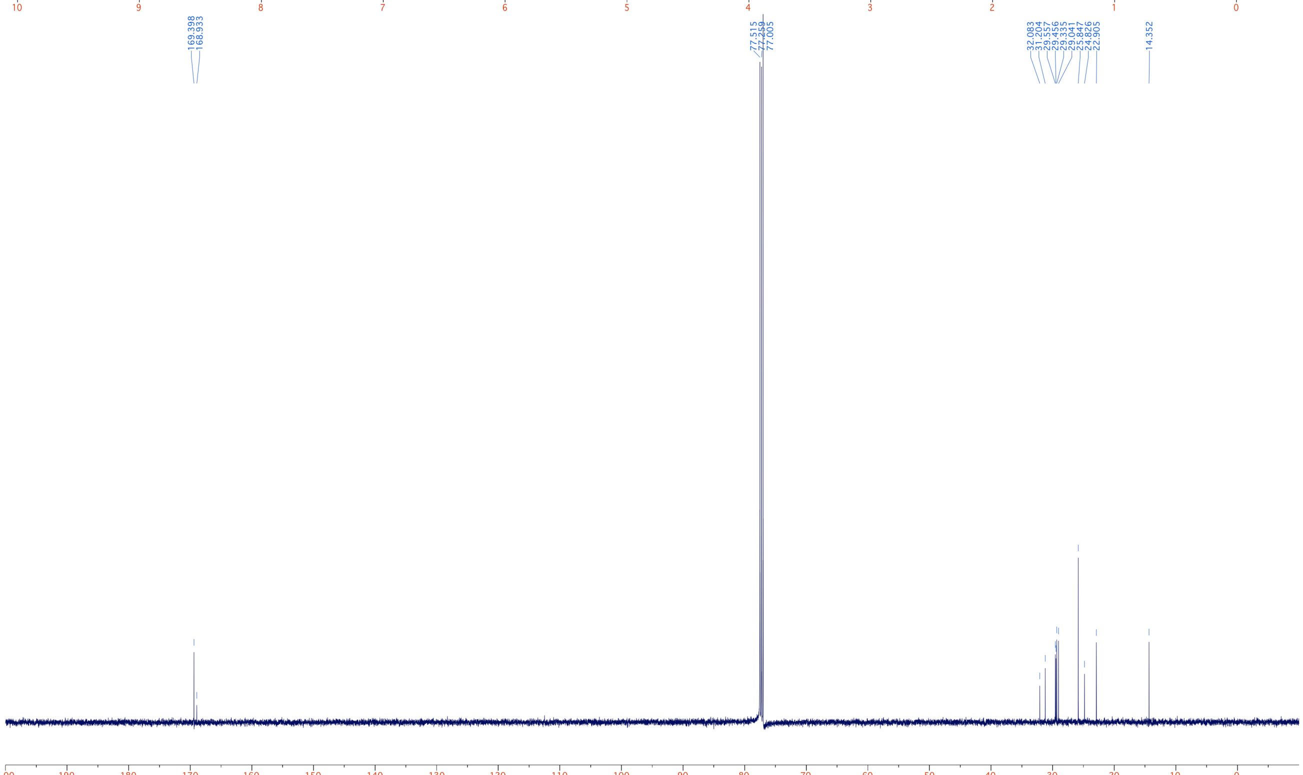
169.398
168.933
77.515
77.259
77.005
32.083
31.204
29.557
29.436
29.335
29.041
25.847
24.826
22.905
14.352
190
180
170
160
150
140
130
120
110
100
90
80
70
60
50
40
30
20
10
0

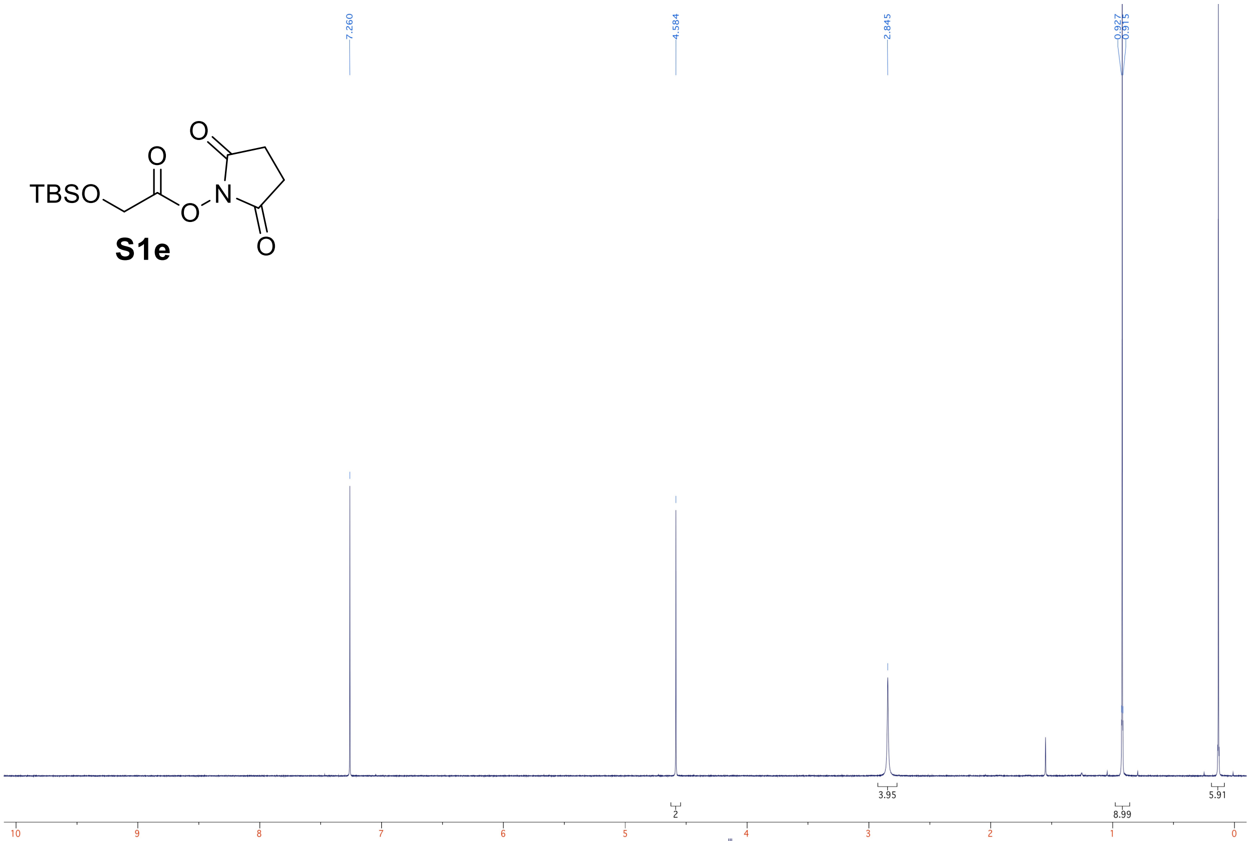
TBSO
S1e
7.260
4.584
2.845
0.927
0.915
3.95
2
8.99
5.91
10
9
8
7
6
5
4
3
2
1
0

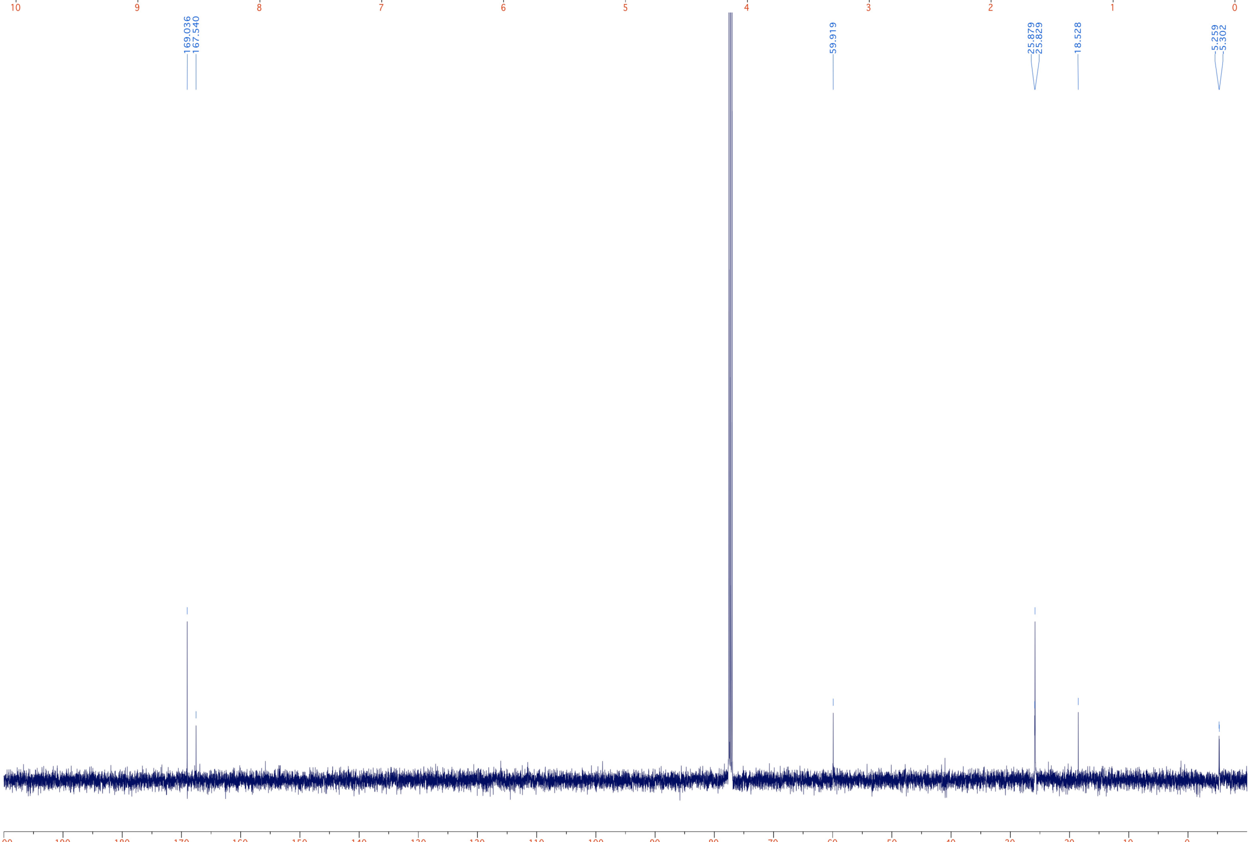
169.036
167.540
59.919
25.879
25.829
18.528
-5.259
-5.302
190
180
170
160
150
140
130
120
110
100
90
80
70
60
50
40
30
20
10
0

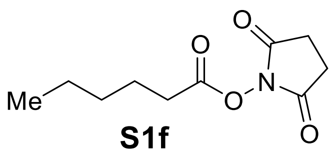

S1f

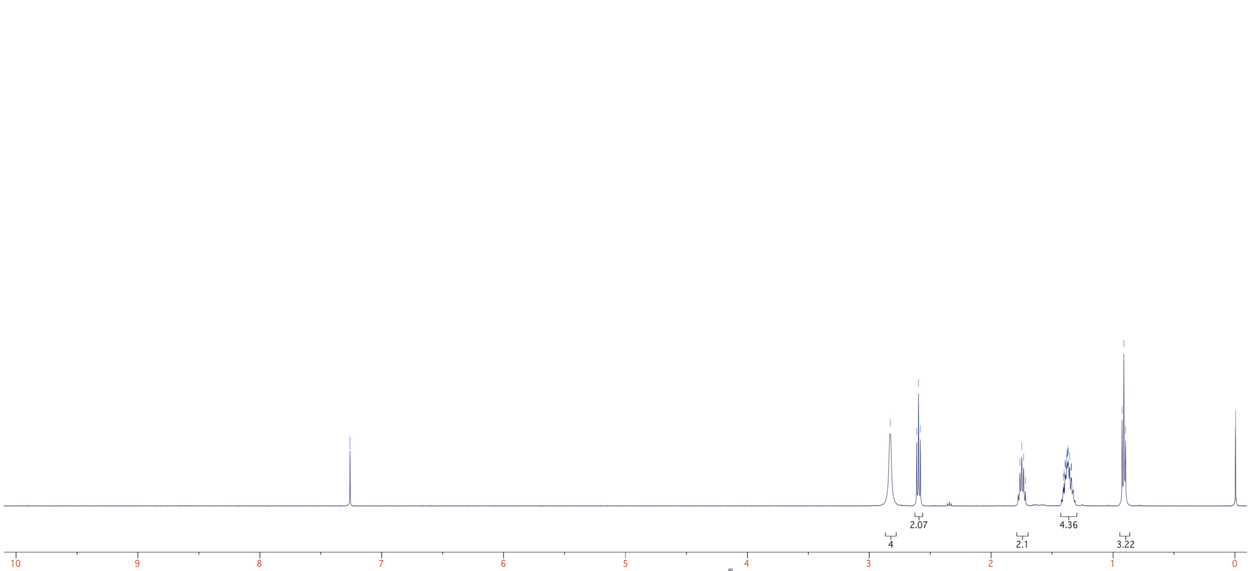

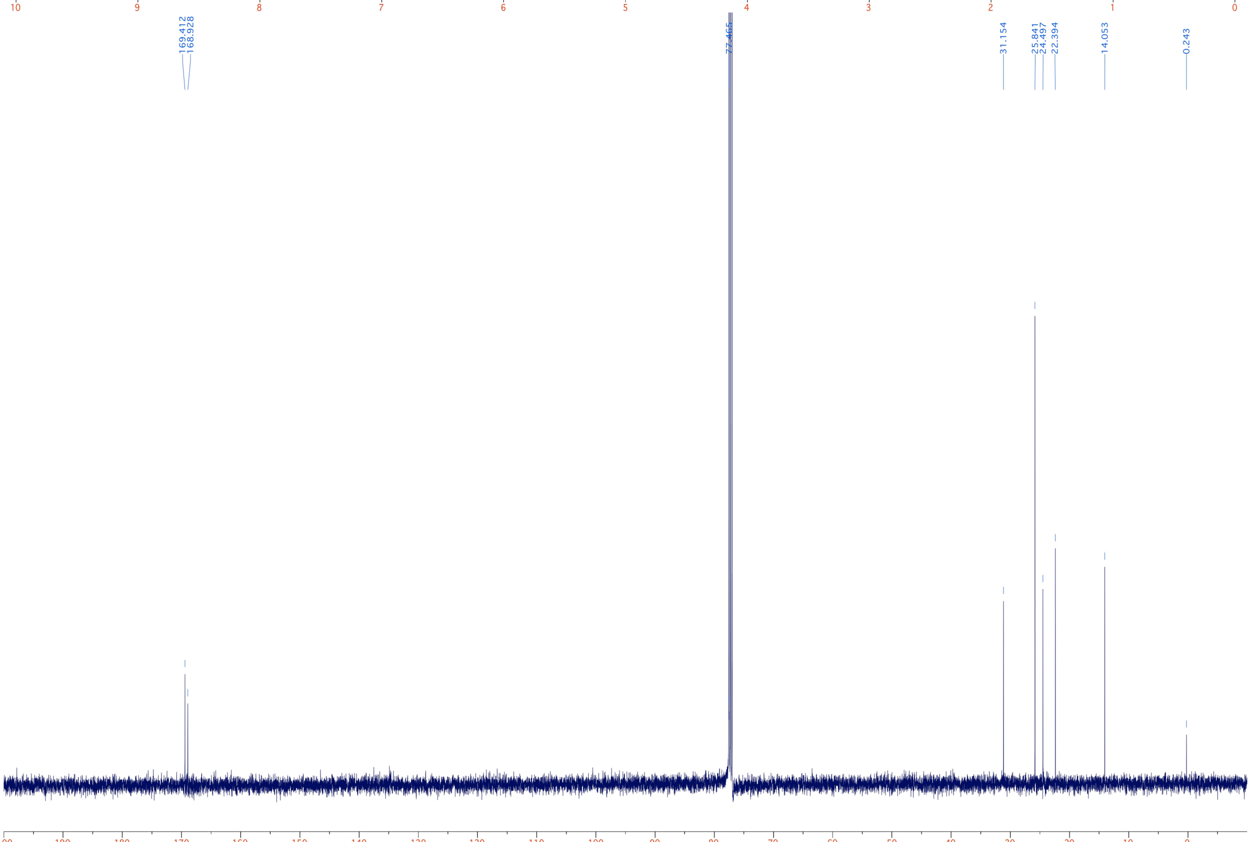

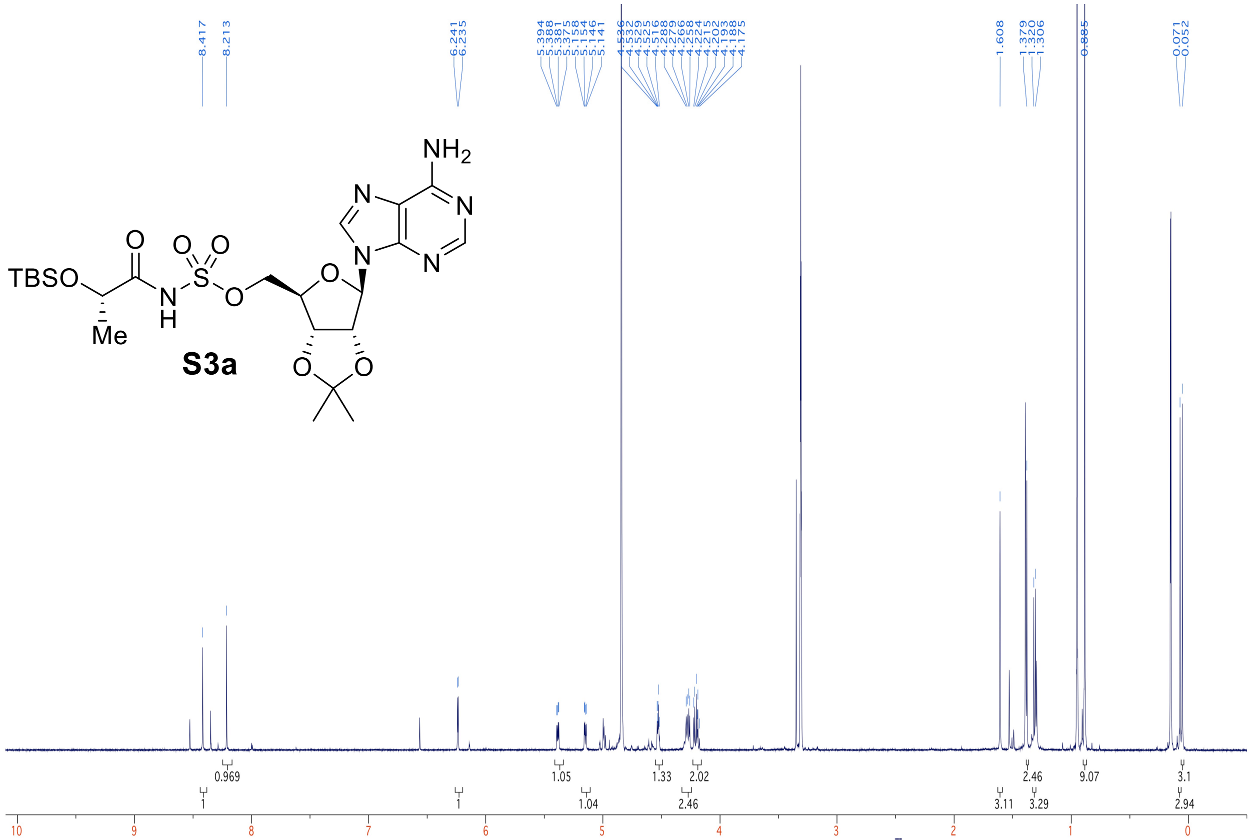

TBSO
Me
NH2
S3a
8.417 8.213
6.241 6.235
5.394 5.388 5.381 5.375 5.158 5.154 5.146 5.141
4.536 4.532 4.529 4.525 4.516 4.288 4.279 4.266 4.258 4.224 4.215 4.202 4.193 4.188 4.175
1.608 1.379 1.320 1.306
0.885
0.071 0.052
0.969 1 1 1.05 1.04 1.33 2.46 2.02 3.11 2.46 3.29 9.07 3.1 2.94
10 9 8 7 6 5 4 3 2 1 0

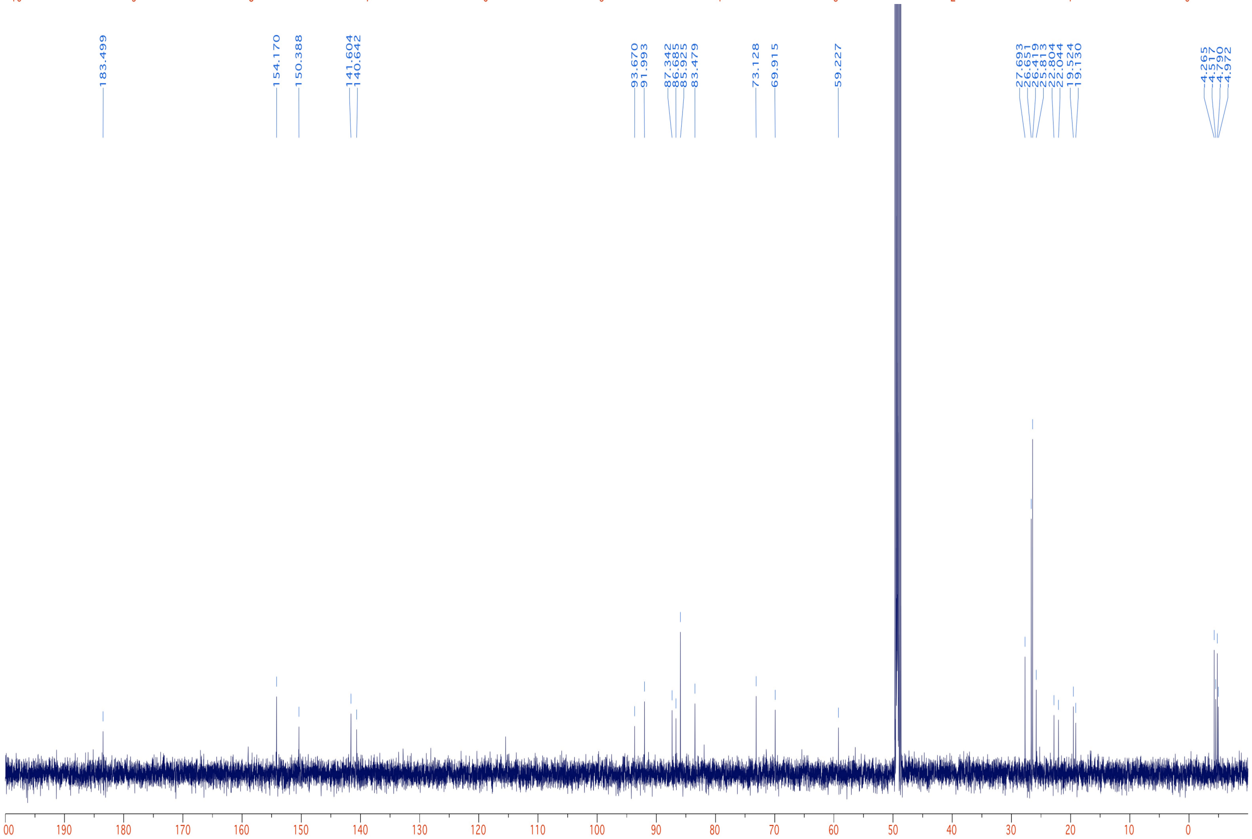

183.499
154.170 150.388
141.604 140.642
93.670 91.993 87.342 86.685 85.925 83.479
73.128 69.915
59.227
27.693 26.651 26.419 25.813 22.804 22.044 19.524 19.130
4.265 4.517 4.770 4.972
00 190 180 170 160 150 140 130 120 110 100 90 80 70 60 50 40 30 20 10 0

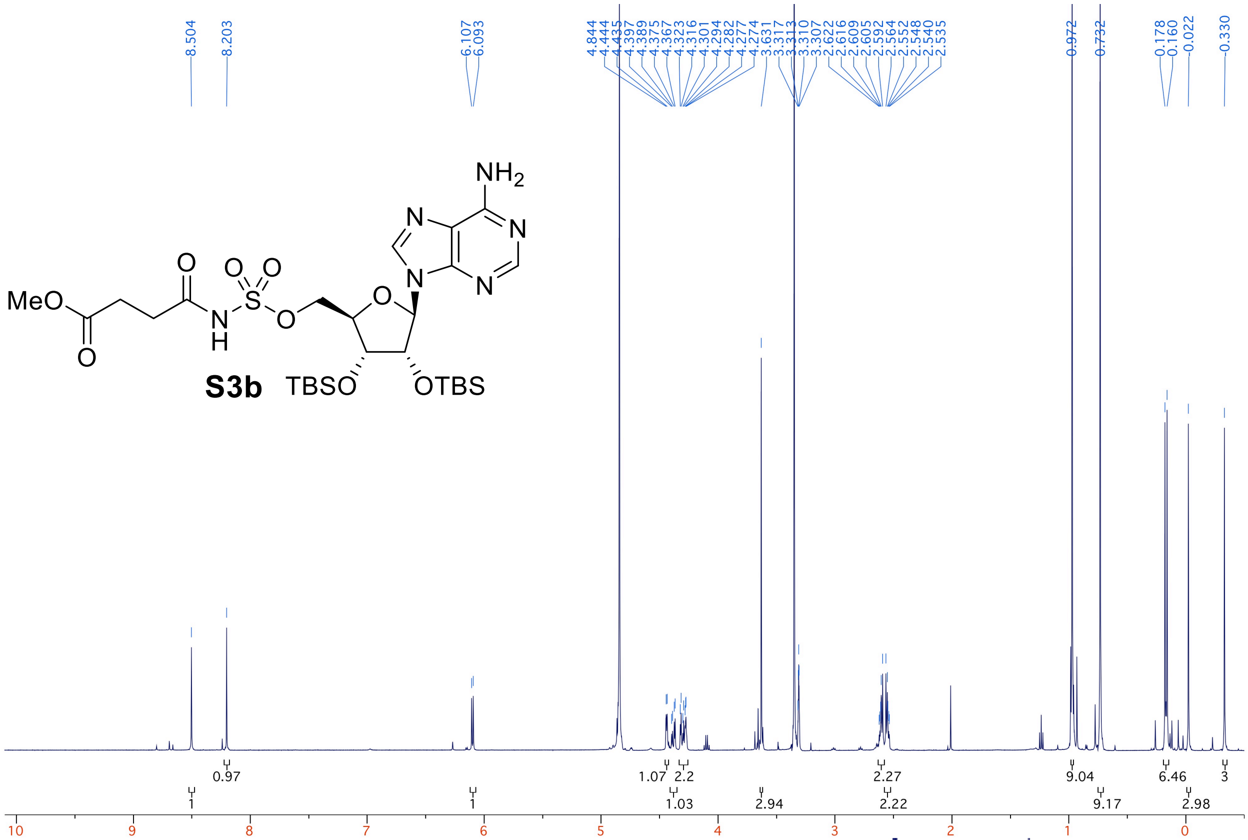

S3b

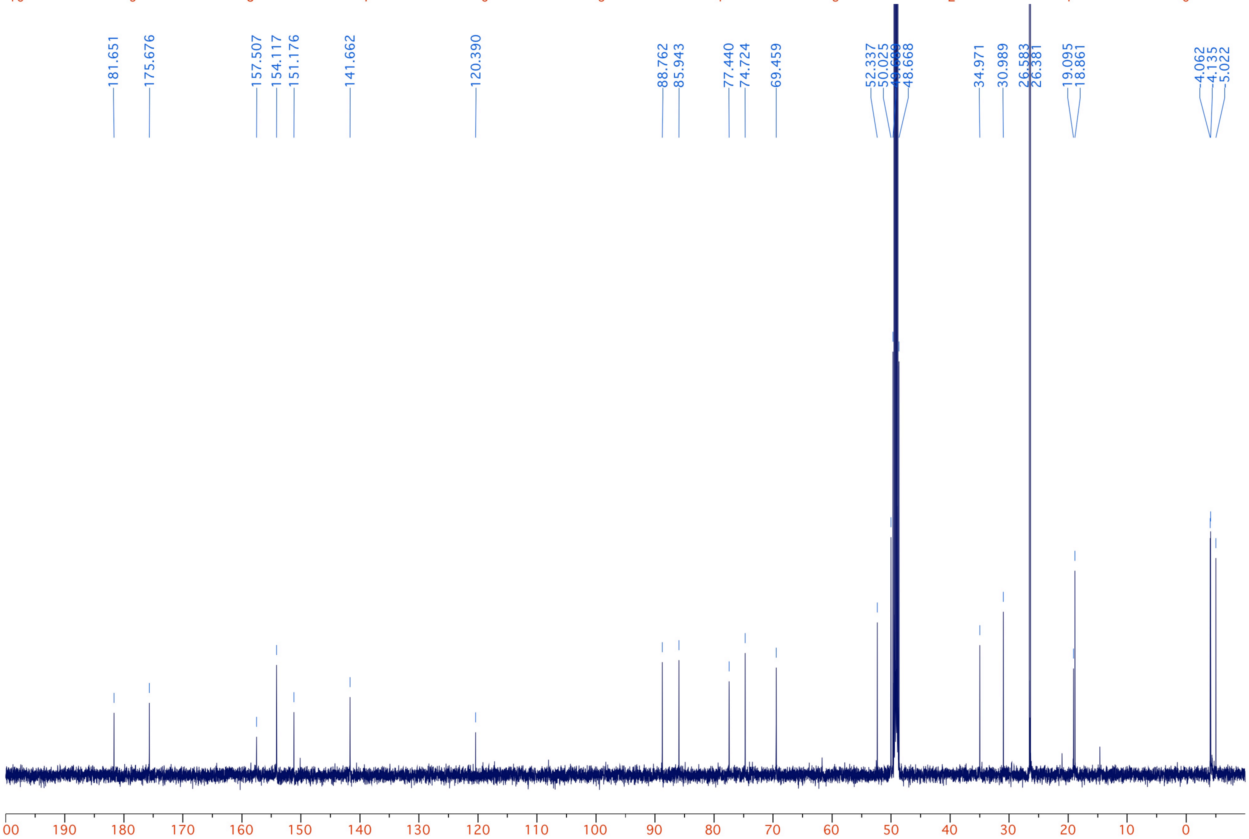

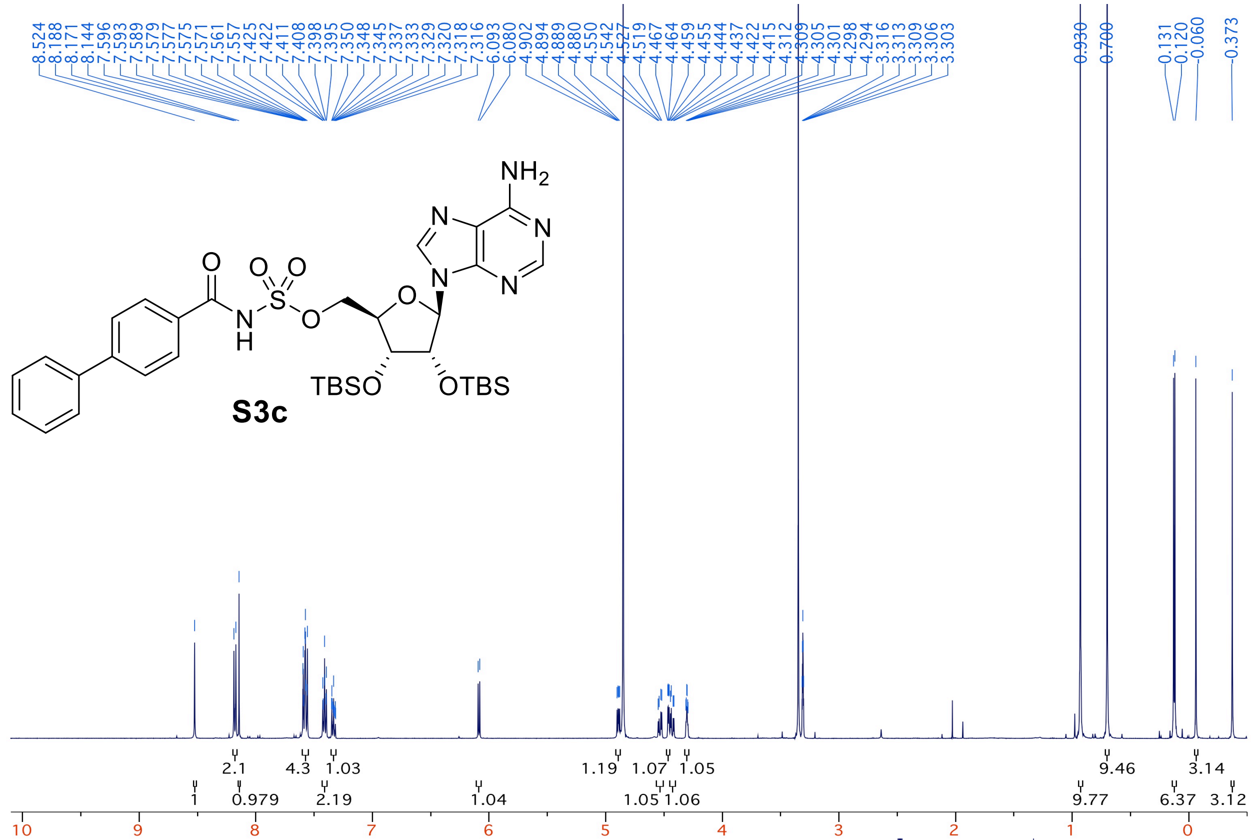
NH2
TBSO
OTBS
S3c

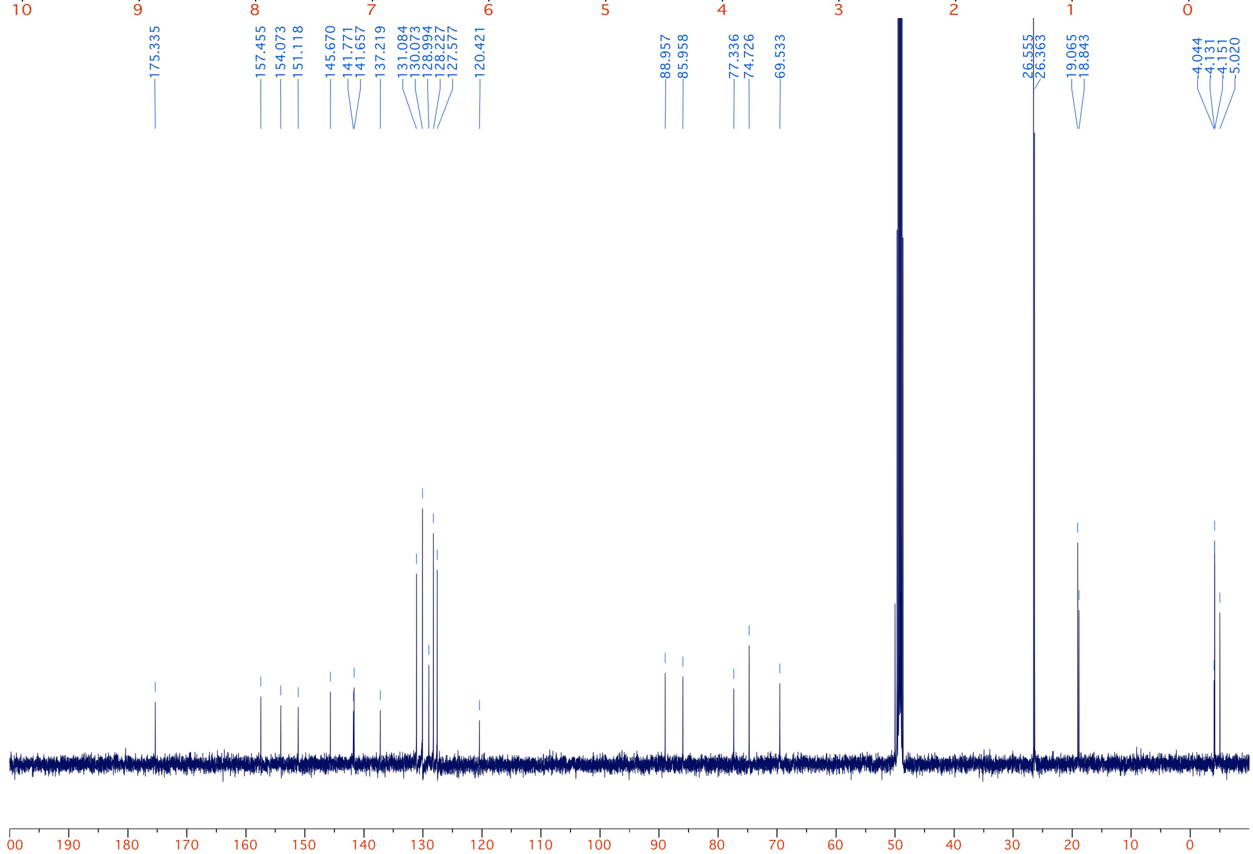

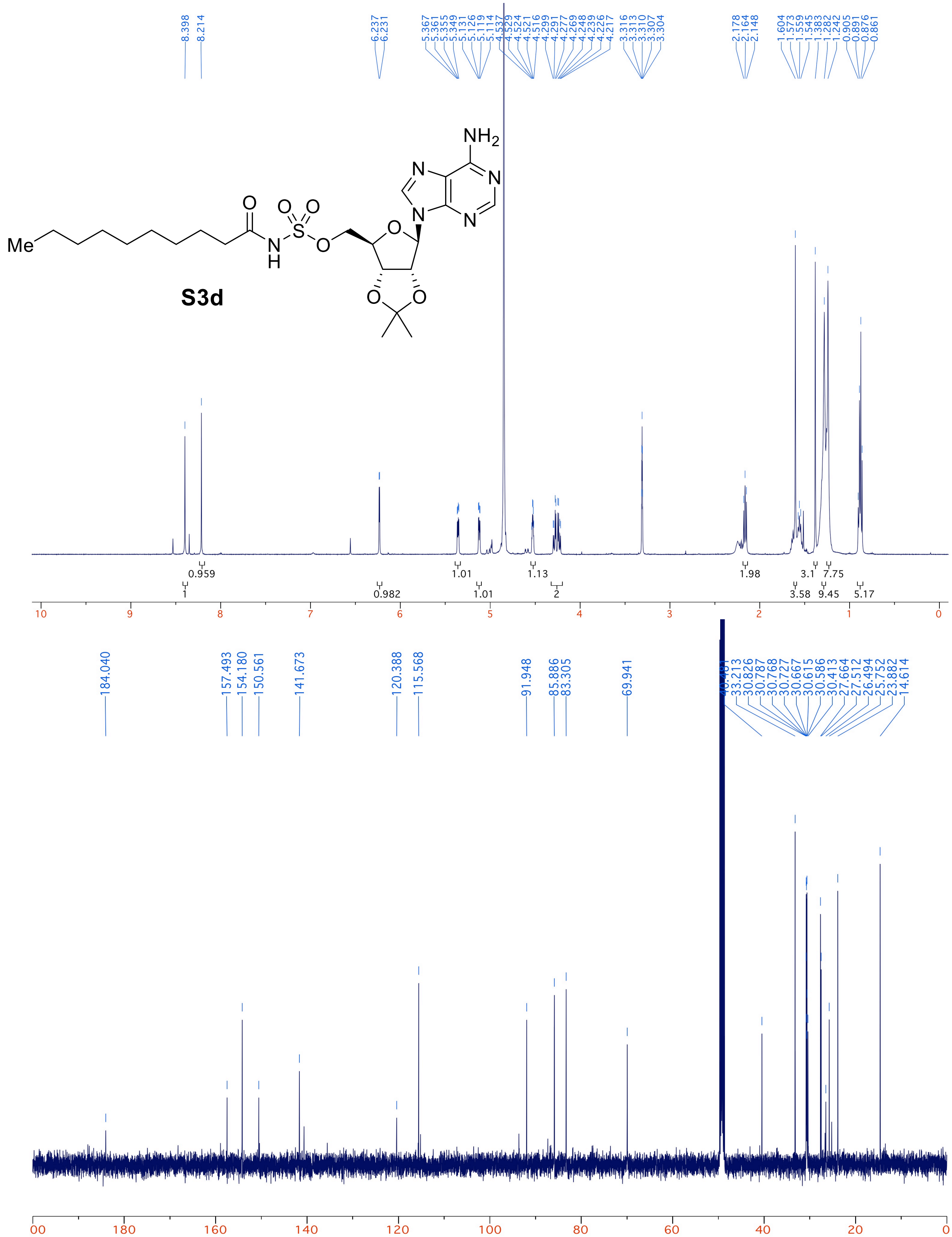
S3d
Me
NH2
N
O
S
H
184.040
157.493
154.180
150.561
141.673
120.388
115.568
91.948
85.886
83.305
69.941

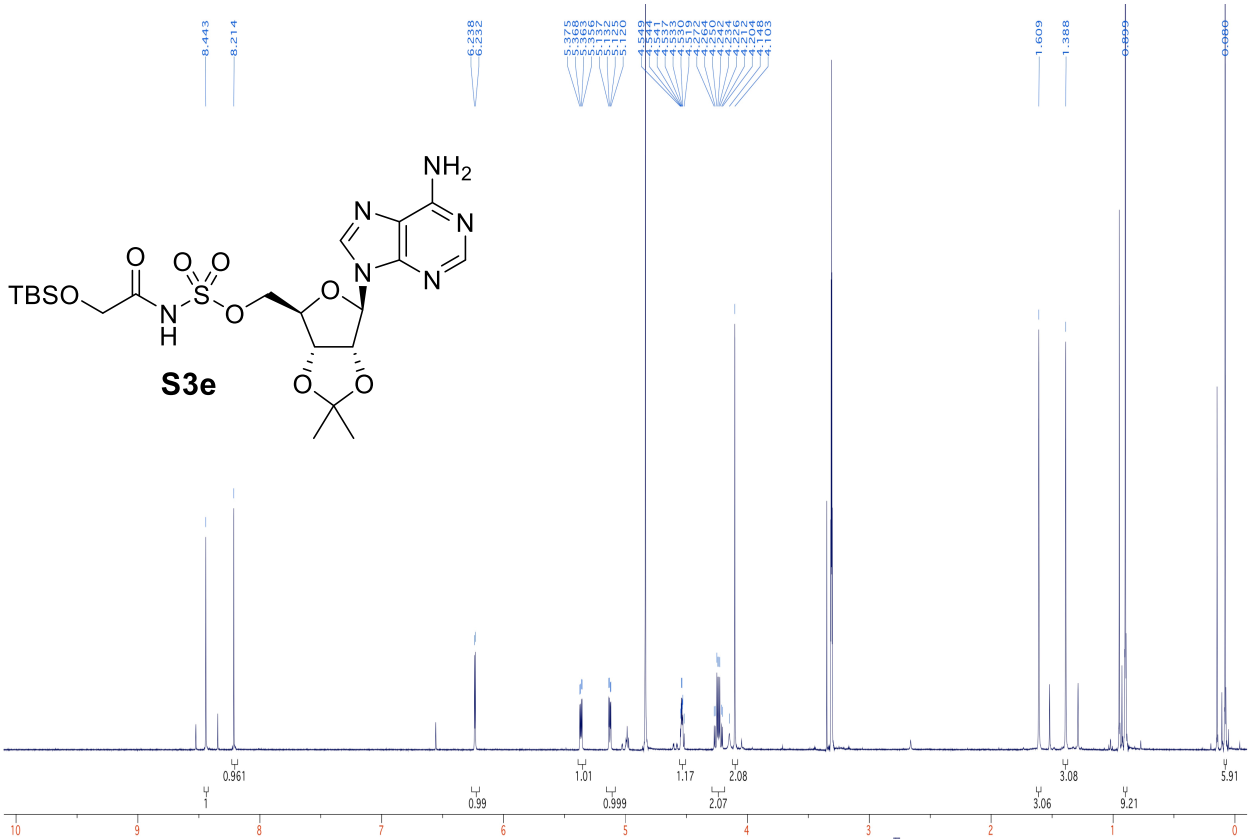

S3e

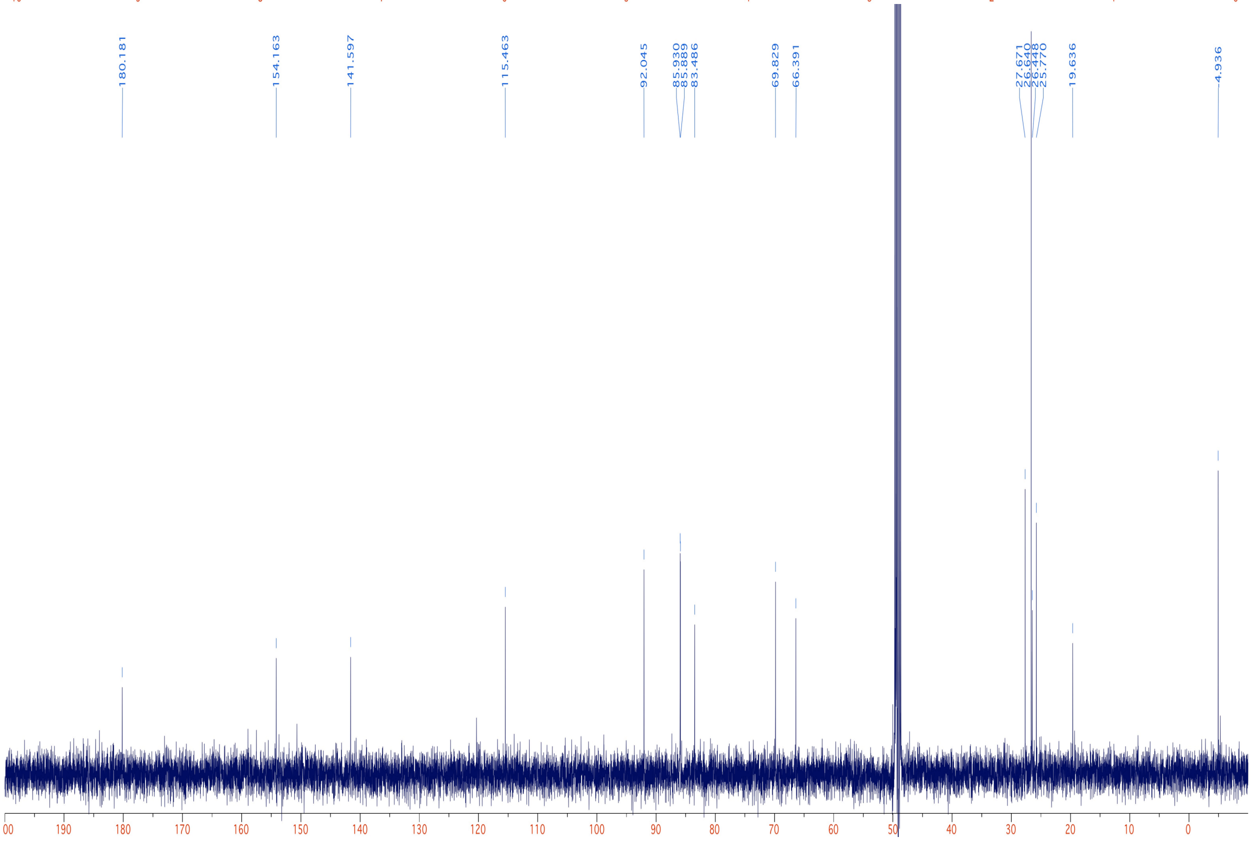

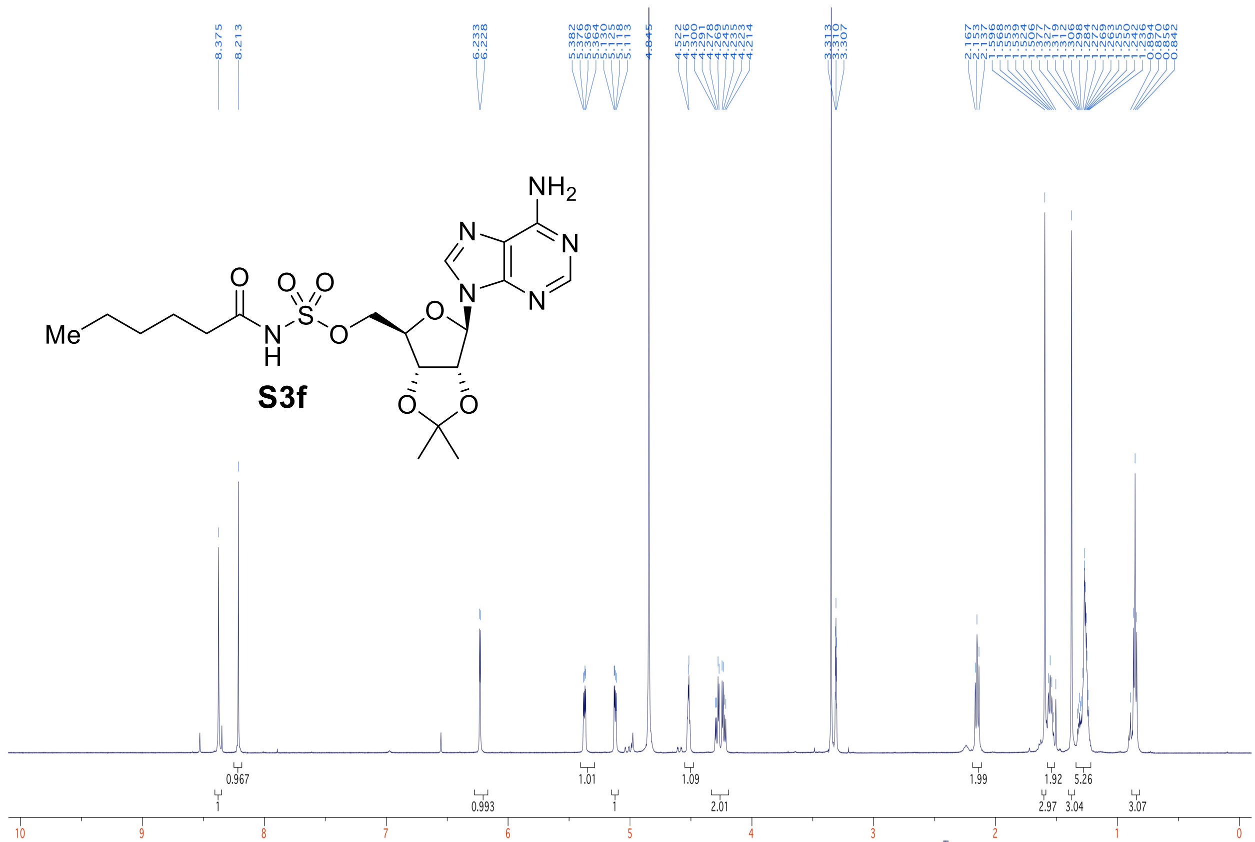
S3f
Me
NH2
8.375
8.213
6.233
6.228
4.845
3.313
3.310
3.307
0.967
1
0.993
1.01
1
1.09
2.01
1.99
1.92
5.26
2.97
3.04
3.07

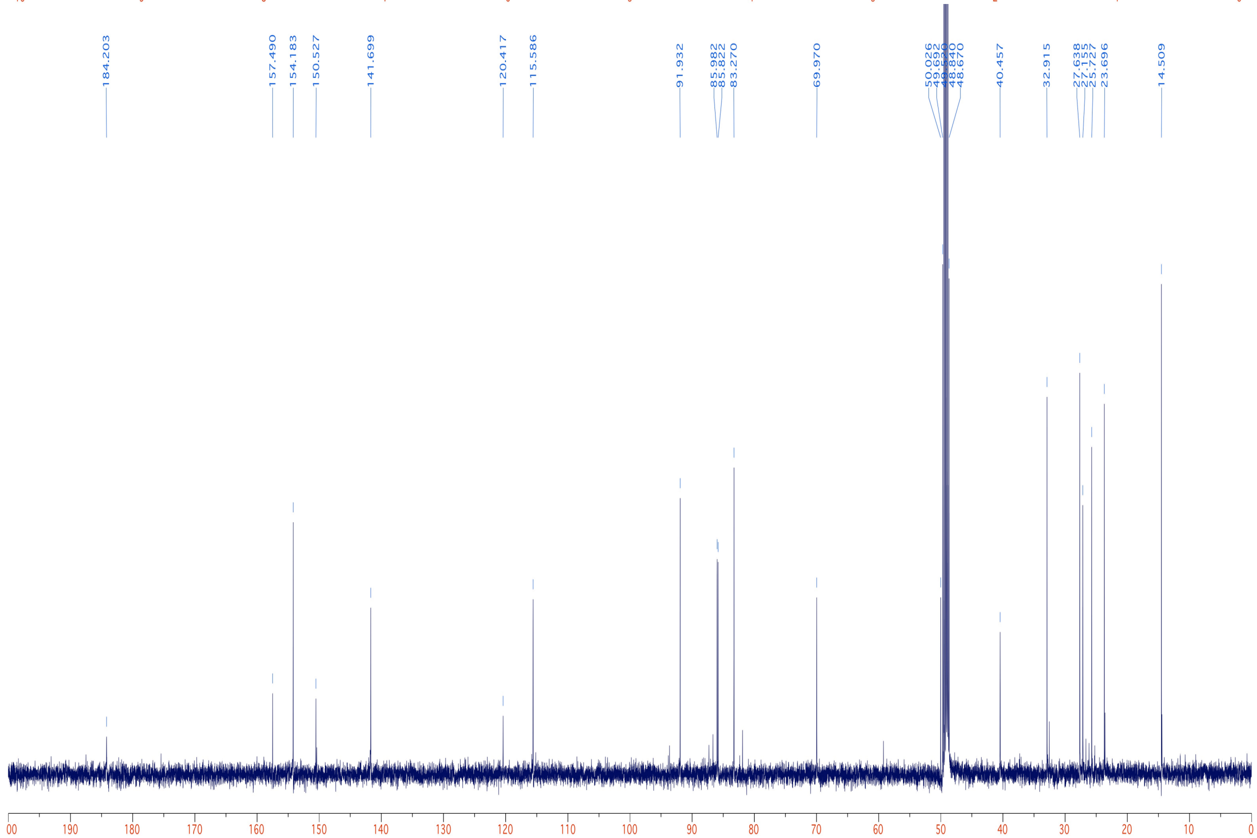
184.203
157.490
154.183
150.527
141.699
120.417
115.586
91.932
85.982
85.822
83.270
69.970
40.457
32.915
27.638
27.155
25.727
23.696
14.509

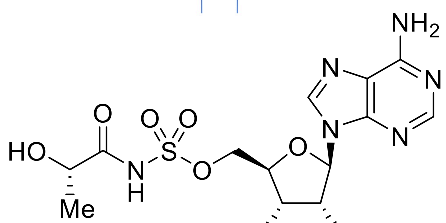
NH2
N
N
N
N
O
HO
O
O
S
N
H
O
O
Me
HO
OH

4

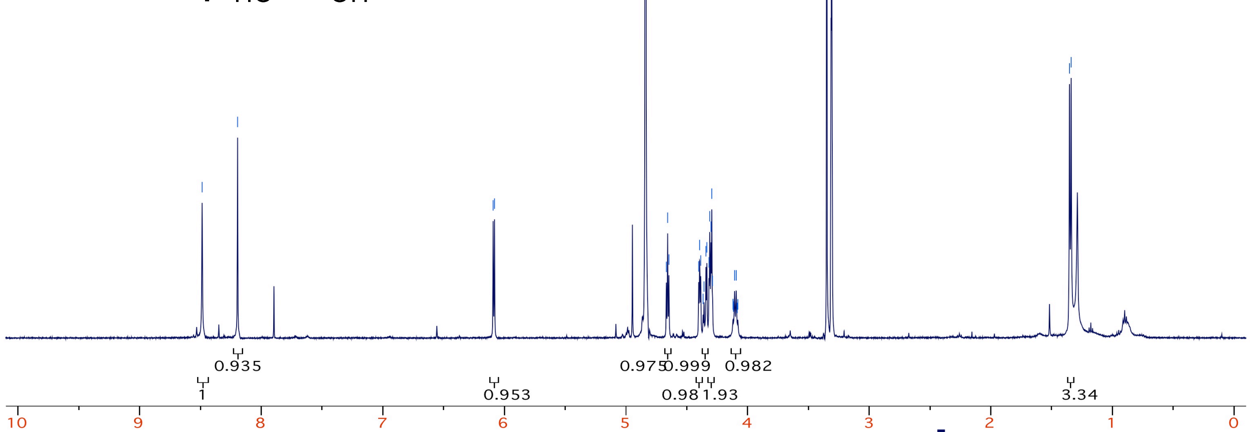
8.486
8.194
6.093
6.082
4.668
4.657
4.647
4.402
4.395
4.385
4.366
4.358
4.343
4.335
4.317
4.311
4.302
4.294
4.289
4.120
4.119
4.117
4.107
4.093
4.085
4.080
1.352
1.339
1
0.935
0.953
0.975
0.999
0.98
1.93
0.982
3.34
10
9
8
7
6
5
4
3
2
1
0

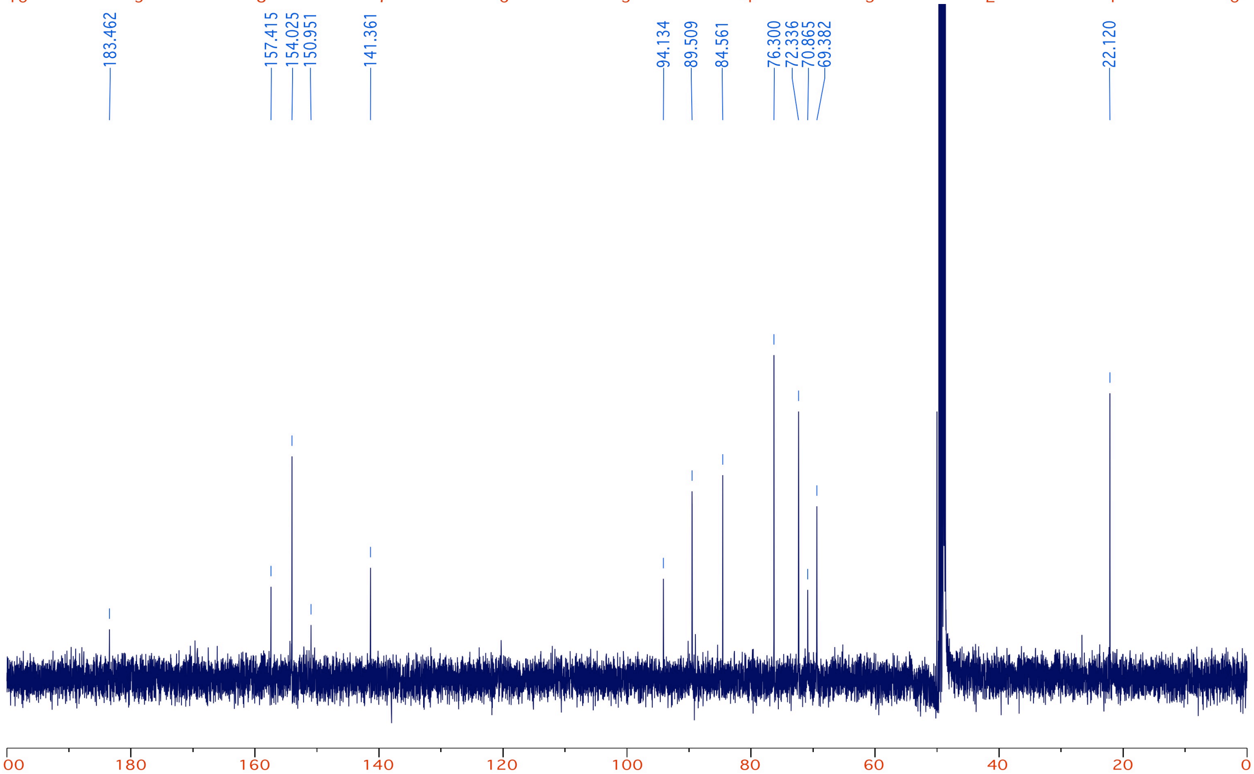
183.462
157.415
154.025
150.951
141.361
94.134
89.509
84.561
76.300
72.336
70.865
69.382
22.120
00
180
160
140
120
100
80
60
40
20
0

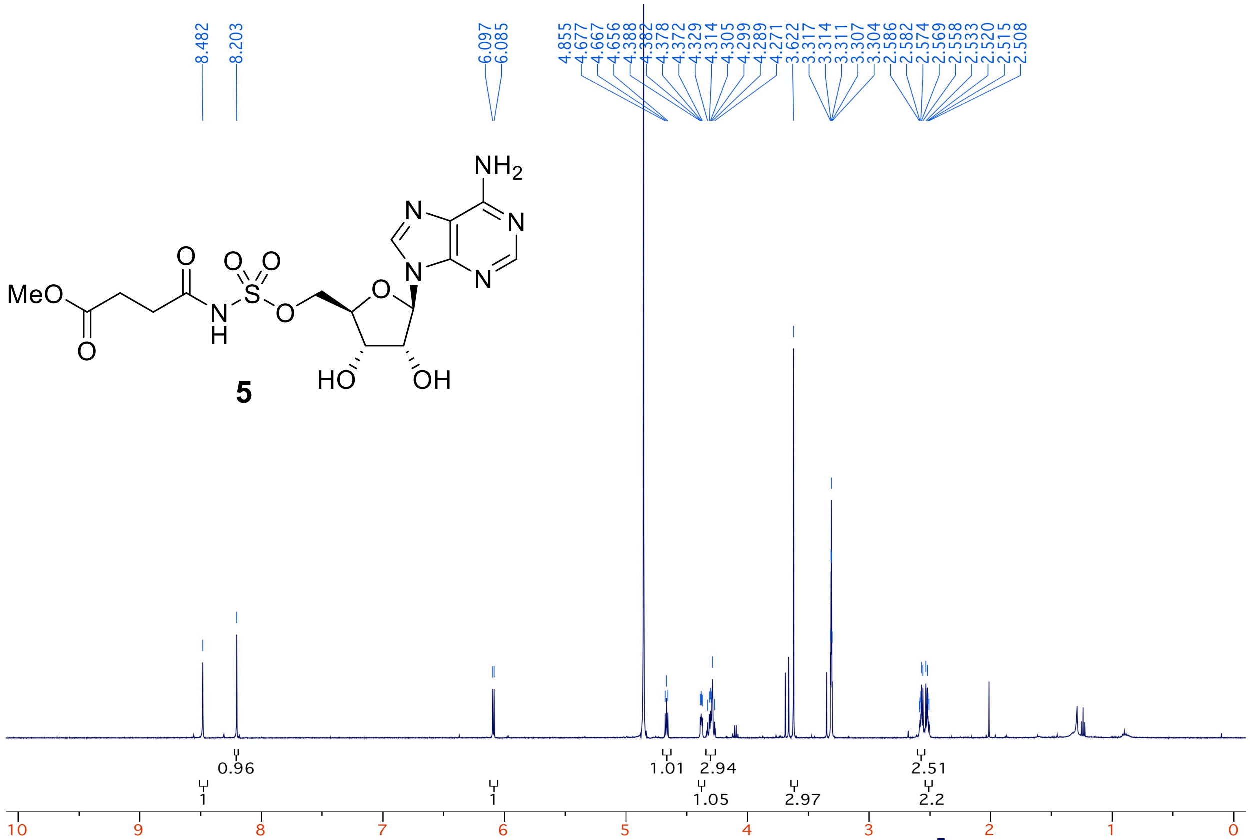
8.482
8.203
6.097
6.085
4.855
4.677
4.667
4.656
4.388
4.382
4.378
4.372
4.329
4.314
4.305
4.299
4.289
4.271
3.622
3.317
3.314
3.311
3.307
3.304
2.586
2.582
2.574
2.569
2.558
2.533
2.520
2.515
2.508
NH_2
MeO
N
H
O
HO
OH
5
0.96
1.01
2.94
2.51
1
1
1.05
2.97
2.2
10 9 8 7 6 5 4 3 2 1 0

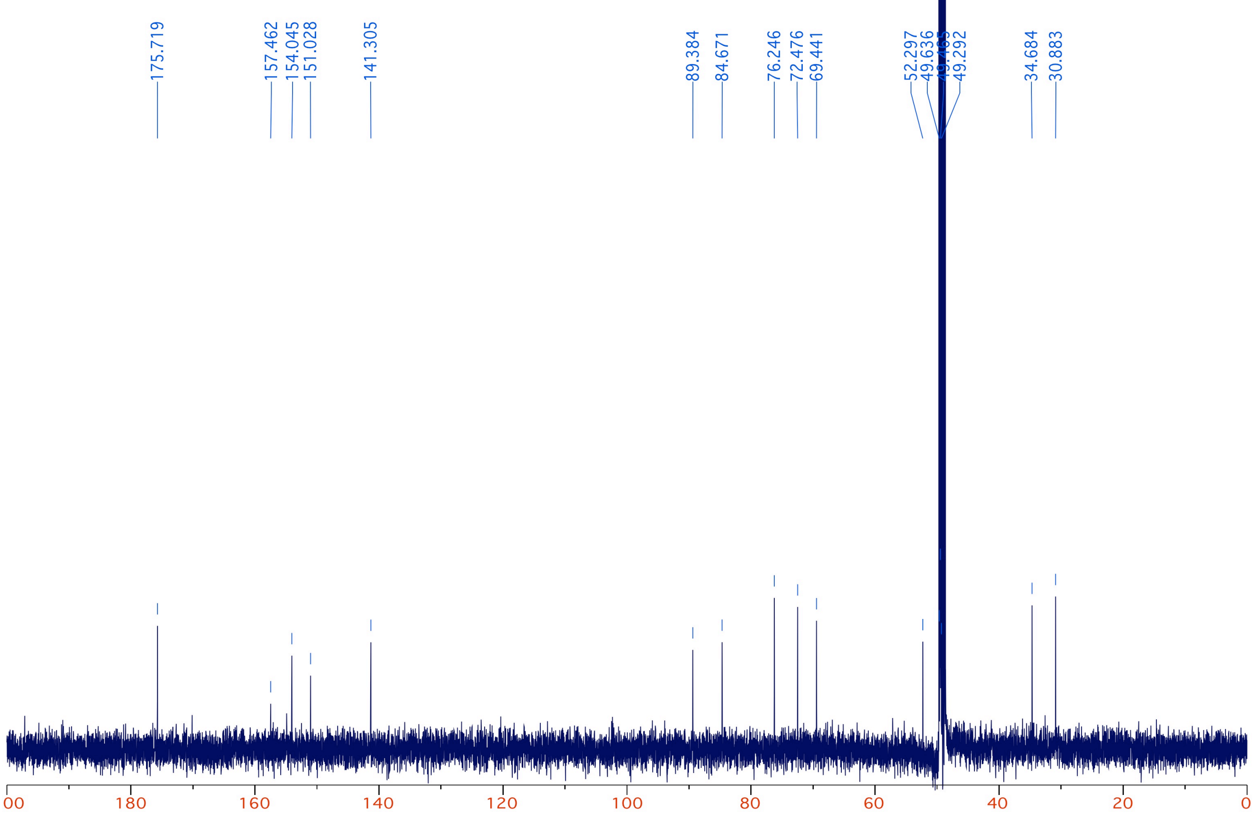
175.719
157.462
154.045
151.028
141.305
89.384
84.671
76.246
72.476
69.441
52.297
49.636
49.292
34.684
30.883
00 180 160 140 120 100 80 60 40 20 0

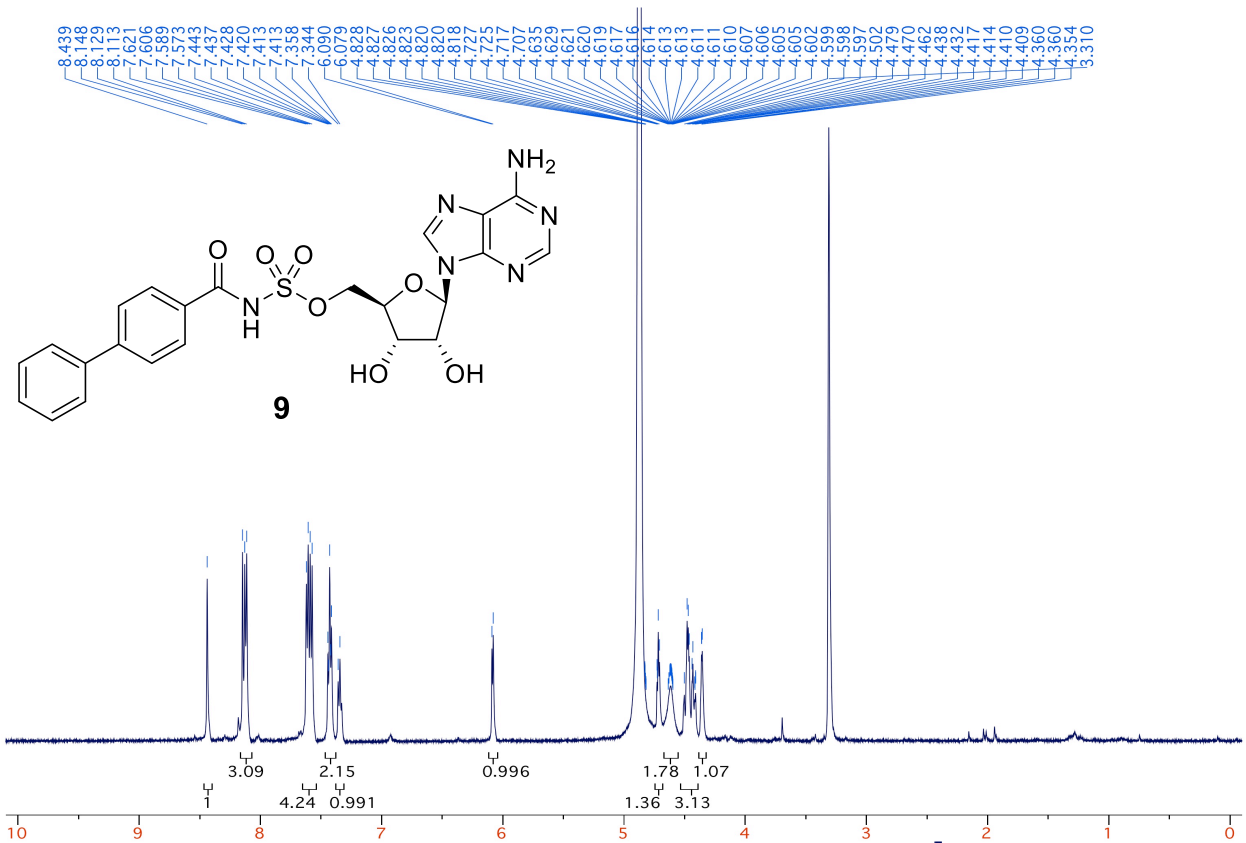
8.439
8.148
8.129
8.113
7.621
7.606
7.589
7.573
7.443
7.437
7.428
7.420
7.413
7.413
7.358
7.344
6.090
6.079
4.828
4.827
4.826
4.823
4.820
4.820
4.818
4.727
4.725
4.717
4.707
4.635
4.629
4.621
4.620
4.619
4.617
4.616
4.614
4.613
4.613
4.611
4.611
4.610
4.607
4.606
4.605
4.602
4.599
4.598
4.597
4.502
4.479
4.470
4.462
4.438
4.432
4.417
4.414
4.410
4.409
4.360
4.360
4.354
3.310
3.09
2.15
0.996
1.78
1.07
1
4.24
0.991
1.36
3.13
10
9
8
7
6
5
4
3
2
1
0
NH2
N
N
N
N
O
O
O
S
N
H
O
O
HO
OH

9

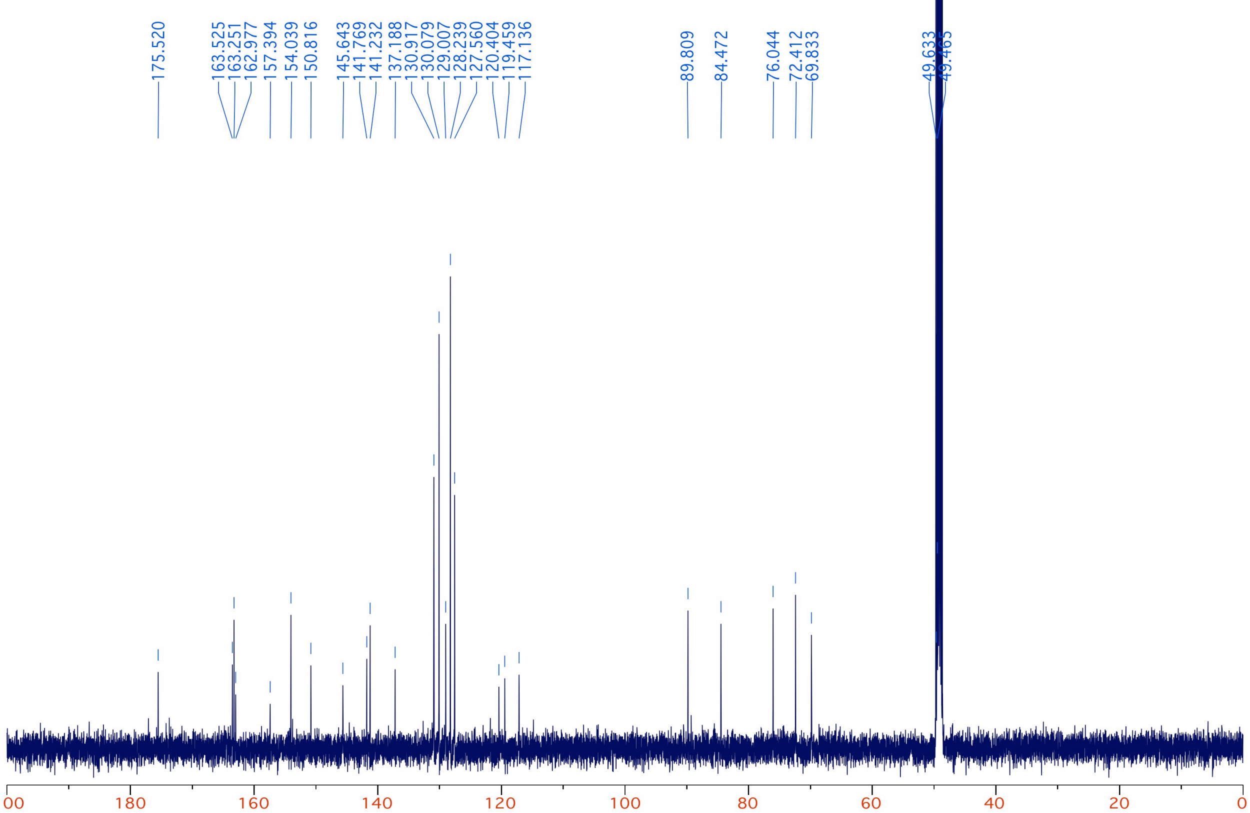
175.520
163.525
163.251
162.977
157.394
154.039
150.816
145.643
141.769
141.232
137.188
130.917
130.079
129.007
128.239
127.560
120.404
119.459
117.136
89.809
84.472
76.044
72.412
69.833
49.633
49.463
00
180
160
140
120
100
80
60
40
20
0

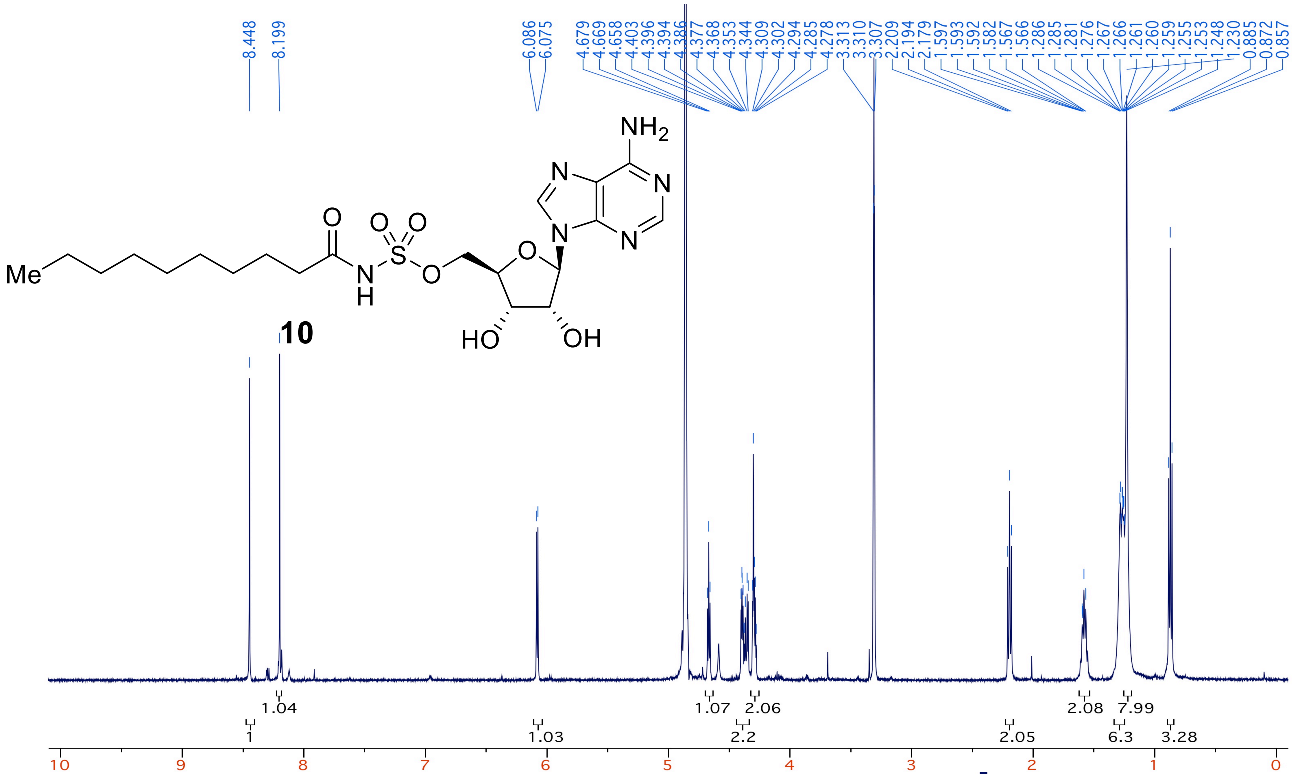

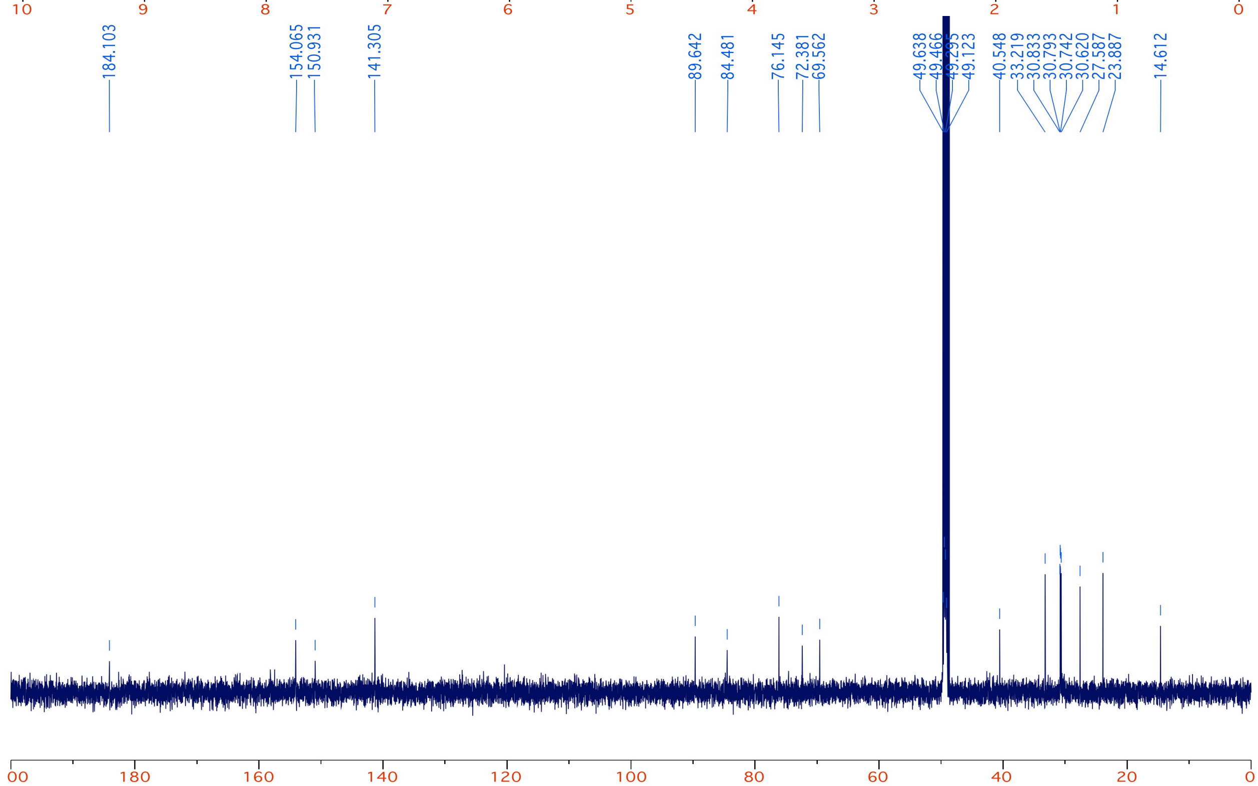

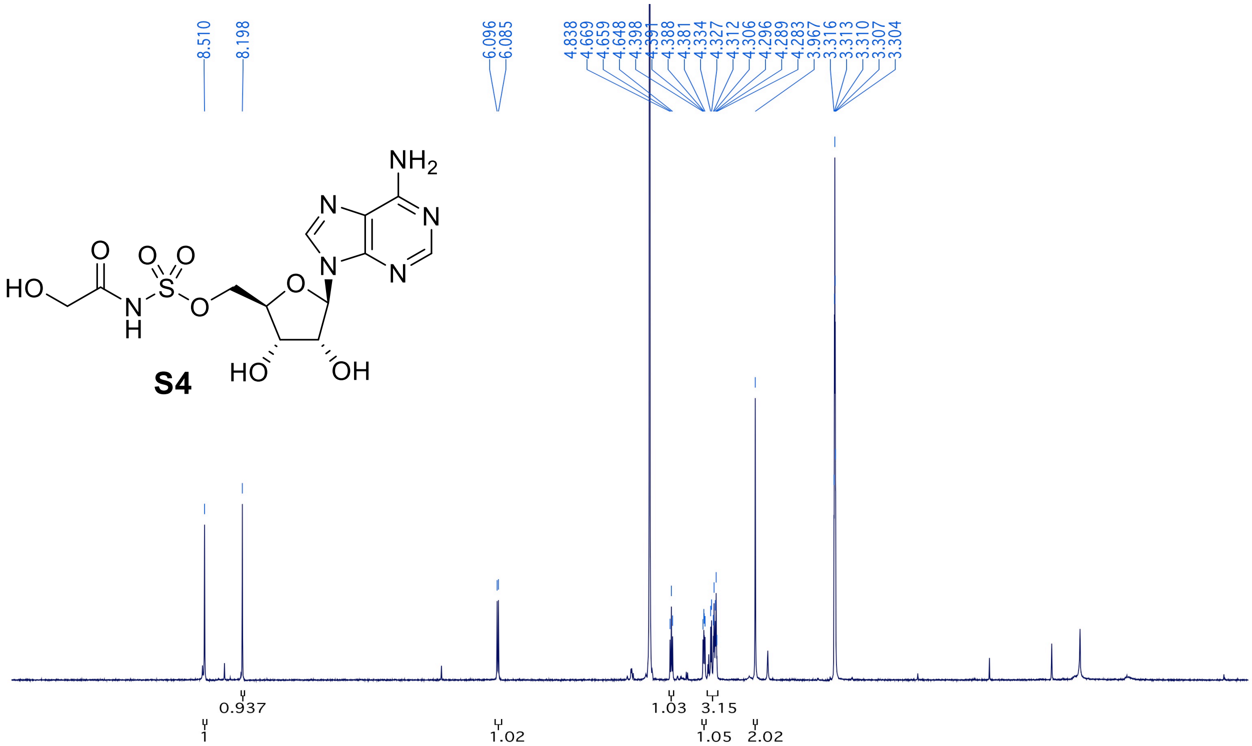

S4

8.510
8.198
6.096
6.085
4.838
4.669
4.659
4.648
4.398
4.391
4.388
4.381
4.334
4.327
4.312
4.306
4.296
4.289
4.283
3.967
3.316
3.313
3.310
3.307
3.304
1
0.937
1.02
1.03
1.05
3.15
2.02
10 9 8 7 6 5 4 3 2 1 0

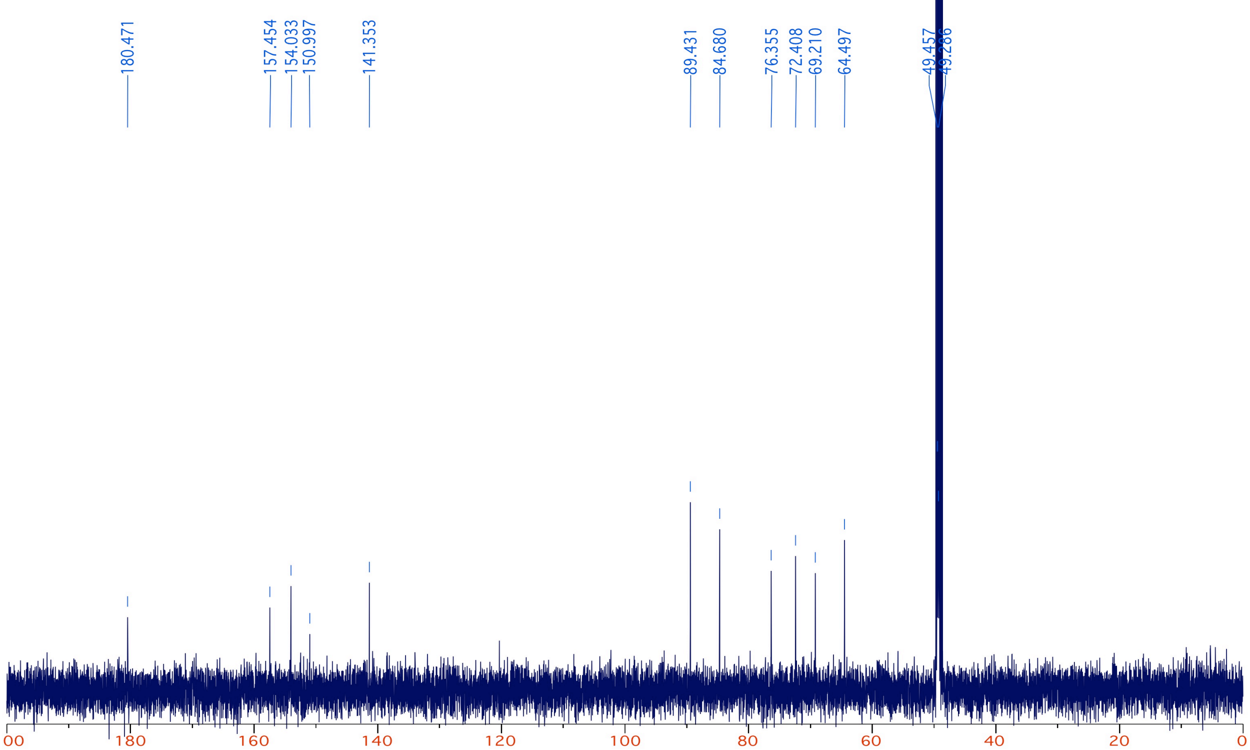
180.471
157.454
154.033
150.997
141.353
89.431
84.680
76.355
72.408
69.210
64.497
49.457
49.286
00 180 160 140 120 100 80 60 40 20 0

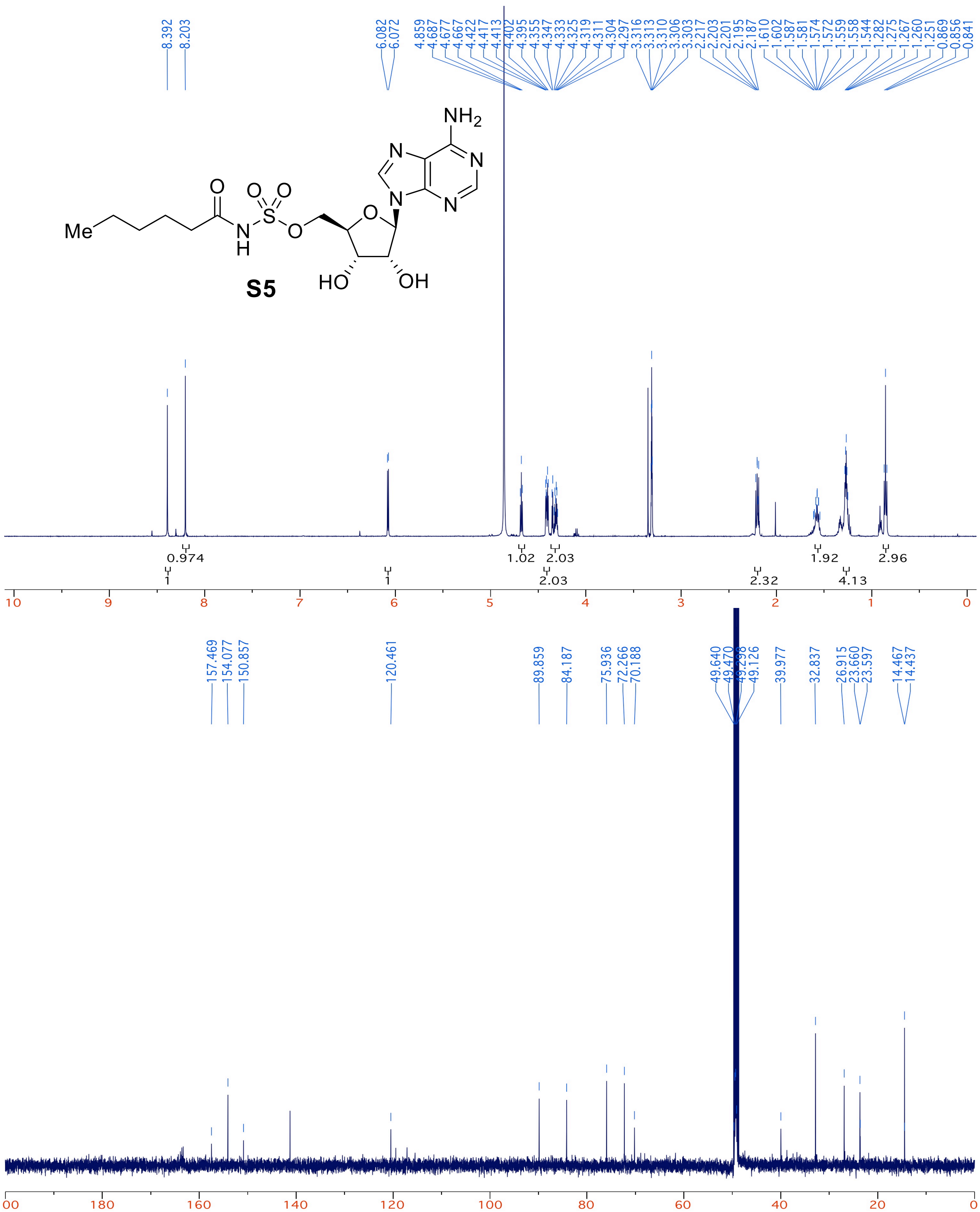
NH2
N
N
N
N
O
O O
O
S
Me
N
H
O
HO
OH
S5
8.392
8.203
6.082
6.072
4.859
4.687
4.677
4.667
4.422
4.417
4.413
4.402
4.395
4.355
4.347
4.333
4.325
4.319
4.311
4.304
4.297
3.316
3.313
3.310
3.306
3.303
2.217
2.203
2.201
2.195
2.187
1.610
1.602
1.587
1.581
1.574
1.572
1.559
1.558
1.544
1.282
1.275
1.267
1.260
1.251
0.869
0.856
0.841
0.974
1
1
1.02
2.03
2.03
2.32
1.92
4.13
2.96
10
9
8
7
6
5
4
3
2
1
0
157.469
154.077
150.857
120.461
89.859
84.187
75.936
72.266
70.188
49.640
49.470
49.298
49.126
39.977
32.837
26.915
23.660
23.597
14.467
14.437
00
180
160
140
120
100
80
60
40
20
0